CHAN, DANIEL CHUEN FONG

BIOPHYSICAL STUDIES OF NUCLEOSOME STRUCTURE BY CIRCULAR DICHROISM, THERMAL DENATURATION AND ESR SPIN LABELING

University of Hawaii PH.D. 1979

BIOPHYSICAL STUDIES OF NUCLEOSOME STRUCTURE BY CIRCULAR DICHROISM, THERMAL DENATURATION AND ESR SPIN LABELING

A DISSERTATION SUBMITTED TO THE GRADUATE DIVISION OF THE UNIVERSITY OF HAWAII IN PARTIAL FULFILLMENT OF THE REQUIREMENTS FOR THE DEGREE OF

DOCTOR OF PHILOSOPHY

IN BIOMEDICAL SCIENCES (BIOPHYSICS)

AUGUST 1979

By

Daniel C.F. Chan

Dissertation Committee

Lawrence H. Piette, Chairman
Roger Cramer
Morton Mandel
Marguerite Volini
Kerry Yasunobu

ACKNOWLEDGEMENTS

I would like to express my appreciation to Dr. Lawrence H. Piette, who supervised this project, for his advice, criticism, encouragement, guidance and financial support throughout this work.

I am very grateful to Dr. Jean-Jacques Lawrence for all of his advice, guidance and friendship.

I thank Drs. Marguerite Volini, Jim Bearden, Tom Grover and Judy Ramseyer for their valuable help and discussions.

I am grateful to Ellen Wildman, Pat Harwood, Winnie Yiu, Clara Abe, Susan Hayashida, Terry Jooss, Giovanni Bartolini and Peter Harney for their valuable assistance in many phases of this work.

Thanks go to Gordon Lee for typing this dissertation.

To the State Poutry Processors, Inc., Honolulu, Hawaii, for their courtesy of supplying the chicken blood.

To my parents for their encouragement, support and understanding.

Special thanks to Eva for her continual encouragement, support, assistance and consideration throughout this work.

ABSTRACT

Rat liver nuclei were digested very briefly by the Ca^{+2}, Mg^{+2} dependent Endogeneous Endonuclease. The digested chromatin was analyzed using exponential sucrose gradients. By plotting the weight average number of subunits released against digestion time, a slowing in the rate of change of chromatin fragments was found in the region of around six subunits. This suggested that the nucleosomes were possibly folded into a chain of discrete superstructures, with 6 to 8 subunits per superbead, and that the DNA between such superbeads was more susceptible to the nuclease digestion than the linker DNA between the nucleosomes.

The conformational state of DNA in the native chromatin and its subunits was analyzed by thermal denaturation and circular dichroism. Monophasic melting profiles were obtained for both the chromatin and its subunits, suggesting that the electrostatic stabilization of the DNA by the histones (H1, H2A, H2B, H3 and H4) was evenly distributed on the chromatin and its subunits. The chromatin and its subunits showed suppressed DNA ellipticities in their circular dichroism spectra. However, upon assembly of the nucleosomes to form a chromatin fiber, the ellipticity increased until the value of chromatin was achieved. We found that at least 8 nucleosomes were required to give the ellipticity of the chromatin, implying that the nucleosomes were possibly folded in an asymmetric fashion.

An imidazole spin label (IMDSL) was used to study the accessibility and conformational state of tyrosines in both the nucleosome core particles and histone core extracted from chicken erythrocytes. About 40% of the tyrosines in the histone core can be labeled under nondenaturing conditions.

However, less than 15% of the tyrosines in the nucleosome core particle can be labeled even at 200- to 300-fold molar excess of IMDSL. Conformational changes in the spin labeled histone core and nucleosome core particles due to external perturbations, such as urea, NaCl, pH and temperature, were studied. The nucleosome core was more sensitive than the histone core to urea denaturation. Several conformational transitions in the labeled nucleosome core were observed in the range of 1 mM to 2.5 M NaCl. A small change was detected at 10 mM NaCl and three major transitions were found between 0.1 M to 0.6 M, 0.7 M to 1.8 M and 2 M to 2.5 M NaCl. The labeled nucleosome core particle appeared to be unaffected by changes of pH in the range of $4.5 < pH < 9.5$. A thermal denaturation profile, obtained by the ESR method, showed that gradual conformational changes occurred within the inner histone core before the DNA melted.

The mode of reconstitution of nucleosome core particles was studied. A mixture of spin labeled histone cores and core DNA was reconstituted by salt step-gradient dialysis. At each step of dialysis, the labeled proteins were examined by ESR. It was found that the histone core bound progressively to the DNA in the range of 2 M to 0.3 M NaCl. Full association between histone core and DNA occurred when the ionic strength was less than 0.3 M. The reconstituted nucleosome complexes, purified by isokinetic sucrose gradients, were found to have identical physical properties as the native particle.

The role of tyrosines in the reassociation process for the nucleosome core was also investigated. It was found that spin labeling the surface tyrosines on the histone core did not interfere with proper reassociation of the nucleosome core complex. However, when "buried" tyrosines in the histone core were exposed by urea treatment and then spin labeled with

IMDSL, additional histone-DNA complexes were formed with properties different from those of native nucleosome cores. This suggests that some of the "buried" tyrosines are essential for the specific histone-histone interactions leading to the histone core structure.

TABLE OF CONTENTS

LIST OF TABLES

LIST OF ILLUSTRATIONS

Figure | Page

LIST OF ABBREVIATIONS

$\overset{o}{A}$	Angstrom
$A_{260,\ 236}$	Absorbance at wavelength 260 nm or 230 nm
ΔA	Change of absorbance
CD	Circular Dichroism
$D_{20,w}$	Diffusion coefficient
E	Extinction coefficient
ESR	Electron Spin Resonance
f	Frictional coefficient
H_+, H_o, H_-	ESR derivative peak heights of the low, central, and high field lines
H1, H2A, H2B H3, H4, and H5	Normenclature for different histone fractions
ΔH_o	Line width of ESR spectrum central component
hr	Hour
IMDSL	Imidazole Spin Label
min	Minute
mM	Millimole
M	Mole
NO	Number
nm	Nanometer
rpm	Revolution per minute
SL	Spin label
sec	Second
S_{20w}	Sedimentation coefficient
tyr	Tyrosine
ΔT	Change of temperature

τ	Rotational correlation time
(θ)	Ellipticity
UV	Ultraviolet
λ	Wavelength
w	Weight

I. INTRODUCTION

(A). BACKGROUND

The term chromatin was first introduced by Flemming in 1882 to describe the basic staining material in the eukaryotic cell nucleus. Chromatin, currently, is thus the diffuse interphase form of the eukaryotic chromosome. It is a complex consisting in addition to DNA, of about an equal weight of histones, a variable amount of highly heterogeneous nonhistone proteins and small amounts of RNA (1,2,3).

(1) Components of chromatin

(a) Nucleic Acids

(i) DNA

DNA contains the genetic information of the cell. A typical cell contains an amount of DNA roughly 1 m long, somehow folded into a nucleus about 10^{-3} cm in diameter. It was found that while all of the different kinds of cells in an eukaryotic organism contain the same nuclear DNA, only a small fraction of that DNA is transcribed in any given tissue (4).

DNA in aqueous solution exists primarily in the B-conformation, which is one of the several double-helicle states of DNA. However, in chromatin, some segments of DNA are found to exist in the C-conformation (46). Dimensions of DNA in different conformations in solutions are given in Table I (5).

(ii) RNA

Various amounts of RNA are found in the isolated chromatin. Bonner, et. al. (6) first reported the existence of chromosomal RNA, which recently was shown to be derived from the high molecular weight nuclear heterogeneous RNA (HnRNA) (7).

TABLE 1

Dimensions of the Different Forms of DNA

Conformation	Salt	Residue turn	Pitch	Translation turn	Angle between helical axis and plane of basis	Dihedral angle between base plane
A						
75% r.h.	Na	11	28.15	2.55	20	16
B						
92% r.h.	Na	10	34.6	3.46	-	-
B						
66% r.h.	Li	10	33.7	3.37	2	5
C	Li	9.3	31	3.32	6	10

The chromosomal RNA is about 40 to 60 base-pairs long, and contains 5-10% of dihydroxypyrimidine in addition to the common bases (8). It hybridizes to native DNA sequences and is species and tissue specific (9,10).

(b) Histones

Histones are basic proteins that comprise the major protein component of the chromosomes of higher plants and animals (for a recent review, see 11). In virtually all the eukaryotic organisms studied, chromosomes have been found to contain a weight ratio of histone to DNA that is close to 1:1. There are five main histones all containing 25% to 30% of the basic amino acids. Lower eukaryotics, such as yeasts and some protozoa, appear to have different histone composition, for example, yeast has neither H1 nor H3 (1,2,11).

Characterization and nomenclature of histones are given in Table 2 (1,11-14).

The complete amino acid sequences of several histones have been determined (11,12) and are given in the Appendix-I. It is interesting to note that with the exception of H1, all the other four histones have basic residues concentrated in the N-terminal region, with a secondary basic cluster at the C-terminal; the intermediate region is dominated by hydrophobic and acidic amino acid residues. There is no tryptophan in any of the histones, and only one or two cysteines in H3. The arginine rich histones (H3,H4) are the most conserved in primary sequence from species to species. It is found that there are only two residues different in H4 from calf thymus and pea. Histone H3 as well as H2A, H2B are also highly conserved. H1 (and H5 in chicken) is the longest histone and shows heterogeneity not only in the sequences of the subfractions isolated from the same origin but also when different

TABLE 2

Characterization and Nomenclature of Histones

Main histone	Ciba Sym. (current)	Gordon	John W.	Proposed	Mlecular wt	Mole% lys	Mole% Arg	Total Residues
lysine rich	H1	KAP	F1	Ia Ib	21,000	24.8	2.6	215
slightly lysine rich	H2A	ALK	F2a2	IIb1	14,004	16	6.4	129
	H2B	KSA	F2b	IIb2	13,774	10.9	9.3	125
arginine rich	H3	ARK	F3	III	15,324	9.6	13.3	135
	H4	GRK	F2a1	IV	11,282	10.8	13.7	102
other histones								
unique lysine rich histone from nucleated erythrocytes	H5	KAS	F2c	V	17,000			
lysine rich	H6	AKP		T				

species are compared (11,12). Most of the basic residues are clustered at the carboxyl half of the molecule. It is found that H1 is very prone to proteolysis and phosphorylation. The charge distributions of the five histones at pH 7.0 are given in appendix-II.

Because of their particular primary structures, the hydrophobic regions of the histones H2A, H2B, H3 and H4 appear to interact strongly with each other forming some kind of particulate structure within the chromatin while the N-terminal regions interact ionically with DNA. This will be discussed in more detail later.

The lack of diversity of the histones makes them poor candidates for the specificity element in control of transcription of chromatin DNA, although they still remain as important candidates for the role of general repressor initially suggested by Stedman and Stedman (15).

(c) Nonhistone Proteins

Nonhistone proteins comprise 50% or more of the chromosomal mass. In contrast to histones, the nonhistone proteins are extremely heterogeneous and include in all probability proteins ranging from structural to metabolically active types, like DNA polymerase. The nonhistone proteins are heterogeneous with respect to their molecular weights and isoelectric points; the molecular weight ranging from 15,000 to over 100,000 daltons (16), and the isoelectric points, as measured by isoelectric focusing, range from 2 to above 9.0 (17). Amino acid analysis which does not distinguish between acids and amides indicates that these proteins are largely acidic, so they are sometimes known as nuclear acidic proteins. Comparison of nonhistone proteins prepared from different sources shows quantitative and qualitative

species and tissue specificity (2,18,19,20).

(2) Current structural models for chromatin

The earlier regular (21) or irregular (22) supercoil model of chromatin structure is outdated by the current and well supported beads-on-a-string-like subunit structure of chromatin (1-3,23, 24). The former model was based on the low-angle X-ray diffraction studies of chromatin fibers and gels. The diffraction pattern showed rings at about 110, 55, 38, 26 and 22 Å. It was then proposed that this 110-22 Å set are successive orders of reflection from a supercoil of double helical DNA having 100 Å diameter and 120 Å pitch (21,22). However, this supercoil model can only account for the DNA compact packing in the chromosome and it does not say anything about the contribution of the histones to the structural integrity of chromatin. The X-ray diffraction data were not sufficient to support this model.

The subunit structure (nucleosome) model envisioned a periodic repeating structure of histone-DNA complex along the DNA fiber, suggesting that the first level of DNA compaction in chromatin and nuclei is by wrapping of DNA about a histone core. This model has been well supported by nuclease digestion (27,28), electron microscopy (39-44), low-angle X-ray diffraction, neutron scattering (49-52), and histone-interaction studies (57-64). This evidence supported a model of chromatin structure based on a repeating unit about 100 Å in diameter, comprising eight histones (two of each H2A, H2B, H3 and H4) surrounded by 150-200 base pairs of DNA.

(a) Nuclease Digestion Studies

In 1970, Williamson observed that DNA isolated from the cytoplasm of mouse embryonic liver cells after culture resembles

nuclear DNA and occurs in fragments of discrete size, each being a multiple of a unit molecular weight of approximately 135,000; but they claimed that this may be an artifact and suggested that the isolated cytoplasmic DNA is a degradation product of nuclear DNA (25). In 1971, Clark and Felsenfeld found that only about 50% of the DNA in calf thymus chromatin could be readily digested by Staphylococcal Nuclease (26). They interpreted that histones are not evenly distributed in chromatin; about half of the DNA is "open" and not covered by proteins. Until 1973, Hewish and Burgoyne (27) correctly identified a series of discrete size DNA fragments as the result of nuclear autolysis. By digesting chromatin with a Ca-Mg dependent Endogeneous Endonuclease of rat liver nuclei, they showed that the DNA was released in a set of discrete sizes, which appeared to be integral multiples of about 200 base pairs in length. Digestion of free DNA with the same endonuclease failed to give such discrete sizes. Their data significantly indicated that DNA was structured within chromatin so as to provide regularly repeating sites of enhanced accessibility to nucleases. Noll (28) later improved and confirmed this repeating structure of chromatin by using the exogenous Staphylococcal nuclease. Since then, such periodic repeating structures of chromatin have been observed in a broad range of eukaryotic cells, such as rat liver (27,28), calf thymus (29), trout testes (30), duck erythrocyte (31), pea (32), yeast (33), sea urchin sperm (34), cells grown in culture (35), aspergillus (36), etc. (for a review, see 3).

It is found that the chromatin appears to be first cut into multimers and monomers (nucleosomes) which contain a histone core (two each of the four histones H2A, H2B, H3 and H4) com-

plexed with a repeat length of about 200 base pairs of DNA. Further digestion of the nucleosomes yields the nucleosome core particles containing the histone core and a constant 140 base-pairs of DNA (37,38). The nucleosome core particles are connected in close apposition by DNA linkers, which vary in length (depending on the cell type), forming a continuous chromatin fiber. Histone H1 (and H5) is found to be associated with the linker DNA and is involved in maintaining and generating higher order chromatin structures (3,23,24).

(b) Electron Microscopy Studies

In 1973, Woodcock (39) and Olins' group (40) separately reported the "string of beads" chromatin structure in electron microscopy studies. Olins and Olins (40,41) coined the term "nu" bodies (ν-bodies) for the spheroid chromatin units. They found linear arrays of spherical chromatin particles about 70 Å in diameter, close packed or connected by 15 Å diameter 'strings' appeared to be the major structural unit of the formaldehyde fixed chromatin. They have estimated an approximate molecular weight of 160,000 per body with an equal weight for both DNA and proteins associated. Later, Senior and the Olins (42) showed that extensive sonication of formaldehyde fixed chromatin yielded a subpopulation consisting of homogeneous ν-bodies of molecular wt 300,000 with 200 base-pairs of DNA and about an equal weight of histones. Oudet and Chambon (43) found the same result namely that chromatin is composed of a flexible chain of spherical particles, about 125 Å in diameter, connected and packed closely by DNA filaments. They renamed the ν-body or the PS particles as "Nucleosome". However, Kornberg's group (44) and Varshavsky's group (45) who have observed the same result but indicated that the native structure of chromatin to be

a closely packed fiber. Van Holde's group (46) confirmed the structural similarities between the nucleosomes and the PS particles. But it is clear that the mononucleosome is larger than their 'PS' particle. Several investigators (40,46,47,48) favored the existence of the spacer regions between the nucleosomes. They suggested that very mild digestion or sonication will break the chromatin fibers randomly in the spacer regions; the first mononucleosomes to be produced will then contain 150-200 base-pairs of DNA. Further degradation of the exposed DNA tails will give the ultimate PS particles or the nucleosome core particle with 140 base-pairs DNA. However, several other investigators (3,44,45) insisted that the nuclease accessible DNA is not a spacer but a linker and is not physically extended.

(c) X-Ray and Neutron Scattering Studies

Earlier studies of chromatin by X-ray diffraction (21,22) lead to the proposal of a regular or irregular "super-coil" model. But such data were insufficient to support the validity of such a model. In 1974, Kornberg and Thomas (49) applied the X-ray diffraction method on the reconstituted histone-DNA complex. They were able to demonstrate that, except for H1, all the other histones H2A, H2B, H3 and H4 are required for the generation of a normal diffraction pattern. However, no refined analysis of the 110, 55, 37, 27, 22 Å series were provided. Bradbury's group (50) extended this work by using neutron scattering which gives scattering patterns similar to X-ray patterns but provides a more refined analysis of the data. By using the method of contrast variation, (i.e. matching the scattering of the solvent ((D_2O/H_2O)) with that of either DNA or histone), they were able to show that the 110 Å and 37 Å reflections come from the protein and that the 55 Å and 27 Å

reflections arise from DNA. The 110 Å peak which is concentration dependent represents the basic repeat of the subunits along the chromatin fibril. Later, Bradbury's group (51) was able to show that this 110 Å peak was slightly off the meridian of the oriented chromatin fiber, suggesting a superhelical arrangement of the nucleosomes of pitch 100 Å and outer diameter of approximately 300 Å; with about six nucleosomes per turn of the chromatin fiber. Such results were consistent with several recent biophysical studies (88,110), X-ray (52,53), and electron microscopy data (54), suggesting a Solenoidal model for superstructure in chromatin. In about the same period, Bradbury (55), Richards and Pardon (56) using low-angle neutron scattering, tried to measure the size and shape of the internal structure of the nucleosome. They were able to propose a spherically averaged structure with most of the histones closely packed into a core of radius 32 Å surrounded by a loosely packed DNA-rich shell of 20 Å thickness resulting in a particle of 52 Å average radius.

(d) Histone Interactions, Cross-linking and Reconstitution Studies

Histones interact with one another in specific ways (49,57-64) and such interactions are very important in maintaining the histone core structure in the chromatin. Using fluorescent anisotopy and circular dichroism methods. Isenberg et. al. (see ref. in 57) had shown that there are: three strong interactions leading to the formation of two dimers, (H2A-H2B) and (H2B-H4), and one tetramer $(H3\text{-}H4)_2$; two weak interactions, H2A-H4 and H2B-H3; and one intermediate interaction, H2A-H3. The association constants for the histone cross-complexing patterns in solution are shown in Table 3 (see ref. in 57-59).

TABLE 3

HISTONES CROSS-COMPLEXING IN SOLUTION

H3	H4	H2B	H2A	
	STRONG (TETRAMER) 0.7×10^{21} M^{-3}	WEAK (DIMER)	INTERMEDIATE (DIMER) 10^{5} M^{-1}	H3
STRONG		STRONG (DIMER) 10^{6} M^{-1}	WEAK (DIMER) 4×10^{4} M^{-1}	H4
WEAK	STRONG		STRONG (DIMER) 2×10^{6} M^{-1}	H2B
INTERMEDIATE	WEAK	STRONG		H2A

Note: The term dimer used in chromatin research only refers to a complex of two different molecules. It is different from the conventional definition for the dimer.

The H2A-H2B dimer and the $(H3\text{-}H4)_2$ tetramer were also found by several other investigators (62,63,49,64). However, Weintraub et. al. (60) found a heterotypic tetramer composing each of H2A, H2B, H3 and H4 from chromatin, when treated in 2M NaCl.

Using different chemical cross-linking agents, many laboratories have also found such histone complexes from chromatin, nuclei or whole cells. For example, H2A-H2B, H2B-H4 were cross-linked by formaldehyde, glutaraldehyde, dimethyl suberimidate, tetranitromethane, and UV irradiation (65-69), while H3-H4 were cross-linked by carbodiimide (70), glutaraldehyde, dimethyladipimidate (66) and dimethyl suberimidate (67), respectively. The cross-linked histone pairs in chromatin are presented in Table 4.

It should be noticed that the tetranitromethane, UV irradiation and carbodiimide are zero length cross-linkers, and such cross-linking (for example, H2B-H4, H2A-H2B and H3-H4) implies that these cross-linked histone pairs had previously been in contact, and hence presumably interacting. Comparison of Table 3 and Table 4 clearly shows that all the strongest interacting histone pairs (H3-H4, H2B-H4 and H2A-H2B) have been linked in chromatin by zero length linkers and no other pairs have been so linked. Therefore, it suggests that the histones which interact strongly <u>in vitro</u> are also in close proximity to each other in the chromatin.

The highly conserved arginine rich histones (H3,H4) may play a special role among the histone complexes. Camerini-Otero et. al. (73) showed that the H3-H4 tetramer largely determine the organization of DNA into a subunit structure, judged by the periodicity of nuclease-sensitive sites in the reconstituted DNA-histone complexes.

TABLE 4

HISTONES CROSS-LINKING IN CHROMATIN

H3	H4	H2B	H2A	
X	X			H3
X		X	X	H4
	X		X	H2B
	X	X		H2A

X MEANS CROSS-LINKED

Bosely et. al. (74) supported this observation by showing that the reconstituted H3, H4 & DNA complexes could give the typical small-angle X-ray diffraction patterns, i.e. the 110 Å - 22 Å series. Oudet et. al. (75) had also found that the reconstituted H3, H4 and DNA complexes showed nucleosome-like particles in electron micrographs. Furthermore, H3 and H4 appeared to be bound at the 5' and 3' ends of each DNA strand, respectively, in the nucleosome core DNA, as shown by histone-DNA cross-linking studies (76,77). Thus, it has been suggested that the conservation in length of the core DNA (140 base-pairs) in the nucleosome core particle, is due to the conservation in the structure of the histones H3 and H4, while the variation in length of the linker DNA is due to variation in structure of H1, H2A and H2B (2,3,11,23,24).

Based on the above abundant data, two main models proposed for the chromatin subunit (nucleosome) structures are worth mentioning:

(i) Kornberg (3,49) proposed a structure in which 200 base-pairs of DNA associated in some manner with a group of nine histones molecules, comprising two each of H2A, H2B, H3 and H4, and one H1 molecule, to generate the bead or subunit structure. A chromatin fiber consists of many such units forming a flexible jointed chain. The unit is about 100 Å in the fiber direction and about 90 Å in diameter, with DNA wrapping on the outside of the unit, and the histone on the inside. The histones are arranged as an $(H3)_2(H4)_2$ tetramer and H2A-H2B polymer.

(ii) Van Holde and co-workers (38,46) favored a model whereby 140 base-pairs of DNA wrapping on a protein core formed by two molecules each of H2A, H2B, H3 and H4 to form beads or subunits

which are then separated by a 60 base-pairs spacer region. H1 was postulated to interact with the DNA of the spacer or interbead region. The protein core is formed by the interactions (hydrophobic) of the C-terminal halves of the histones, leaving the N-terminal regions free to interact with DNA.

Some of the physical parameters of the monomer subunits from the chicken erythrocyte have been characterized by hydrodynamic studies (37,38,94) and are shown in Table 5.

(B) STATEMENT OF THE PROBLEM

The nucleosome, as a subunit structure for chromatin, is now well established from morphological, biochemical and biophysical studies (see Background). Most of the experimental data are best met by a model of nucleosome core particle consisting of a central histone core associated on its circumference with a supercoiled DNA dyad of about 140 base-pairs. Recently, the X-ray diffraction pattern of the nucleosome core particle crystals has been obtained and is shown to be consistent with this model (78). The nucleosome core particle is found to be roughly a disc-shaped particle of diameter 110 Å with a thickness of 57 Å, somewhat wedge-shaped with the core DNA (140 base pairs) being wrapped around the histone core into about 1 3/4 turns of a flat superhelix with a pitch of about 28 Å (78). These crystallographic dimensions are in good agreement with those determined by electron microscopic techniques (79) and with those of the model proposed on the basis of neutron-scattering and X-ray scattering data (80,81). However, the present X-ray crystallographic data with a 25 Å resolution (78), do not give definite conclusions concerning the

TABLE 5

Physical Properties of Chicken erythrocyte core particles

Sedimentation coefficient, $S_{20,w}$	:	11.4S
Partial specific volume, $\bar{v}$	:	0.68 cm^3/gm
Extinction coefficient, $E(\frac{1cm}{mg.ml})$	:	9.3 mg^{-1}/m^{-1}
Molecular weight	:	208,000 $\pm$ 10,000
Composition, gmprotein/gm DNA	:	1.25
Effective diameter in solution	:	106Å
$D_{20,w}$	:	3.9F
f/f_o	:	1.44
a/b prolate axial ratio	:	8.2 - 8.7
a/b oblate axial ratio	:	9.7 - 10.3

Fig. 1 Model of Nucleosome Core Particle

(A) Representation of 1 3/4 turns of the 140 base pairs DNA superhelix proposed for the nucleosome core with 80 base pairs per turn. Numbering is from the 5'-end of one strand.

(B) Shaded areas represent groups of sites of low or medium cutting frequency by DNase I. The arrow indicates the dyad axis. * means high frequency DNase I cutting.

Adapted from Finch et al (78).

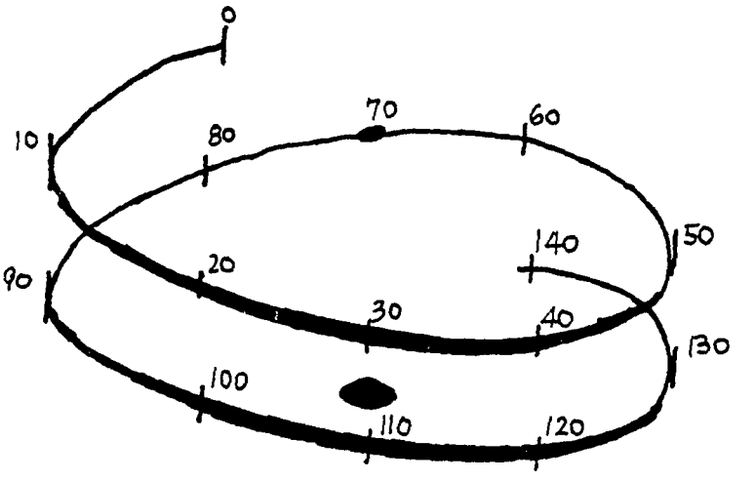
0
10
80
70
60
50
90
20
140
30
40
130
100
110
120

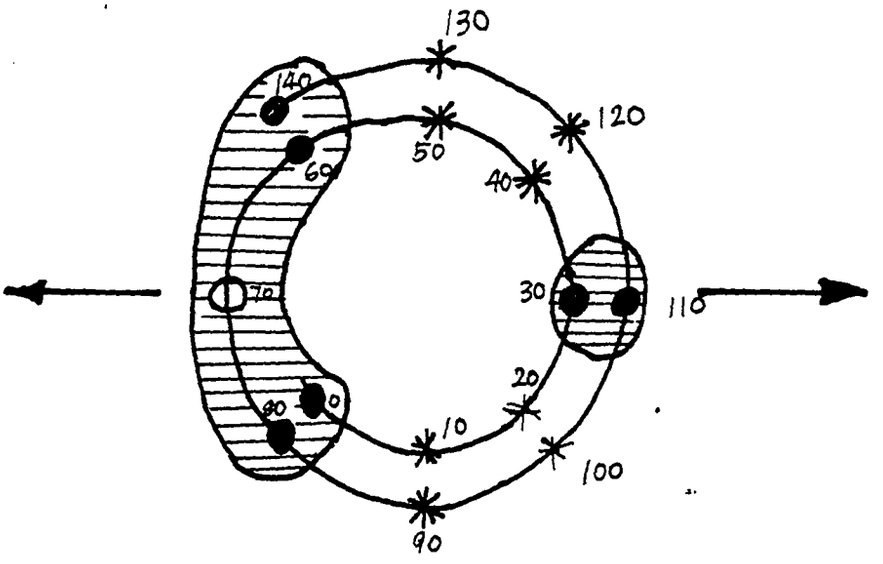
130
140
120
50
60
40
70
30
110
20
80
0
10
100
90

organization of the inner histone core. The internal architecture of the nucleosome is not well understood. The exact path followed by the DNA in the core is still unknown. The evidence that the core DNA is accessible to cleavage by DNase I at intervals of 10 nucleotides along both stands (82-84), suggests that the enzyme either cuts at points on smoothly bent DNA (non-kinked model) which are 'maximally exposed' (85) or at 'kinks' in the DNA where the structure is distorted (86,87). Furthermore, it has been found that the DNase I sensitive sites are not equally frequent every 10 bases (82-84), and it has been assumed that the frequency of cutting reflects differential protection of different tracts of the DNA by the histone interactions. Based on the X-ray crystallographic data (78) and the DNase I digestion studies (82-84), Finch et. al. (78) has proposed a more refined model for the nucleosome core particle structure, and this is shown in Figure 1.

Although a detailed structure of the nucleosome will probably eventually be solved by high-resolution X-ray diffraction methods, until such time, it is still worthwhile to study the DNA-histone and histone-histone interactions within the nucleosome, using indirect methods which will provide additional information on the nucleosome structure. The overall aim of this research project is to study such interactions in the nucleosome and in the reconstituted histone-DNA complexes by several physical, biochemical methods, namely, nuclease digestion, sedimentation, circular dichroism, thermal denaturation and ESR spin labeling. The specific aims are:

(a) to characterize the conformational state of DNA in native chromatin and in its subunits,

(b) to analyze the distribution of the digested

products at the early stage of endonuclease digestion,

(c) to study the accessibility and conformational state of specific tyrosine residues in the nucleosome core particles and in the histone core,

(d) to study the conformational changes of the nucleosome and histone core due to perturbations, and

(e) to establish the role of tyrosine residues in the reconstitution of nucleosome complex.

II. METHODS AND EXPERIMENTAL PROCEDURES

(A). MATERIALS

Commercial material	Supplier
Acetic Acid, Glacial	Mallinckrodt
Acetone	Mallinckrodt
Acrylamide	Bio-Rad
Agarose	Bio-Bad
Bio-Gel HTP	Bio-Rad
Bis-acrylamide	Bio-Rad
Ammonium Persulfate	Bio-Rad
Bovine Albumin	Sigma
1-Butanol	Baker
Calcium Chloride	Baker
Calf thymus DNA	Sigma
Calf thymus histones	Sigma
Citric Acid	Mallinckrodt
Coomassie Brilliant Blue	Sigma
Chloroform	Mallinckrodt
Disodium-ethylene-dinitrilo-tetraacetic Acid (EDTA)	Sigma
Ethnol	Commercial Solvents Corp.
Ethylene-glycol-bis (-aminoethylether) N, N'-tetraacetic Acid, (EGTA)	Sigma
Ethidium Bromide	Sigma
Floin Ciocalteau phenol reagent	Sigma
Glycine	Bio-Rad

Hydrochloric acid	B & A
Magnesium Chloride	Mallinckrodt
2-Mercaptoethanol	Aldrich
Nonidet P40	BOH
N-acetylimidazole	Aldrich
Nuclease, Micrococcal	Worthington
Phenylmethyl Sulfonyl fluoride, (PMSF)	Sigma
n-Propanol	Mallinckrodt
Potassium Chloride	Mallinckrodt
Potassium phosphate, mono & dibasic	Mallinckrodt
Potassium sodium Tartrate	Mallinckrodt
Sodium Chloride	Mallinckrodt
	MCB
	Sigma
Sucrose	Sigma
Spermidine	Sigma
Sephadex G-25, fine	Pharmacia
Sephadex G-100	Pharmacia
Sodium carbonate	Sigma
Sodium Lauryl Sulfate, SDS	Sigma
Sodium Hydroxide	Sigma
TEMED	Bio-Rad
Trizma Base	Sigma
Urea	Sigma & Bio-Rad

(B) PREPARATION OF NUCLEAR COMPONENTS

(1) Tissues

(a) Calf Thymus

Commercial Calf Thymus DNA, whole histones and histone fractions were purchased from Sigma Chemical Company.

(b) Livers

Livers from freshly killed adult rats were used immediately for nuclei extraction.

(c) Chicken Erythrocyte

Chicken blood was collected from freshly exsanguinated white chickens (courtesy of State Poultry Processors, Inc., Honolulu, Hawaii).

(2) Nuclei

(a) Small Scale

Rat liver nuclei were extracted according to the procedures of Hewish and Burgoyne (27) with some modifications. Fresh livers (60 gm to 120 gm) were homogenized rapidly in at least 8 ml of Buffer B-1/gm of liver. The homogenate was filtered through four layers of gauze and was centrifuged at 6,000 rpm for 15 minutes. The pellets were resuspended in Buffer-B2 (one half volume of B-1) and centrifuged at 12,000 rpm for 15 minutes. The nuclear pellets were resuspended in at least 8 volumes of Buffer C, layered on 12 ml of the same buffer and centrifuged at 27,000 rpm for 90 minutes. The nuclear pellets were washed twice in Buffer D and resuspended in the same buffer at a concentration of 1.5 to 2×10^8 nuclei/ml. The white nuclei were used immediately for chromatin extraction or were frozen at $-80^{\circ}C$ for later use. Usually, nuclei were well preserved with very minor cytoplasmic

contamination as checked by light microscopy.

BUFFER COMPOSITION

Buffer A: 60 mM KCl; 15 mM NaCl, 0.5 mM Spermidine, 15 mM Tris-HCl, 15 mM β-Mercaptoethanol, pH 7.4 (titrate with HCl).

Buffer B-1: 0.34 M Sucrose, 2 mM EDTA, 0.5 mM EGTA, in Buffer A.

Buffer B-2: 1.37 M Sucrose, 1 mM EDTA, 0.25 mM EGTA, in Buffer A.

Buffer C: 2.4 M Sucrose, 0.1 mM EDTA, 0.1 mM EGTA, in Buffer A.

Buffer D: 0.34 M Sucrose, 0.1 mM EDTA, 0.1 mM EGTA, in Buffer A.

(b) Large Scale

Large quantities of chicken erythrocyte nuclei were extracted according to the method of Olins et. al. (94). Blood was collected from eight freshly exsanguinated chickens. One tenth volume of anticoagulant citrate dextrose was added. The blood was filtered through four layers of gauze, diluted with one half volume of STM Buffer, and centrifuged at 6,000 rpm for 15 minutes. The loose erythrocyte pellet was suspended in 1,500 ml of STMN Buffer, stirred with a magnetic bar for 10 minutes, and centrifuged at 6,000 rpm for 15 minutes; the entire washing cycle was repeated three more times. The resulting nuclear pellets were diluted to a concentration of $1x10^9$ nuclei/ml in STMN Buffer, and were used immediately for nucleosome extraction or were frozen at -80^oC for later use.

BUFFER COMPOSITION

Buffer STM: 10 mM NaCl, 10 mM Tris-HCl, 3 mM $MgCl_2$, pH 7.4

Buffer STMN: 10 mM NaCl, 10 mM Tris-HCl, 3 mM $MgCl_2$, 0.5% Nonidet P40, pH 7.4

(3) Chromatin

Nuclei were digested with Ca^{+2}, Mg^{+2} dependent endogeneous endonuclease or with Micrococcal Nuclease (Worthington), according to Hewish (27) and Noll (28), with minor modifications. 0.2 mM phenylmethyl sulfonylfluoride (PMSF) was present at all times during isolation and digestion of the nuclei.

(a) Very brief digestion

To extract large segments of native chromatin, low units of nuclease and short digestion time was used. Rat liver nuclei were suspended in Buffer D at 1.5 to $2x10^8$ nuclei/ml. The nuclear solution was made 1 mM $CaCl_2$ and incubated at 37°C for 5 minutes. 15 U/ml of micrococcal nuclease was added. The digestion was stopped 20 seconds later by adding 1 mM EDTA and chilled quickly on ice. The nuclei were then sedimented at 2000xg for five minutes, yielding a pellet of nuclei and a first supernatant. The pellet was lysed by resuspending in 0.2 mM EDTA, 0.2 mM PMSF (Phenyl methyl Sulfonyl Fluoride), pH 7.0. The suspension was sedimented at 2000xg for two minutes and the chromatin was recovered in the supernatant; the yield was estimated by measuring the absorbance at 260 nm.

(b) Mild digestion

To get a distribution of monomers, and multimers, a higher nuclease concentration and digestion time were used (44). The digestion condition was the same as (a) except that the concentration of

nuclease is about 200 to 300 U/ml, and digestion time varied from 30 seconds to 5 minutes.

(c) Digestion by rat liver nuclear endogeneous endonuclease

Digestion conditions were as described by Hewish and Burgoyne (27), with some modifications. Rat liver nuclei were resuspended in Buffer D at a concentration of 1.5 to $2x10^8$ nuclei/ml. The solution was made 1 mM $CaCl_2$ and incubated at 37°C for 5 minutes. Digestion was activated by adding a final concentration of 10 mM $MgCl_2$ to the incubated nuclear solution. Digestion time was varied from 2½ minutes to 6 hours and the reaction was terminated by adding 4 ml of 0.02M K-Phosphate buffer with 5 mM EDTA, pH 7.5, and chilled quickly on ice for 2 minutes. The suspension was centrifuged at 2,300 rpm for 5 minutes, yielding the first supernatant and the digested nuclear pellet. The pellet was lyzed with 0.2 mM EDTA and 0.2 mM PMSF, pH 7.0, for 5 minutes and centrifuged at 1,300 rpm for 2 minutes. The supernatant was saved and its absorbance was measured at 260 nm.

(d) Fractionation of monomers, dimers, and multimers by isokinetic sucrose gradients

The isokinetic sucrose gradients were prepared according to Lawrence et. al. (88). One to two ml of the mild digested chromatin (A_{260} = 30 to 50/ml) was layered on the preformed isokinetic sucrose gradients in the nitrocellulose tubes and ultracentrifuged at 27,000 rpm for 20 hours in a Beckman SW27 Rotor.

Fifty fractions of 20 drops each were collected per lot by a Gilson fractionator and its absorbance was measured at 260 nm with a Beckman 25 Spectrophotometer. Fractions corresponding to

the three highest optical density values of each peak were pooled and extensively dialyzed against 1 mM NaCl, 0.2 mM EDTA, pH 7.0.

(4) Nucleosome core particles

H1 and H5 depleted chromatin was prepared from the chicken erythrocyte nuclei according to Tatchell and Van Holde (89) with minor modifications. The chromatin was digested at 37°C with 50 U/ml micrococcal nuclease (Worthington), according to Noll (28) for 3 hours. The limited digested chromatin was centrifuged through 5-25% isokinetic sucrose gradients according to Lawrence et. al. (88), in an SW27 Rotor. The monomer fractions were pooled and dialyzed against 10 mM Tris HCl, 2 mM EDTA, pH 7.2, at 4°C.

(5) DNA

DNA was extracted according to Noll et. al. (90) from commercial calf thymus, native chromatin and fractionated subunits by making them in 2 M NaCl, 1% SDS and extracted twice with a chloform-isoamyl alcohol (24:1) mixture. The aqueous phases were dialyzed against water overnight and lyophylzed or dialyzed against the desired buffer.

(6) Histones

(a) Whole histones

Histones from chromatin and its subunits were extracted with 0.25 N HCl according to Johns (91). The precipitated DNA was removed by centrifugation at 10,000 rpm for 20 minutes. The supernatants were re-extracted with 0.25 N HCl and centrifuged again for 20 minutes. The combined supernatants were dialyzed overnight against water and lyophylzed.

(b) Histone cores

The procedure of Tatchell and Van Holde (89) was also used to isolate histone cores from the H2 and H5 depleted chromatin. The chromatin solution in 2 M NaCl, 10 mM Tris HCl, 0.2 mM EDTA, pH 7.2, was centrifuged at 50,000 rpm for 8 hours with an Ti 50.2 Rotor to pellet the DNA away from the histone cores. The supernatant was chromatographed through a Sephadex G-100 column equilibrated with 2 M NaCl, 10 mM Tris HCl, 0.2 mM EDTA, pH 7.2 and the histone core fractions were pooled, concentrated with an Amicon ultrafiltration cell, and dialyzed against 2 M NaCl, 10 mM Tris HCl, 0.2 mM EDTA, pH 7.2.

(c) Histone pairs H2A + H2B and H3 + H4

Histone pairs H2A + H2B and H3 + H4 from chromatin or spin labeled nucleosome were purified by hydroxylapatite column according to Simon and Felsenfeld (92) with modifications. Native or modified chromatin was dialyzed overnight at 4°C against 0.63 M KCl, 0.1 M potassium phosphate, pH 6.7. An amount of chromatin containing 5 mg of DNA was applied to a 2x18 cm hydroxylapatite column that had been equilibrated with the same buffer at 4°C. The column was then washed with 120 ml of the starting buffer while 40 fractions (containing mainly H1 and H5) were collected and the absorbance of fractions was measured at 230 nm and 260 nm. The running buffer was then stepped to 0.93 M KCl, 0.1 M potassium phosphate, pH 6.7, and 60 ml was washed through the column. A single peak containing H2A + H2B was eluted. Next 80 ml of linear KCl gradient from 0.93 M to 1.2 M KCl, plus 0.1 M potassium phosphate pH 6.7 was run through the column. Another peak containing H3 + H4 was eluted when 60 ml of 2 M KCl, 0.1 M potassium phosphate, pH 6.7 was run through the column. Finally, the buffer was

changed to 0.5 M potassium phosphate, pH 6.7 and the protein-free DNA was eluted from the column.

(C) BIOCHEMICAL METHODS

(1) Kinetics of nuclease digestion

The kinetics of micrococcal nuclease digestion of DNA in chromatin were followed by measuring the amount of DNA rendered acid soluble. The conditions for activation and termination of nuclease digestion on chromatin were the same as described in Chapter II, section B, part 3 of this report. The acid soluble DNA was determined by the addition of perchloric acid to 0.8 N to the first supernatant, followed by chilling 10 minutes at $0^{\circ}C$ and centrifugation at 8000xg for 10 minutes. The absorbance at 260 nm of this supernatant (which contains mostly mononucleotides and short oligonucleotides) was measured and divided by a factor of 1.67 to correct for the hyperchromic effect (95).

(2) Gel-electrophoresis

Polyacrylamide gel electrophoresis of DNA extracted by digested chromatin or fractionated subunits was carried out in 12 cm x 0.8 cm diameter Plexiglass tubes, employing a Tris-acetate-EDTA (TAE) buffer system, according to Leoning (96). 2.5% polyacrylamide and 0.5% agarose TAE gels were used. ΦX174 RF DNA-Hae III Digest (New England Biolabs) was used as a standard to calibrate the DNA sizes. Histones were analyzed by the polyacrylamide slab gels containing SDS method of Laemmli (97), using running gels of 18% polyacrylamide.

(3) Concentration determination

Histone concentration was analyzed by the method of Lowry et. al. (98), using calf thymus histones as standards. Extinction coefficients used to determine the DNA and histone concentrations

were: DNA, $E^{1\%}_{1\ cm}$ = 200 at 258 nm; histone core protein, $E^{1\%}_{1\ cm}$ = 3.69 at 275.5 nm (99).

(4) Reconstitution of nucleosome core particles

Nucleosome complexes were reconstituted from core DNA and (native or spin labeled) histone core by salt step-gradient dialysis method, according to Tatchell and Van Holde (89), with 4 hour steps of 2M, 1.5M, 1.2M, 1.0M, 0.8M, 0.6M, 0.4M, 0.1M NaCl and, finally, 2 changes of 10 mM Tris HCl, 0.2 mM EDTA, pH 7.2 at 4°C. At the end of reconstitution, the material was first concentrated using either an Amicon Ultrafiltration cell (Model 12 with a PM 10 membrane) or Amicon Centriflo Membrane Cones (CF 25). The concentrate was then centrifuged through 5-20% isokinetic sucrose gradients according to Lawrence et al. (88) in a Beckman SW27 Rotor at 27,000 rpm for 26 to 30 hours.

(D) BIOPHYSICAL METHODS

(1) Sedimentation Velocity

Sedimentation velocity experiments were performed on a Beckman Model E Ultracentrifuge, equipped with a Schlieren optical system, operating at 48,000 rpm with a temperature of 20°C. All data were corrected for temperatures and buffer effects to yield $S_{20,w}$ values. The concentration of the samples were kept at 2-3 mg/ml of DNA.

(2) Circular Dichroism

The CD spectra of the chromatin, its subunits, native and spin labeled nucleosome core particles or reconstituted nucleosome complexes were recorded at room temperature with a Cary 61 Spectropolarimeter (88). The spectra were calculated, after correction for base-line deviation, in terms of ellipticity (deg-cm^2/decimole) on the basis

of DNA concentration.

(3) Thermal Denaturation

Thermal melting profiles of the samples were recorded with a Gilford Spectrophotometer (88), at a heating rate of 0.25°C/min. Derivative curves were calculated and normalized by a linear least square fit. The materials were dialyzed against 0.2mM EDTA, pH 7.0, prior to use in the thermal denaturation experiments.

(E) ESR SPIN LABELING STUDIES

(1) Preparation of Imidazole spin labels

The spin label, N-(2,2,5,5-Tetramethyl-3-carbonylpyrrolidine-1-oxyl)-imidazole, (IMDSL) was synthesized by G. Bartolini of

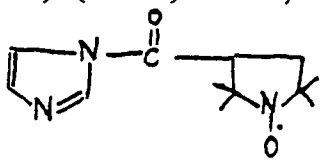

the Cancer Center of Hawaii, University of Hawaii, according to Adackaparayil and Smith (99). To 0.5mM of N-(2,2,5,5-Tetramethyl-pyrrolidine-1-oxyl)-3-carboxylic acid suspended in 10 ml of dry benzene was added 0.5mM of N, N'-carbonyldiimidazole. The mixture was stirred under N_2 for 2 hours. The solvent was removed under a stream of nitrogen and the residue crystallized twice from ether to give 68 mg (57%) of IMDSL: mp 128-129°C; IR (KBr) 1730, 1242 cm^{-1}.

(2) Competition of N-acetylimidazole and spin labeled imidazole

Histone core solutions were first reacted with varying amounts of non spin-labeled N-acetylimidazole for 2 hours at room temperature. Then a constant amount of imidazole spin label was further added to the previous reaction mixture; and the reaction was allowed to proceed for another hour. Unreacted reagents were removed by exhaustive

dialysis against 2M NaCl, 10 mM Tris HCl, 0.2 mM EDTA, pH 7.2.

(3) Labeling of histone protein cores and nucleosome core particles

Histone core solutions were labelled at 0.6 mg of protein/ml in 2.0 M NaCl, 10 mM Tris HCl, 0.2 mM EDTA, pH 7.2, with molar excesses of IMDSL to total tyrosine content. A stock solution of IMDSL at 5 x 10^{-2}M was prepared by dissolving the yellow IMDSL crystals in dry Toluene. Appropriate fractions of the IMDSL stock solution were carefully pipetted into test tubes and dried with N_2. Histone core solutions were then added quickly to the dried IMDSL crystals and stirred gently with a magnetic stirrer. The reaction was allowed to proceed for 2 hours at room temperature and 6 hours at 4°C. Unreacted IMDSL were removed by exhaustive dialysis against 2 M NaCl, 10 mM Tris HCl, 0.2 mM EDTA, pH 7.2 at 4°C or by passage through a 1 x 30 cm column of Sephadex G-25, equilibrated with 2 M NaCl, 10 mM Tris HCl, 0.2 mM EDTA, pH 7.2.

Nucleosome core particles were labeled in a same manner, at a concentration of 0.2 mg of DNA/ml, in 10 mM Tris HCl, 0.2 mM EDTA, pH 7.2, with molar excesses of IMDSL to total tyrosine content. Unreacted or hydrolyzed spin labels were removed by exhaustive dialysis or by passage through a 1 x 30 cm column of Sephadex G-25, equilibrated with 10 mM Tris HCl, 0.2 mM EDTA, pH 7.2.

(4) Labelling of nucleosome core particles in the presence of NaCl

Nucleosome core particles were labeled in a same manner except that the particles were previously partially denatured by dialysis against 10 mM Tris HCl, 0.2 mM EDTA, pH 7.2, containing various amounts

of NaCl. Unreacted reagents were removed by exhaustive dialysis against 10 mM Tris HCl, 0.2 mM EDTA, pH 7.2, without NaCl.

(5) Urea and Ionic Effects on the spin labeled histone core and nucleosome

A large quantity of histone cores were labeled with molar excess of IMDSL. The unreacted IMDSL were removed by passing through a 1 x 30 cm column of Sephadex G-25. Usually, 20% of the tyrosyls were labeled. Fractions of 0.5 ml each of the spin labeled histone cores were dialyzed against 250 ml of 10 mM Tris HCl, 0.2 mM EDTA, pH 7.2, containing various amounts of Urea (1 M to 10 M urea). After 12 hours dialysis at $4^{o}C$, the samples were taken for ESR measurement.

Nucleosome core particles in 10 mM Tris HCl, 0.2 mM EDTA, pH 7.2 were labeled in a similar manner. After the removal of the unbound spin labels (usually 12% of the tyrosyls were labeled), fractions of 0.5 ml each of the spin labeled nucleosome core were dialyzed either in 250 ml of 10 mM Tris HCl, 0.2 mM EDTA, pH 7.2, containing various amounts of Urea (1 M to 10 M), or in 500 ml of 10 mM Tris HCl, 0.2 mM EDTA, pH 7.2 containing various amounts of NaCl (0.5 mM to 2.5 M). The samples were taken for ESR measurement after 12 hours dialysis.

(6) Reconstitution of spin labeled nucleosome complexes

Native nucleosome core particles at 0.2 mg/ml of DNA were dissociated by dialysis against 10 mM Tris HCl, 0.2 mM EDTA, pH 7.2, containing:

(a) 2 M NaCl,

(b) 2 M NaCl, 4 M Urea,

or (c) 2 M NaCl, 6 M Urea,

respectively, at $4^{o}C$ for more than 12 hours. Various amounts of molar

excesses of IMDSL crystals were then added to the denatured nucleosome solutions in corresponding buffers respectively. The reactions were allowed to proceed for 2 hours at room temperature and 2 hours at 4°C. The labeled mixtures were then reconstituted back by salt step-gradient dialysis as described in Chapter II, section C, part 4, of this dissertation. The final complexes were concentrated and centrifuged through a preformed 5-20% isokinetic sucrose gradients in an SW27 Rotor for 26 hours (88). Gradients were dripped from the bottom and fractions were analyzed by circular dichroism, thermal denaturation and ESR for their integrity of native structure. The denatured nucleosome solutions in 2 M NaCl, 6 M urea, 10mM Tris HCl, 0.2 mM EDTA, pH 7.2 were also reacted with various amounts of non-spin-labeled N-acetylimidazole and reconstituted back by salt step-gradient dialysis. The complexes were fractionated by the 5-20% isokinetic sucrose gradients and analyzed for nativity by sedimentation velocity, circular dichroism and thermal denaturation experiments.

(7) ESR spectroscopy

ESR spectra were recorded at room temperature with a Varian E4 ESR spectrometer operating at 9.5 GHz. Modulation amplitude was set at 4 Gauss. The concentration of the bound spin labels (and thus the concentration of the labeled tyrosine) was quantitated by double integration of the ESR spectra using the On-line V-72 Mini-Computer equipped with software in CLASS for computational analysis and interfaced to the ESR spectrometer. The spin lable, 2,2,6,6-tetramethyl-4-piperidinal-1-oxyl, (TEMPOL), was used as the standard to calibrate the bound spin concentration. For melting experiments, a Varian V-4540 Variable Temperature controller was used. The temperatures were calibrated with a copper vs. constantan thermocouple.

III. RESULTS

(A) NUCLEASE DIGESTIONS OF NUCLEI

(1) Micrococcal Nuclease digestions of nuclei

The kinetics of micrococcal nuclease digestion of DNA in rat liver nuclei were monitored by measuring the amount of DNA rendered acid soluble. There is a fairly linear rise in acid-soluble products and a limit is reached when 40% of the DNA has been digested, as shown in Fig. 2. At various points in the digestion of the nuclei, the digested products were analyzed by sedimentation on an isokinetic sucrose gradient. Typical results are shown in Fig. 3a and 3b respectively. It can be seen that at the very early stage of digestion, the chromatin has been cut into higher molecular weight multimers first. As digestion proceeds, the smaller fragments are increased with the consumption of the larger fragments. Up to 8 resolvable fractions are resolved on the isokinetic sucrose gradients for a typical 3 minute digested product (Fig. 3b).

The use of an isokinetic sucrose gradient provides better resolution than a simple linear gradient. It is especially designed to keep the sedimentation rate (of particles of a given density) constant throughout the length of the centrifuge tube. The gradients are made in such a way that the linear increase in the driving force acting on a particle with increasing distance from the center of the rotor is exactly compensated by an equivalent increase in the opposing forces of viscous drag and buoyancy (100). We have used the isokinetic sucrose gradients not just for preparative isolation but also for sedimentation analysis of the digested chromatin products.

The constancy of nucleosome sedimentation rates in

Fig. 2 Kinetics of Micrococcal Nuclease digestion

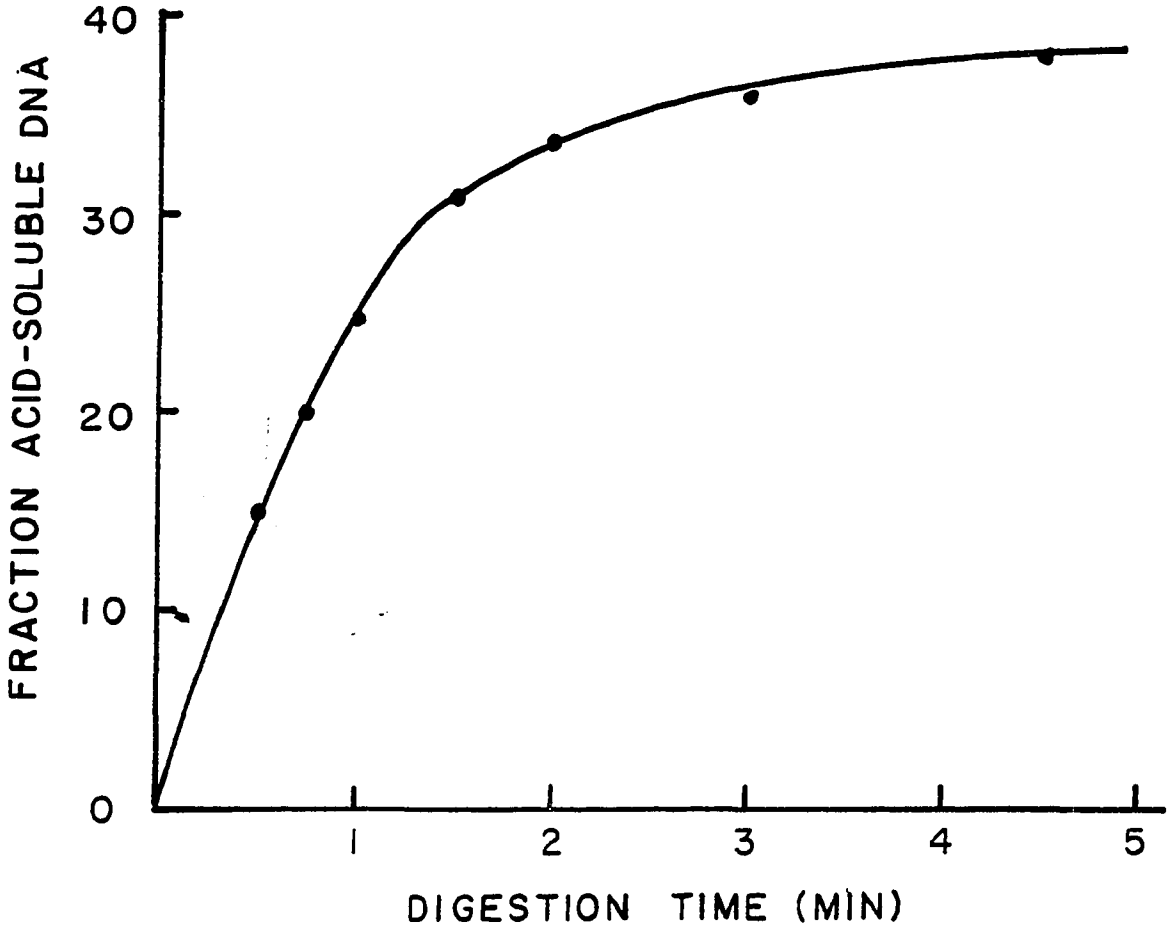
FRACTION ACID-SOLUBLE DNA
40
30
20
10
0
1
2
3
4
5
DIGESTION TIME (MIN)

Fig. 3 Fractionation Profile for the nuclease digested chromatin

Rat liver nuclei were digested with 300 U/ml of Micrococcal Nuclease for different length of time:

(A) _____ 30 sec.

- - - - - - - 45 sec.

_ . _ . _ . _ 60 sec.

(B) _____ 90 sec.

- - - - - - - - 120 sec.

_ . _ . _ . _ 180 sec.

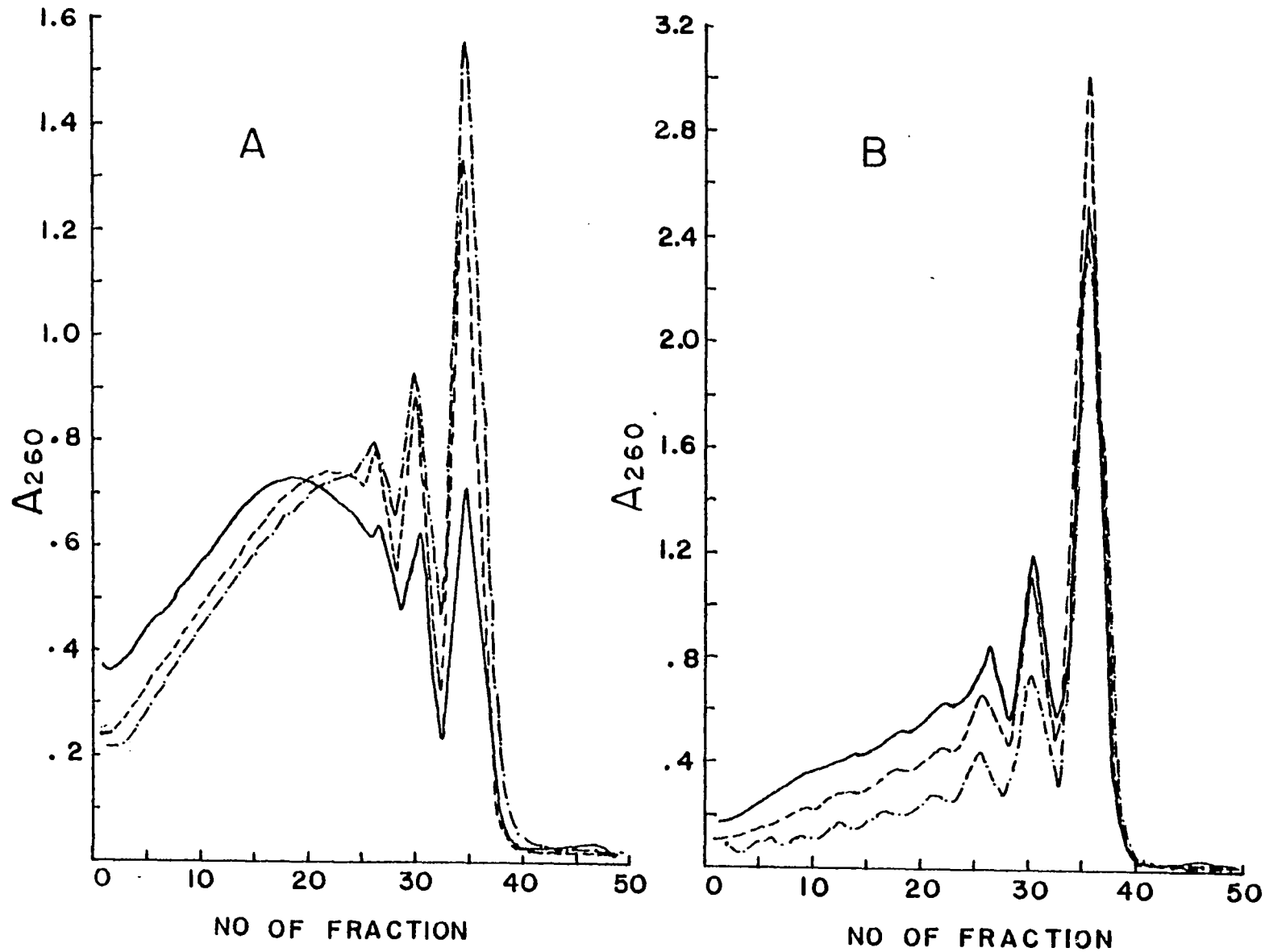
A
B
A260
NO OF FRACTION
1.6
1.4
1.2
1.0
.8
.6
.4
.2
3.2
2.8
2.4
2.0
1.6
1.2
.8
.4
0
10
20
30
40
50

the isokinetic sucrose gradients is tested by plotting the distance travelled by the various nucleosomal species against the corresponding sedimentation coefficients (So), a straight line is obtained, as shown in Fig. 4. The sedimentation coefficients of the chromatin subunits were obtained by Noll and Kornberg (95).

The size distribution of the DNA in the fractionated chromatin subunits was analyzed by polyacrylamide gel electrophoresis as shown in Fig. 5a, b. A straight line was obtained when the relative mobilities of the bands were plotted against the logarithm of the number of the corresponding subunits, as shown in Fig. 6, indicating that the molecular weight of the DNA fragments in the multimers is multiple of the molecular weight of the smallest species (the monomers). The size of the DNA in the mononucleosome was found to be 185 base-pairs in length, when x 174 RF DNA-Hae III digest (New England Biolabs) was used as a standard.

The histones from the subunits were analyzed by 18% polyacrylamide-SDS gel electrophoresis. The electrophoresis pattern of the rat histones is given in Fig. 7. All the histone fractions (H1, H2A, H2B, H3 and H4) were present in equimolar amounts in the subunits. The presence of the histone H1 indicates that the linker DNA in the mononucleosome or in the multimers has not been extensively degraded.

(2) Ca^{+2} , Mg^{+2} dependent Endogeneous Endonuclease digestions of rat liver nuclei

In order to analyze the distribution of the multimers at the early stage of digestion, rat liver nuclei were digested by the Ca^{+2} , Mg^{+2} dependent Endogeneous Endonuclease. Since there is

Fig. 4 Test for constancy of chromatin subunit sedimentation rates in an isokinetic sucrose gradient

Mobilities of chromatin subunit peaks determined from Fig. 3 are plotted against the sedimentation coefficient of the subunits.

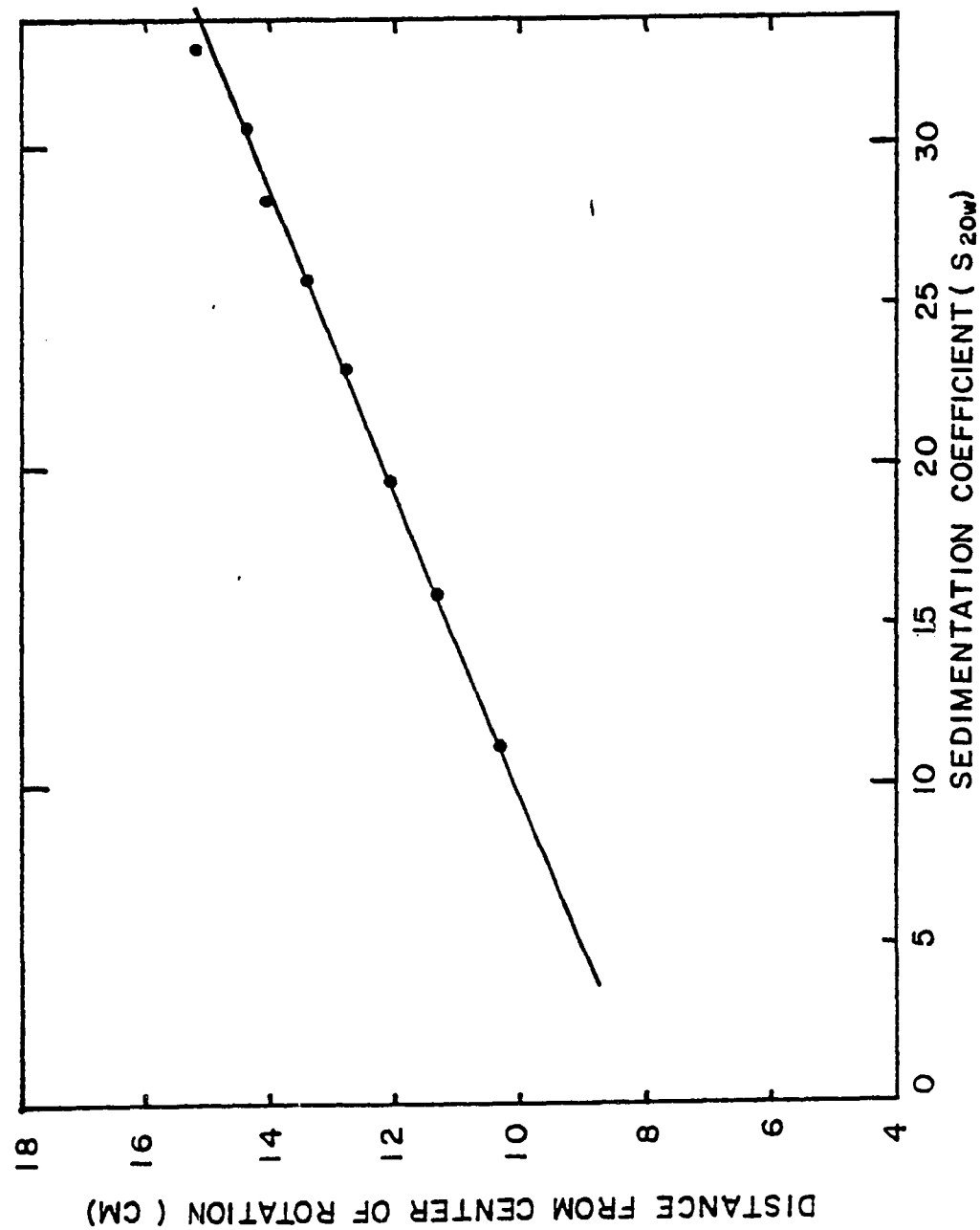
DISTANCE FROM CENTER OF ROTATION (CM)
18
16
14
12
10
8
6
4
0
5
10
15
20
25
30
SEDIMENTATION COEFFICIENT (S20w)

Fig. 5 Polyacrylamide gel electrophosesis for DNA extracted from chromatin and its subunits

C: Chromatin

C_1: Monomer

C_{1s}: Monomer

C_2: Dimer

C_3: Trimer

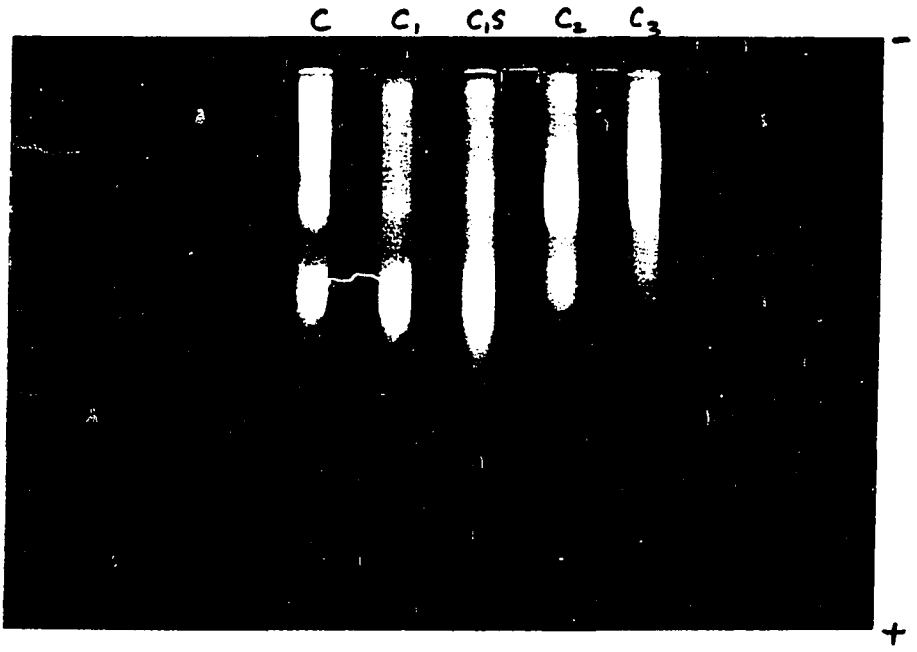
C
C1
C1S
C2
C3
-
+

Fig. 6 Mobility of the DNA extracted from chromatin subunits in the polyacrylamide gel

Number of chromatin subunits is plotted against the distance traveled by the corresponding DNA fragment in the polyacrylamide gel.

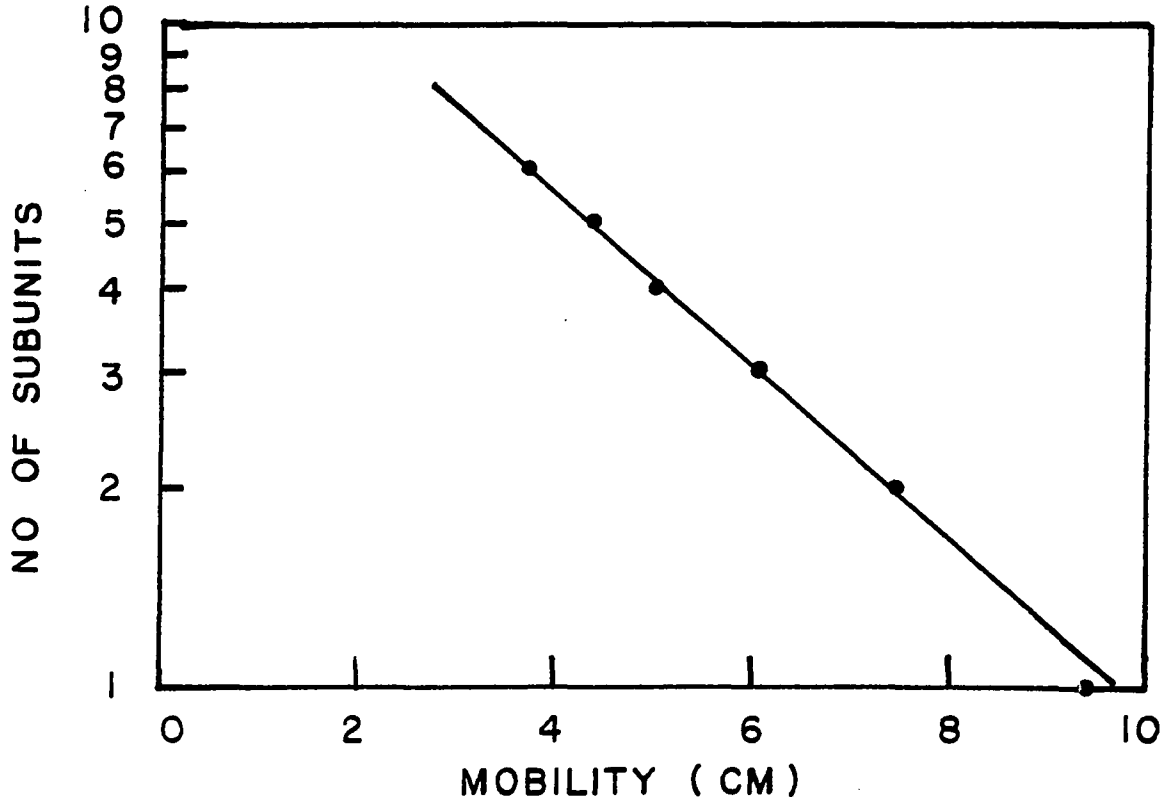
NO OF SUBUNITS
10
9
8
7
6
5
4
3
2
1
0
2
4
6
8
10
MOBILITY (CM)

Fig. 7 18% polyacrylamide-SDS gel electrophoresis for histones extracted from chromatin and its subunits

a) Chromatin

b) Monomer

c) Dimer

d) Trimer

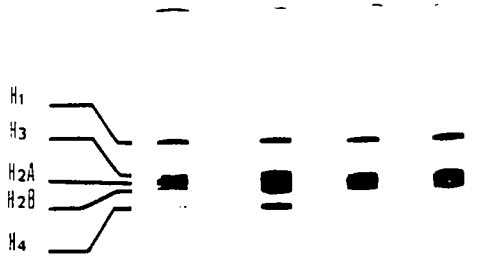

a b c d

same amount of the Endogeneous Endonuclease present in the nuclei, the only variables affecting the digestion will be the cations and the time of digestion. Thus, results are more reproducible.

The time course of digestion of the rat liver nuclei by the Endogeneous Endonuclease was analyzed by centrifuging the digested products on the exponential or isokinetic sucrose gradients as shown in Fig. 8a, b, c, d, respectively. It can be seen that the time scale of digestion by the Endogeneous Endonuclease is quite different from that of the Exogeneous Micrococcal nuclease. This may be due to differences in the nuclease concentration or in the specific activities of the two nucleases. It is obvious that chromatin is cut into smaller fragments, and finally into trimers, dimers and mostly monomers; and eventually, into the monomer core particles, as the limited digestion is reached.

When the large segments of the briefly digested products were analyzed by centrifuging through the steeper exponential sucrose gradients (non-isokinetics) a broad, Gaussian-like distribution curve was obtained. This suggests that a homogeneous species is dominant at each time interval of digestion. The weight average DNA size in each broad peak was analyzed by agarose gel electrophoresis, using the DNA fragments from the tetramer, trimer, dimer and monomer, as the standards. When the weight average number of subunits is plotted against the digestion time, a slowdown in the rate of change of chromatin fragments in the region of around six subunits is observed, as shown in Fig. 9. With longer digestion, the broad peak has shifted to smaller fragments, and finally into resolvable components (Fig. 8d). Comparing the digestion products from the Micrococcal Nuclease and

Fig. 8 Fractionation profiles for the rat liver Chromatin digested by the Mg^{+2}, Ca^{+2} dependent endogeneous endonuclease

The briefly digested chromatin was centrifuged through preformed different exponential or isokinetic sucrose gradients in an SW27 rotor at 27000 rpm for 20 hours. The absorbance for the fractions was monitored at λ = 260 nm.

(A) ——— 2.5 min. (B) ——— 10 min.
------ 5 min. ------ 15 min.
—·—·—·— 7.5 min.

(C) ——— 20 min. (D) ——— 20 hr.
------- 30 min. ------ 3 hr.
—·—·—·— 40 min. —·—·—·— 4 hr.
—··—··— 6 hr.

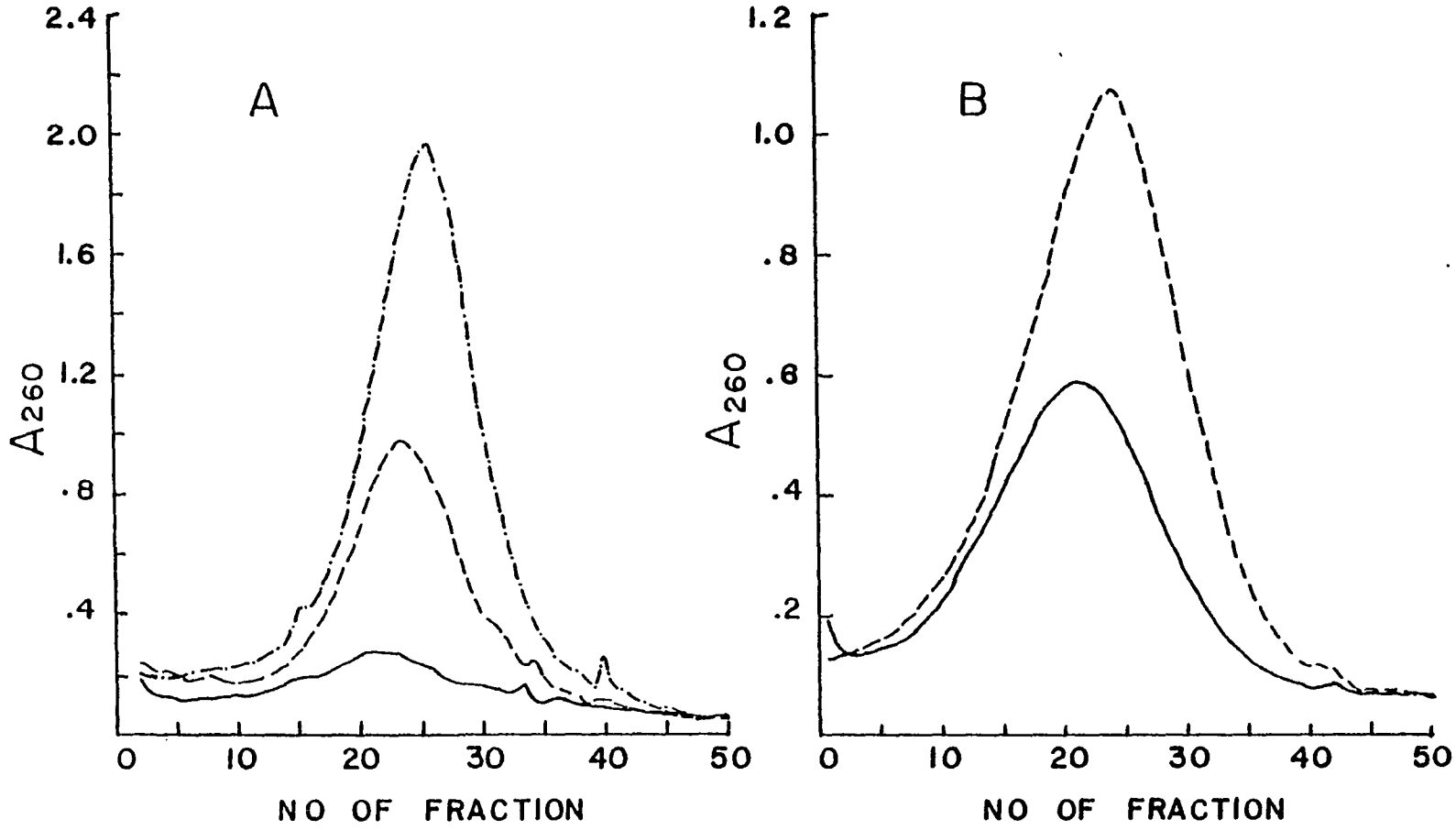
A
B
A_{260}
2.4
2.0
1.6
1.2
.8
.4
1.2
1.0
.8
.6
.4
.2
0
10
20
30
40
50
NO OF FRACTION

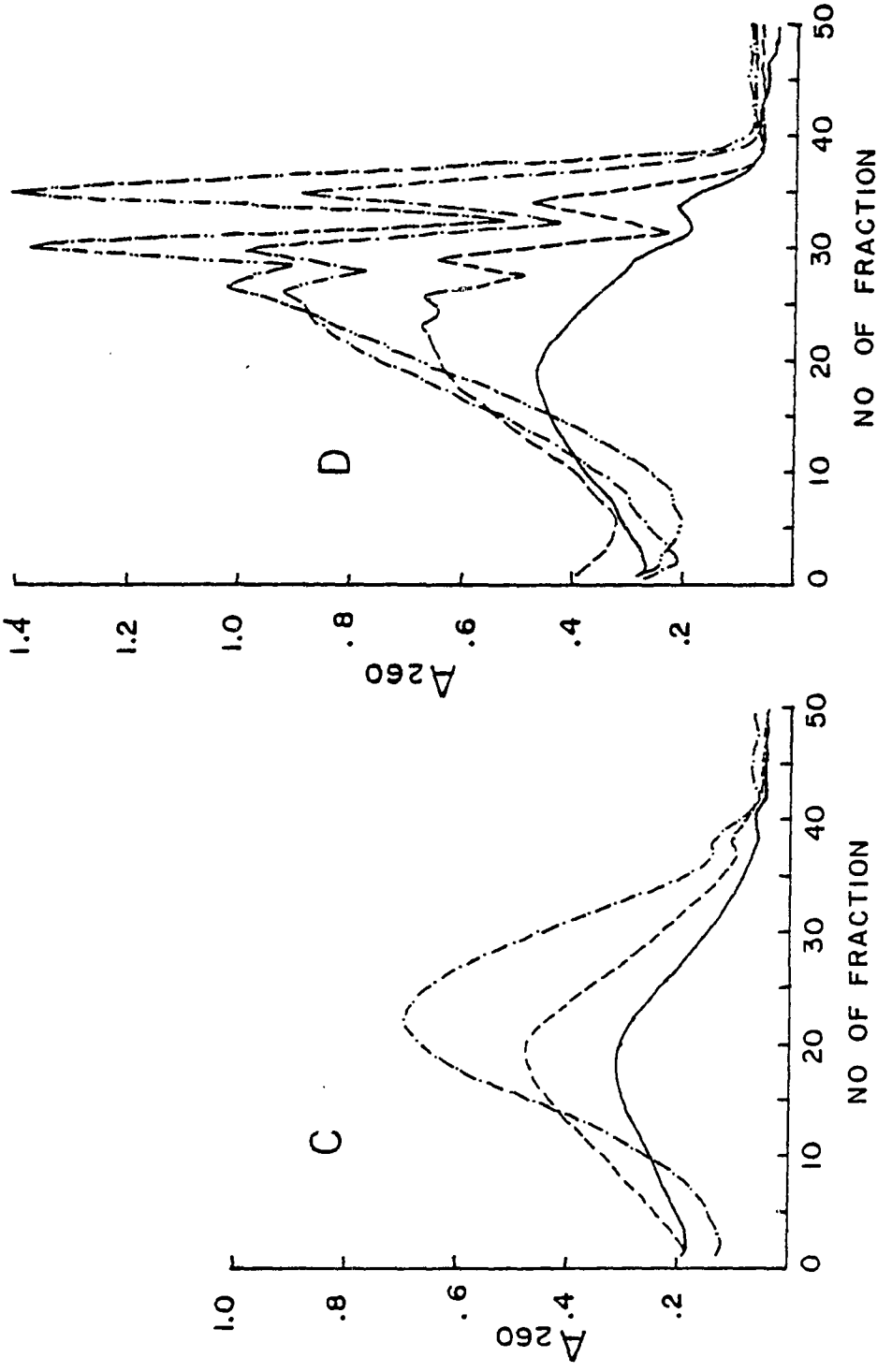
D
C
A260
NO OF FRACTION
1.4
1.2
1.0
.8
.6
.4
.2
0
10
20
30
40
50

Fig. 9 Weight-Average Number of chromatin subunits vs. Digestion time

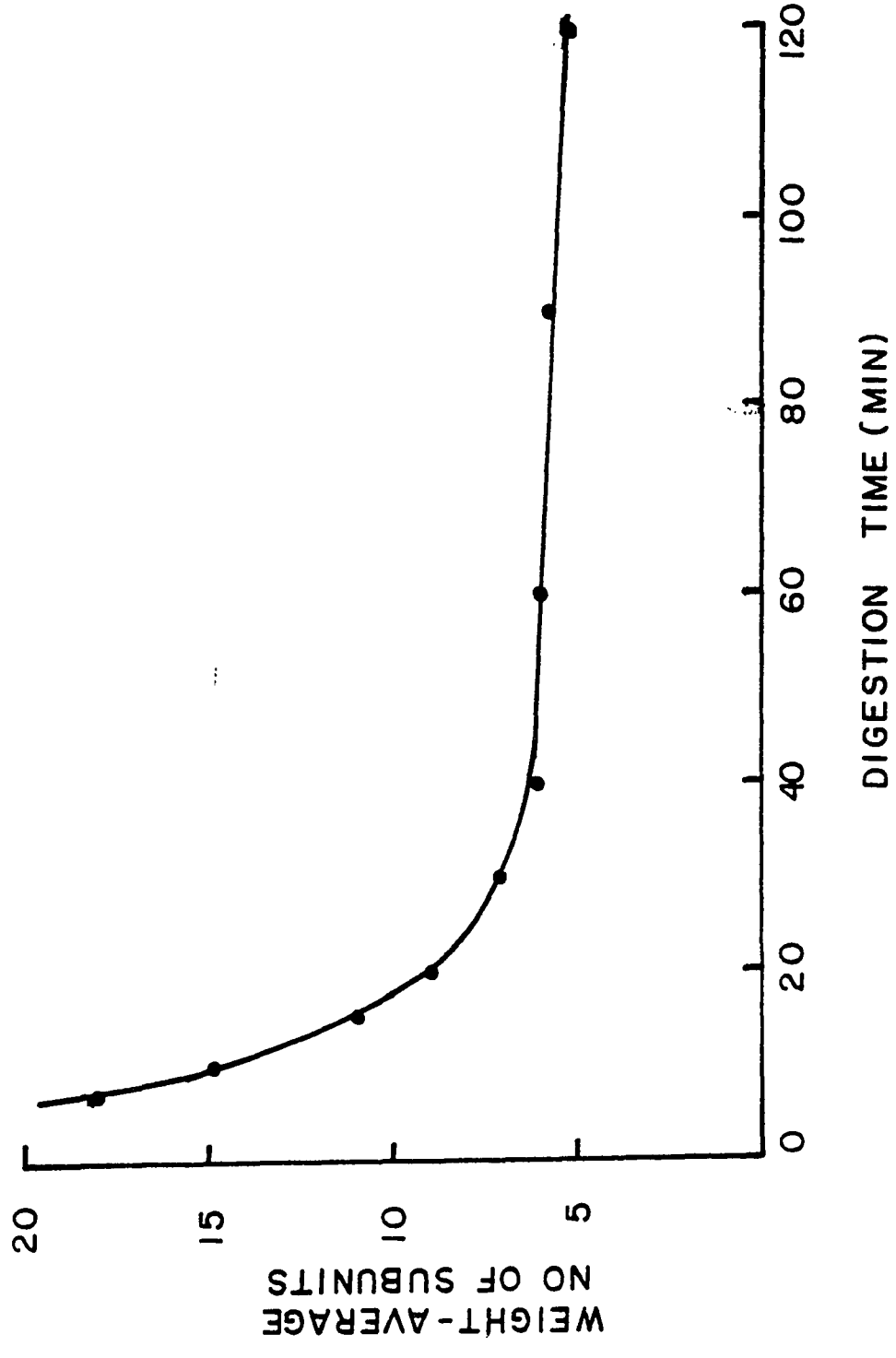
WEIGHT-AVERAGE
NO OF SUBUNITS
20
15
10
5
0
20
40
60
80
100
120
DIGESTION TIME (MIN)

the Endogeneous Endonuclease, we see that the fractionation pattern of the one-minute digestion by the Micrococcal Nuclease (Fig. 3a) is very similar to a six-hours digestion by the Endogeneous Endonuclease (Fig. 8d).

The observation of the slowing of the rate of change of the digested chromatin fragments at about six subunits may suggest that there is superstructural organization of the nucleosomes in the chromatin. It is possible that the nucleosomes are somehow organized into a chain of granular or knobby superstructures, with 6 to 8 subunits per superbead. It can be that the DNA between such superbeads is more susceptible to the Endogeneous Endonuclease than the linker DNA between the smaller subunits. Thus, the nuclease first cuts between the superbeads, relaesing an average of 6 to 8-subunit fragments, or multiple of these fragments; further digestion cuts between the subunits within the superbeads; and limited digestion degrades the mononucleosomes into the core particles of 140 base-pairs of DNA.

(B) CIRCULAR DICHROISM

Circular dichroism, the approach used in the present study of the conformation of chromatin and its subunits, is particularly advantageous in that the individual contributions of nuclei acids and proteins to the observed circular dichroism spectrum are easily separable due to differences in the wavelength of their absorptions. The two requirements necessary for optical activity (circular dichroism) are absorption and asymmetry. The four main bases (thymine, cytosine, adenine and guanine) in the DNA are the basic chromophores responsible for light absorption in the ultraviolet region. The main electronic transitions responsible for these absorptions are the $\pi \rightarrow \pi^*$ and $n \rightarrow \pi^*$

transitions. It is the asymmetric helical arrangement of these base-pairs in the nucleic acid chain which plays the most significant role in the CD spectra. More precisely, the circular dichroism of DNA is the result of the interaction of electronic transition moments and polarizabilities in one DNA base with bases asymmetrically arranged above and below it in the helical structure of the DNA. Consequently, the circular dichroism of any helical arrangement of a DNA polymer is due directly to the distance and angle between the transition moments and polarizabilities of any given base and bases above and below it in the DNA strucuture in question.

There are three kinds of asymmetry for the chromophoric moiety that can lead to circular dichroism (optical activity) in a native protein. First, the polypeptide chain is made up of L-residues, and the inherently asymmetry of the α carbons of the L-residues in the primary structure of the protein constitutes one source of optical activity. Second, the helical arrangement of residues in the secondary structures of the protein results in optical activity for electronic transitions either in the chain backbone or in helically arrayed side groups. Third, an asymmetric distribution of charge or dipoles about a chromophore, resulting from the rigid tertiary structure of a macro-molecule, can also provoke optical activity. The analyses of these sources can be divided into two approaches depending on the nature of the electronic transition. If the transitions have strong absorption bands (e.g. $\pi \rightarrow \pi^*$ transition), i.e., large electric transition dipole moments, rotational strength is derived in large measure from the dynamic coupling with electric transition dipole moments in vicinal chromophores. If the electronic transition in the inherently symmetric chromophore is of low absorption intensity and contains a substantial

magnetic transition dipole moment such as with $n \rightarrow \pi^*$ transitions, (corresponding to promotion of lone-pair electron of the peptide carbonyl oxygen atom into the π-system), a large rotational strength leading to strong optical activity is also derived. For example, in a helical peptide, there are three observable Cotton effects in the low ultraviolet: one, which is negative, comes from the $n \rightarrow \pi^*$ transition, a second, also negative, from the first (parallel polarized) limb of the $\pi \rightarrow \pi_{11}^*$ transition, and a third, which is positive, from the second (perpendicularly polarized) $\pi \rightarrow \pi_{1}^*$ transition (101-107,168).

X-ray analysis of DNA has demonstrated three canonical forms termed A, B, and C conformation (108). These forms differ in the number of residues per turn, pitch, translation per residue, angle between perpendicular to helical axis and bases, etc. (see Table I of this dissertation). These various forms can be obtained in oriented fibers of DNA under specific conditions of ionic strength and relative humidity. Under the same conditions, Tunis-Schneider and Maestre (103) found that each of the A, B, and C forms of the DNA had characteristic CD spectra: A form has a large positive peak at 270 nm and a small negative band at 235 nm; B form has a positive peak at 280 nm and a negative but equal amphitude peak at 245 nm; while C form has a very small positive band at 283 nm and two negative bands: one being small and one very large, at 295 nm and 245 nm, respectively. It is obvious that changes of the asymmetry of the DNA double strands without destroying the base-pairing, that is, by tilting the bases relative either to the vertical axis or to the horizontal axis, will cause different transition moment interactions and consequently changes in the CD spectra. Thus, if binding a protein to DNA causes a tightening of the DNA helix, or causes a twisting of the base, i.e., a con-

formational change, a different CD spectrum will be produced (103,105-107).

The analysis of CD spectra of protein has traditionally been based upon the standard circular dichroism arising from a protein or polypeptide in known α-helix protein in β-pleated sheet or protein in random coil configuration. The CD spectra of these three basic protein conformations are easily distinguishable, since the α-helix has two negative troughs at 222 nm and 208 nm and a positive peak at 191 nm; the β-pleated sheet has a negative band at 217 nm and a positive peak at 195 nm; while a random coil has a small positive peak at 217 nm and a large negative band at 197 nm (104,105,107). Thus, the basic CD spectra of DNA in its various forms, plus the basic protein CD spectra of the known secondary structures, are available to interpret the spectra of chromatin and its subunits. However, the complex spectra of chromatin and nucleosome are not so easily unraveled into its component parts.

The circular dichroism spectra of mononucleosome, dimer, trimer, tetramer, chromatin, and DNA extracted from the monomer, chromatin or in the commercial calf thymus DNA are given in Fig. 10 and Fig. 11, respectively. Purified calf thymus DNA shows a typical conservative CD spectrum corresponding to the B form DNA, namely, it has a positive band at 275 nm, a crossover point at 257 nm, and a negative band at 245 nm. The positive ($(\theta)_{275}$ = 8.8 x 10^3 deg-cm^2/decimole) and negative ($(\theta)_{245}$ = -10 x 10^3 deg-cm^2/decimole) bands in this spectrum are of approximately the same intensity and is termed conservative. The DNA extracted from

Fig. 10 Circular dichroism spectra at DNA band

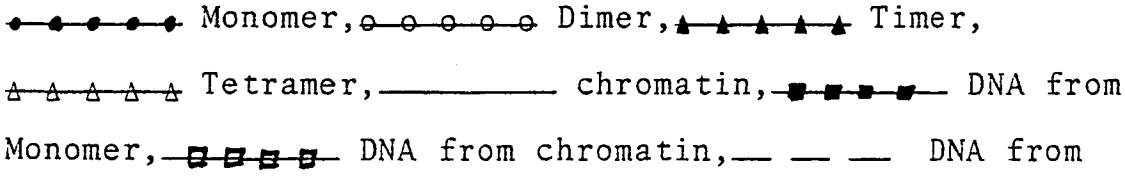

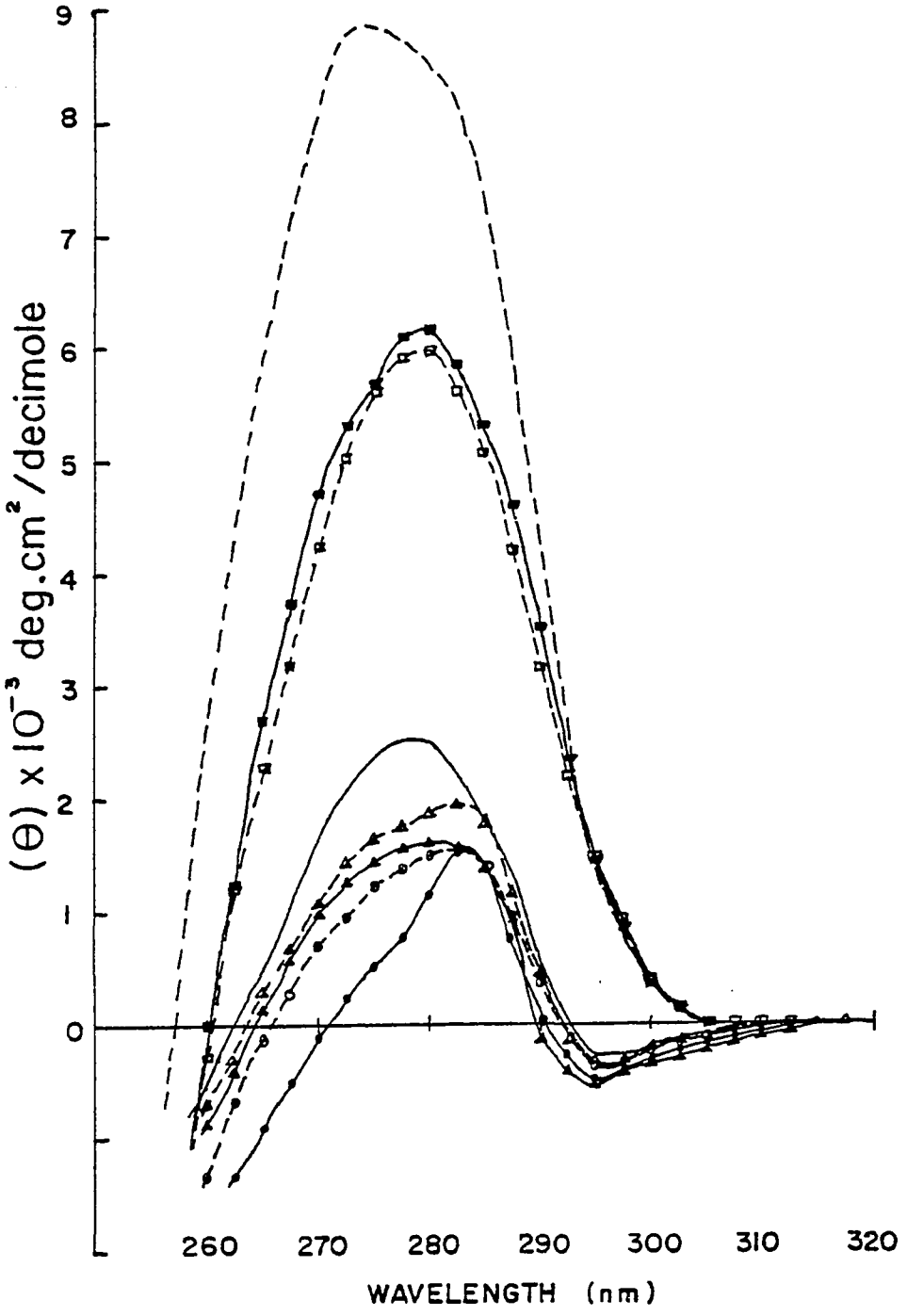
9
8
7
6
5
4
3
2
1
0
(θ) x 10⁻³ deg.cm²/decimole
260
270
280
290
300
310
320
WAVELENGTH (nm)

Fig. 11 Circular Dichroism spectra (320 nm to 210 nm)

———— Monomer, — — — Dimer, —·—·— Trimer,

. . . . Tetramer, —··—··—·· DNA from monomer.

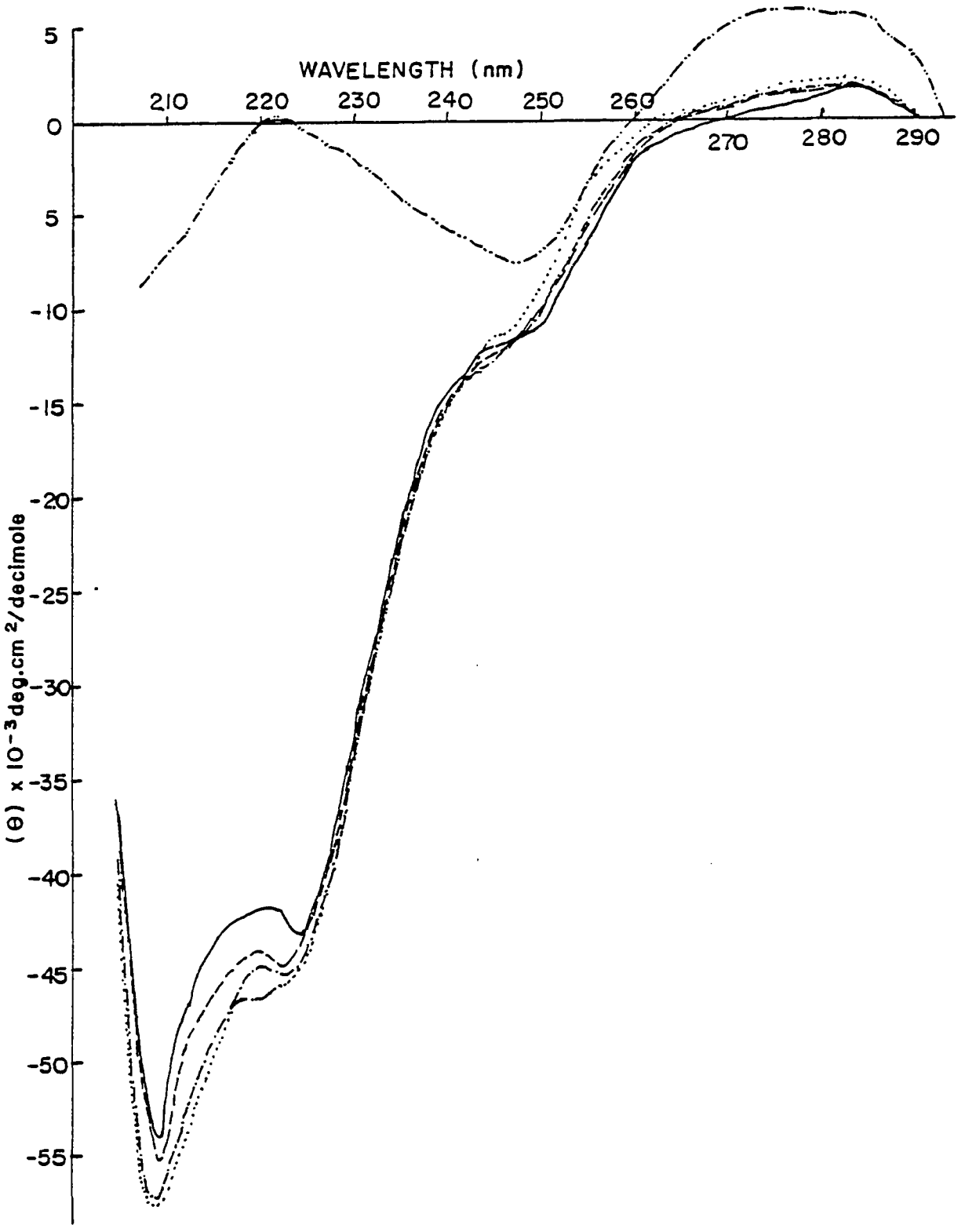
WAVELENGTH (nm)
210
220
230
240
250
260
270
280
290
5
0
5
-10
-15
-20
-25
-30
-35
-40
-45
-50
-55
(θ) x 10⁻³deg.cm²/decimole

the mononucleosome or chromatin gives a similar conservative CD spectrum, with $(\theta)_{280}$ = 6 x 10^3 deg-cm^2/decimole $(\theta)_{247.5}$ = -8 x 10^3 deg-cm^2/decimole, and crossover point at 260 nm. However, the CD spectra for chromatin and its subunits show that DNA in the presence of chromosomal proteins is considerably altered relative to the purified DNA in B form, as shown in Fig. 10. The positive band of DNA at 280 nm (6 x 10^3 deg-cm^2/decimole) is reduced to 2.5 x 10^3 or 1.5 x 10^3 deg-cm^2/decimole. A small negative band is found at 295 nm and the crossover point at 260 nm shows a red shift in the nucleosomes. The CD spectrum for the mononucleosomes is very similar to that for the purified DNA in C conformation (103). It is not yet known what structural changes of the DNA are responsible for the altered CD spectra of DNA in the nucleosome. Two possibilities are that (i) there is a conformational change of DNA due to the compact supercoiling of the DNA around the inner histone core or (ii) that there is a dehydration of the DNA due to intimate contact with the histones (109). When DNA is dissociated from the histone coil by the addition of sodium chloride, the DNA CD spectrum returns to that of purified DNA in B form, suggesting that it is the interaction between DNA and the histone core which is responsible for the altered CD spectrum in the nucleosome or chromatin. Ionic effects will be discussed in more detail later in this dissertation.

Upon assembly of the nucleosomes to form a chromatin fiber, the ellipticity of the positive band at 280 nm increases until the value of chromatin is achieved. When the ellipticity, $(\theta)_p$, at λ = 280 nm is plotted against the number of subunits, as shown in Fig. 12, we find that at least 8 nucleosomes are required to give the ellipticity of the chromatin. It has been suggested by us (88) and other investigators

Fig. 12 Ellipticity at λ= 280 nm vs. number of chromatin subunits

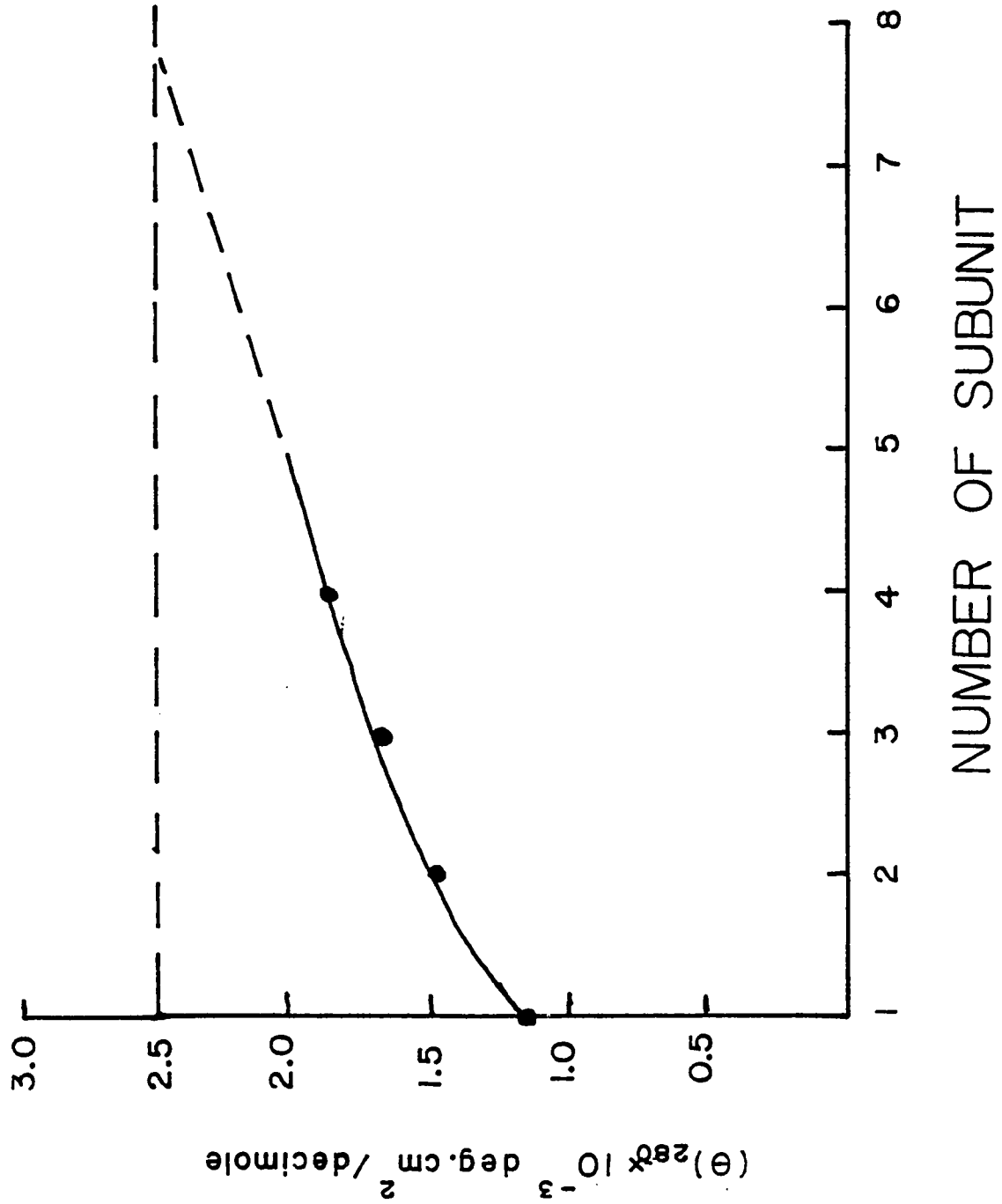
3.0
2.5
2.0
1.5
1.0
0.5
1
2
3
4
5
6
7
8
NUMBER OF SUBUNIT
$(\Theta)_{280} \times 10^{-3}$ deg. cm^2/decimole

(110) that the nucleosomes are probably assembled in an asymmetric fashion, that is, a superhelical array, giving an enhanced ellipticity in the chromatin. It is interesting to see, then, that the superhelical folding of the DNA in the individual nucleosome gives rise to a CD contribution of opposite sense than that found for the superhelical assembling of nucleosomes in the chromatin fiber.

Histones in the chromatin or nucleosomes contain considerable secondary structures as shown in the circular dichroism spectra (Fig. 11). Two negative troughs are found at 222 nm and 208 nm, this suggests a high degree of α-helical content in the histone core. No accurate or actual amount of the α-helical content can be calculated from the CD spectra due to the overlapping contributions from the DNA in the circular dichroism. However, recent laser Raman Spectroscopy studies (111) show that chromatin or histone core contains approximately 50% α-helix, 40% random coil and 10% β-sheet.

(C) THERMAL DENATURATION

Thermal denaturation has been extensively used to study the helix-coil transition in DNA, and as a tool to study the stability and structure of DNA (112), the extent and strength of binding of DNA to polypeptides and proteins (113), and as a probe of chromatin structure (114,115). Both the principles and the applications of thermal denaturation to the study of chromatin structure have been reviewed recently (116). In most of the studies, the thermal transition has been monitored by observing the increase in absorption (hyperchromicity) accompanying the helix-to-coil transitions in DNA. A biphasic melting profile for nucleoprotein complex has been reported (89,112-116). It is suggested that the first transition of the biphasic profiles obtained

by the usual procedure is due to partial DNA strand separation in those regions of the chromatin which become less well protected by histones during the heating process. The melting temperature for the second transition of the biphasic profile for the chromatin is much higher than that for purified DNA in the same buffer system.

The thermal stabilization of DNA within the chromatin strongly reflects the partial neutralization of the negative charges on the DNA backbone by the positive charges introduced by the histones. Presumably, the close proximity of positive charges in the histones to the negatively charged phosphates in the DNA reduces the usual electrostatic repulsion between the two strands of the DNA double helix, so that higher temperatures are required for the double strands to be driven apart by thermal energy. It has been observed that the binding of nonhistone proteins (acidic proteins) to the purified DNA contribute little, if any, thermal stability to the DNA (116). This suggests that electrostatic interactions between histones and DNA usually are dominant in the thermal stabilization. A similar influence of ionic strength of solvent on stabilizing DNA against thermal denaturation has been reported (114). In fact, it has been found that the thermal stability of native DNA in dilute sodium salts of various acids is a function of the log of the sodium ion concentration, rather than the ionic strength of the medium (117).

The normalized melting profiles and their first derivatives for the rat liver chromatin and its subunits are given in Fig. 13. They are essentially monophasic. We do not detect any premelt regions, suggesting that the electrostatic stabilization of the DNA by nucleoproteins is evenly distributed along the chromatin fiber and its subunits, even

Fig. 13 Thermal Melting profiles for the chromatin and its subunits

(A) The DNA helix-coil transition in the samples monitored by a change in the absorbance at λ= 260 nm vs. increasing temperature. The hyperchromicity is normalized for a better comparison.

(B) Normalized first derivative curves ($\Delta A/\Delta T$) vs. increasing temperature; _____ monomer, __ __ __ Dimer, • • • • • Trimer, o o o o chromatin.

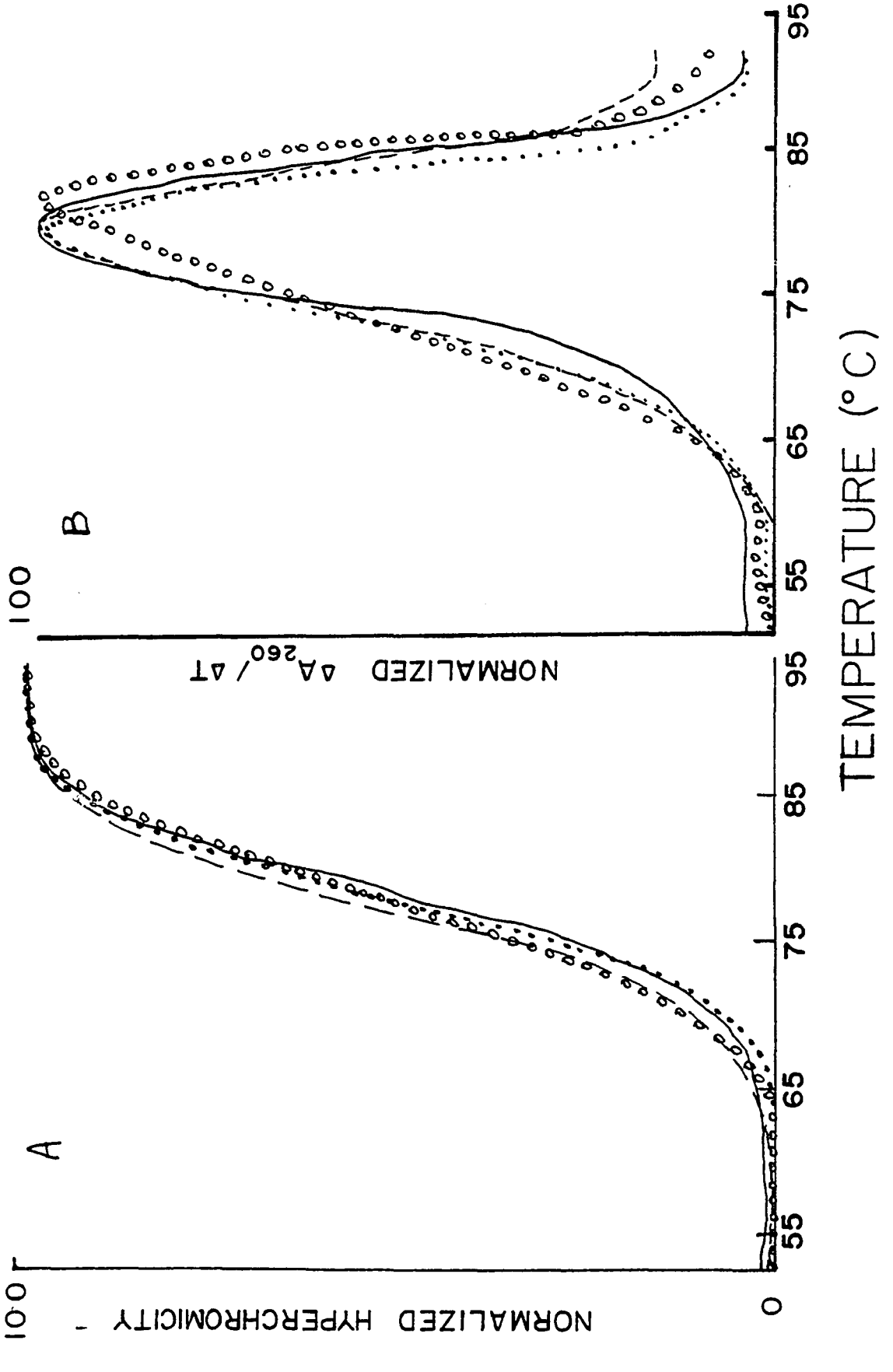
NORMALIZED HYPERCHROMICITY
100
0
A
55
65
75
85
95
NORMALIZED ΔA260/ΔT
100
B
55
65
75
85
95
TEMPERATURE (°C)

in the linker DNA region. This is consistent with a chromatin model proposed by Kornberg (3), that nucleosomes in native chromatin are closely bound to one another, leading to a rather continuous fiber structure. Monophasic melting profiles for chicken embryo chromatin and nucleosomes were also reported by other investigators (118,119). Wittig and Wittig (118) suggested that multiphasic or biphasic melting profiles were originated from in partially denatured nucleosomal material. However, we observed that the removal of histone H1 or H5 had produced biphasic profiles for the same material studied. This kind of biphasic profile for nucleosome core particles will be shown later in this report. Thus, we suggested that the presence of biphasic or multiphasic melting profiles would indicate that some segments of the DNA were not protected by the chromosomal proteins.

The melting profiles and their derivatives for monomer, dimer and trimer are very similar to each other (Fig. 13). The melting temperature is very close to each other also, only varies from 79°C to 80°C. The melting profile and its derivative for the chromatin, although monophasic, has a significantly broader width at the half height of the derivative curve, than for the subunits. Its melting temperature (82°C) is a little bit higher than the subunits (79°C). The broader derivative curve and a higher melting temperature for chromatin may indicate that there is an interaction between adjacent nucleosomes through protein-protein and protein-DNA interactions.

(D) ESR SPIN LABEL STUDIES

The study of the refined structure within the nucleosome and its protein core is of current interest and is the main aim of this dissertation. Selective chemical modification of proteins is one of the

most useful approaches for identification of functional amino acid residues in enzyme active site, delineation of surface topography, determination of the presence of residues invovled in subunit interactions, and evaluation of the presence of exposed and buried groups in the macromolecule (120,121). ESR spin labeling is one of such approaches and is very useful for probing the conformations of protein structures (122-127). The characteristics and sensitivity of the technique are such that binding of small spin-labeled molecules to macromolecules are readily deduced from a careful analysis of their ESR spectra. The spin label technique takes advantage of the fact that most nitroxide spin labels yield anisotropic ESR spectra as a result of either their structure or the environment in which they are attached and it is the change in this anisotropy that is correlated with the interactions being probed. In this dissertation, we want to demonstrate this powerful technique on studying the structures and conformational changes in the nucleosomes and histone protein cores.

(1) Characterization and comparison of native and spin labeled nucleosome core particles

When the H1, H5 depleted, limited digested chicken erythrocyte chromatin is fractionated through a 5-20% isokinetic sucrose gradient, in an SW27 Rotor for 24 hours at 27,000 rpm, the fractionation profile is shown in Fig. 14. The fractions for the mononucleosome peaks were pooled from several gradients and dialyzed against 10 mM Tris HCl, 0.2 mM EDTA, pH 7.2. The DNA was extracted and analyzed by 6% polyacrylamide slab gel, and was found to be 140 base-pairs in length, when Φx 174 RF DNA-Hae III Digest (New England Biolabs) was used as the standard. Histones from the histone core and from the nucleosome core

Fig. 14 Fractionation of nucleosome core particles

Large scale of nucleosome core particles were purified by centrifuging the limited digested chromatin through a 5-20% isokinetic sucrose gradient at 27000 rmp for 24 hours in an SW27 rotor.

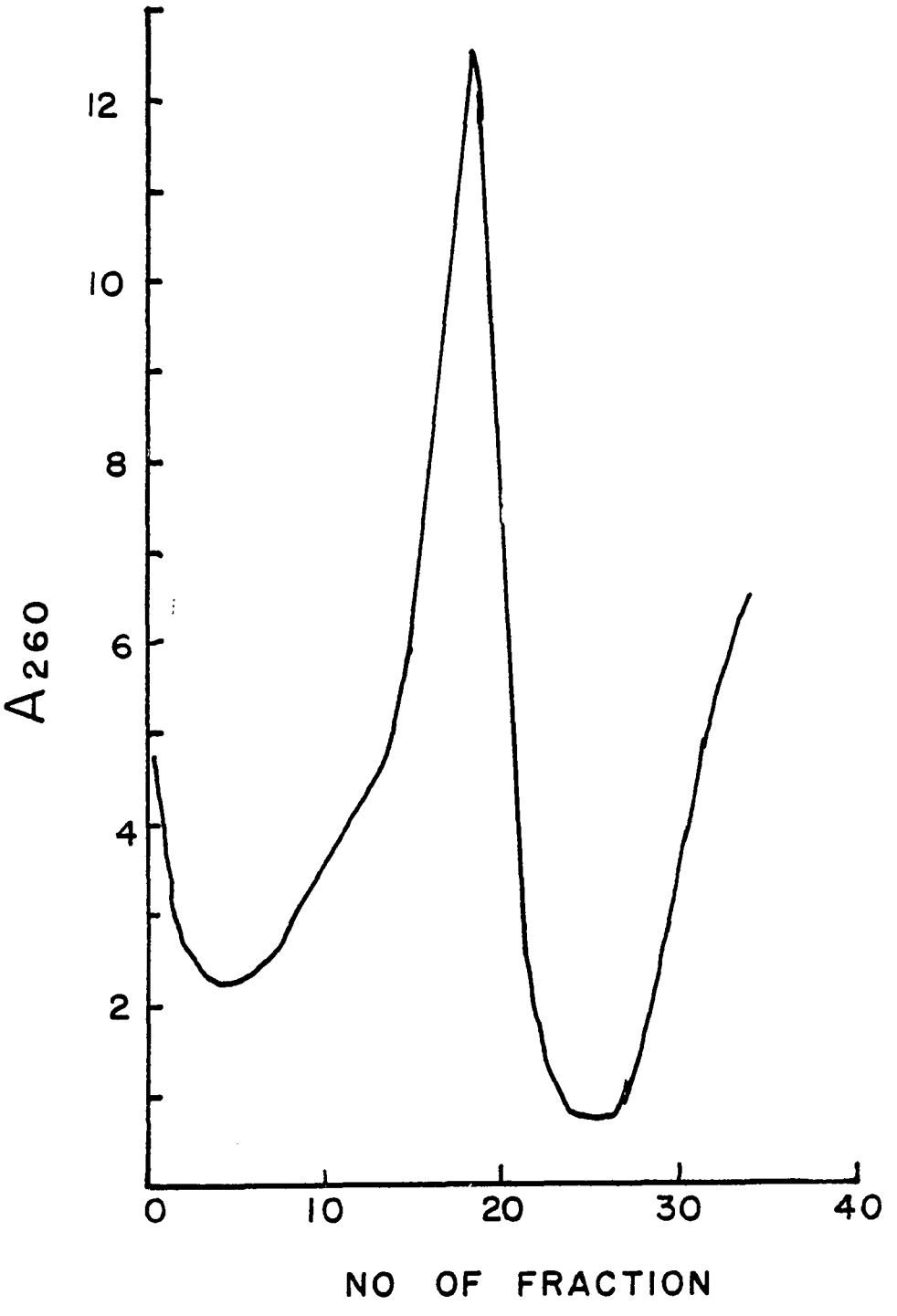
12
10
8
6
4
2
A260
0
10
20
30
40
NO OF FRACTION

particle when extracted and analyzed by SDS-18%-polyacrylamide slab gels, yielded equimolar amounts of histones H2A, H2B, H3 and H4. In both cases, no H1, H5 or nonhistone proteins were detected (Fig. 15a). The spin labeled histones gave a similar migration pattern on the SDS-18%-polyacrylamide gel (Fig. 15b).

Sedimentation velocity experiments were performed for both native and spin labeled nucleosome core particles, and an $S_{20,w}$ of 10.5 ± 0.2 S was measured in each case. A similar value was reported by several investigators (95,119) for the nucleosome core particle without H1. However, a higher value ($S_{20,w}$ = 11.2) was also reported by other investigators (89,94).

Fig. 16 shows the normalized first derivative of the thermal-denaturation profiles for native and spin-labeled nucleosome core particles. Both samples gave nearly identical, biphasic melting profiles, with a premelt region centered at 62°C and a main transition at 75°C. Upon denaturation, 34% hyperchromicity was found for the native nucleosome core particle, while 33% was found for the labeled core particle. Tatchell and Van Holde (89) have reported an identical biphasic melting profile for the nucleosome core particle extracted from chicken erythrocyte nuclei. Therefore, the monophasic melting profile we observed previously (88) for the rat liver nucleosome was possibly due to the presence of histone H1.

Fig. 17 shows the CD spectra of the native and spin-labeled nucleosome particles in 10 mM Tris HCl, 0.2 mM EDTA, pH 7.2. The ellipticity in deg-cm^2/decimole was calculated on the basis of DNA nucleotide concentration. Again, nearly identical CD spectra are obtained for both native and modified samples. Both CD spectra gave a

Fig. 15 18% polyacrylamide-SDS-gel electrophosesis of histones

(a) Extracted from the nucleosome core particle,

(b) Extracted from spin labeled nucleosome core particle.

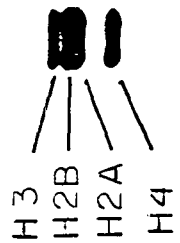

B

A

Fig. 16 Thermal denaturation profiles for the nucleosome core particles

(a) Native particle

(b) Spin labeled particle, and

(c) Reconstituted nucleosome core particle

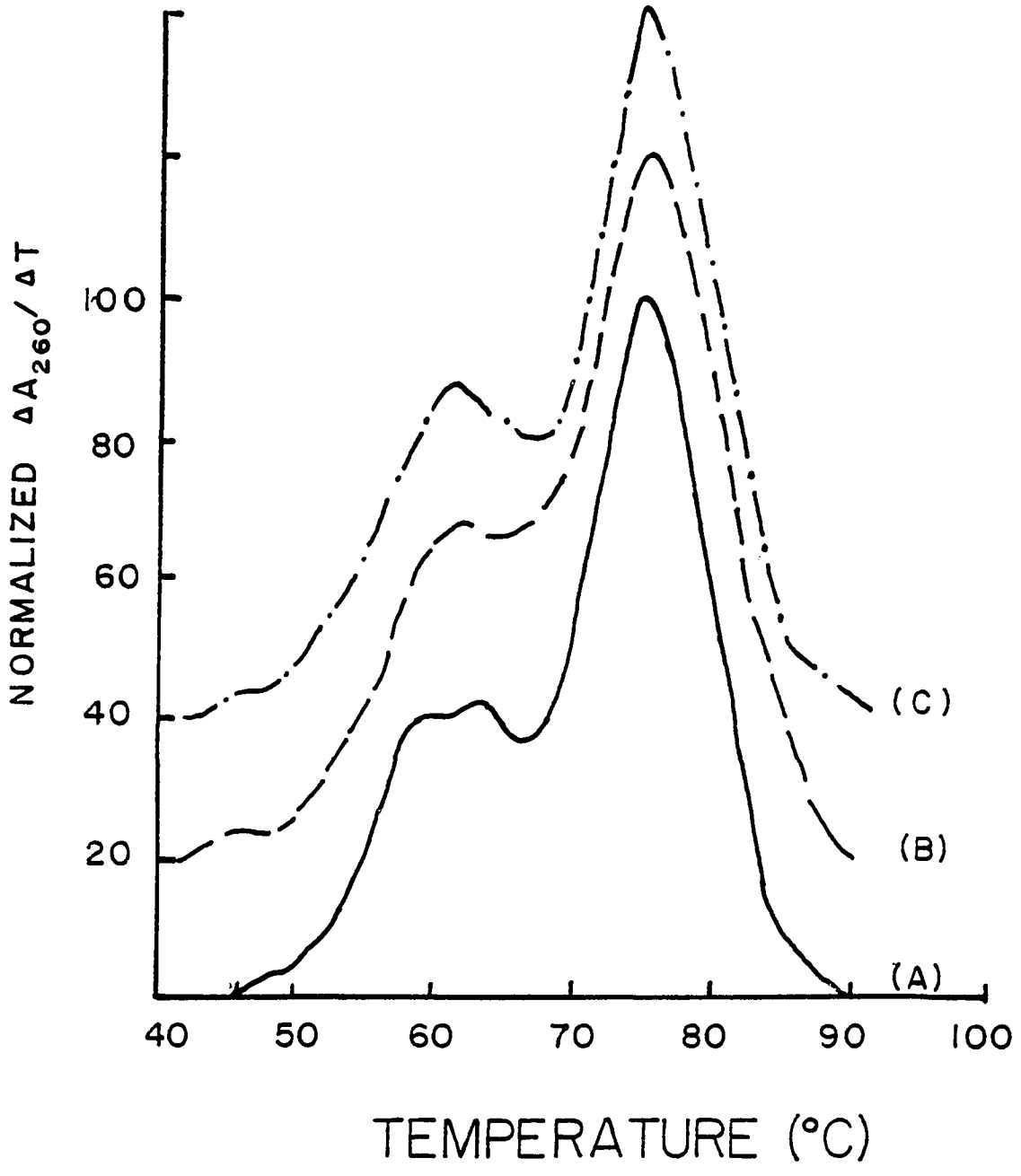
NORMALIZED ΔA260/ΔT
100
80
60
40
20
40
50
60
70
80
90
100
TEMPERATURE (°C)
(C)
(B)
(A)

Fig. 17 Circular dichroism spectra for the nucleosome core particle

_____ : nucleosome core particle,

_ _ _ : spin labeled core particle,

..... : reconstituted core particle

The ellipticity is calculated on the basis of DNA concentration.

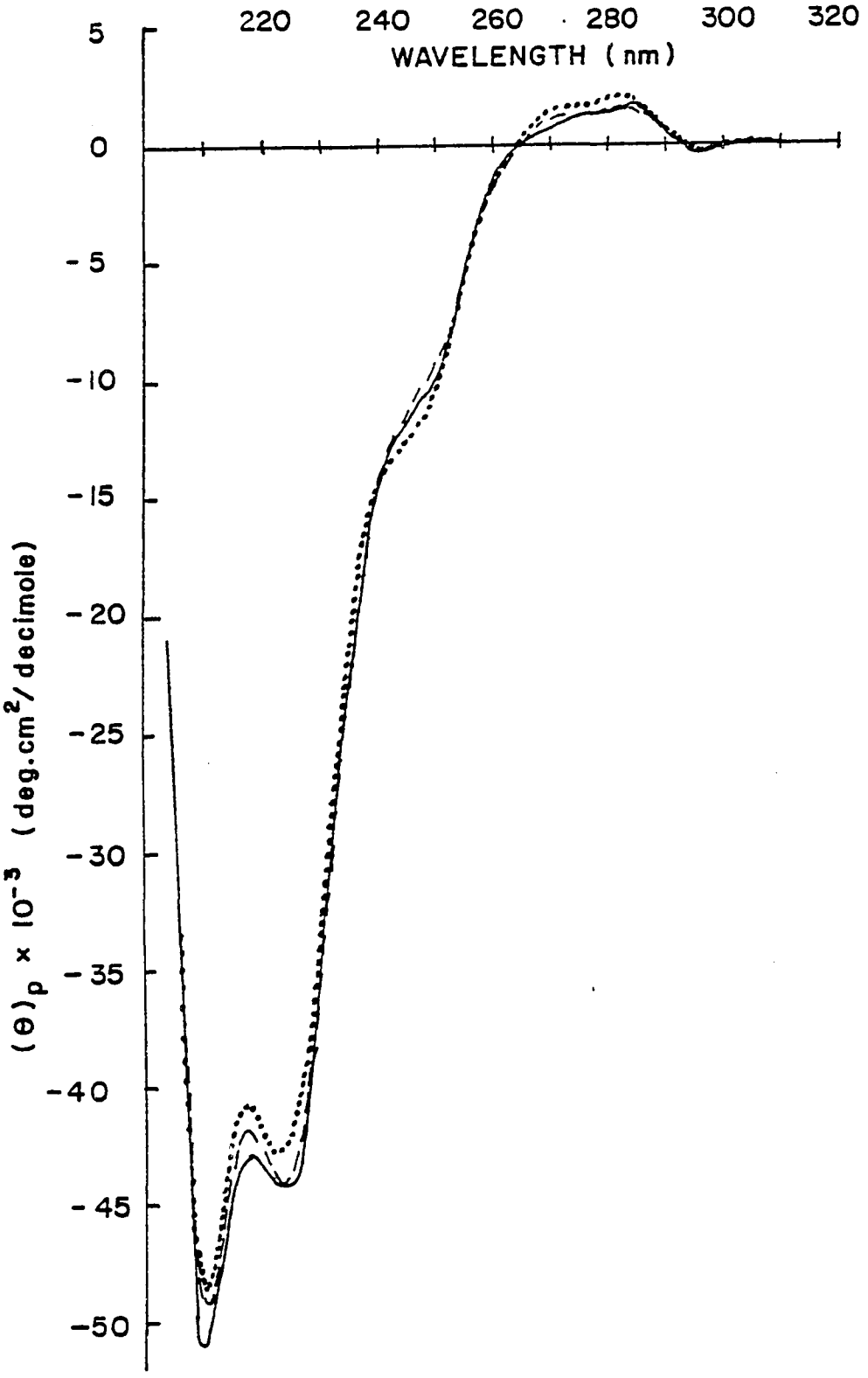
220
240
260
280
300
320
WAVELENGTH (nm)
5
0
-5
-10
-15
-20
-25
-30
-35
-40
-45
-50
$(\theta)_p \times 10^{-3}$ (deg.cm^2/decimole)

suppressed DNA ellipticity but a high α-helical band at 220 nm.

Based on the previous studies, we see that the sedimentation coefficient, the theraml denaturation profile and the circular dichroism are some of the important physical properties for judging the native structure for a nucleosome. Thus, from the above physical studies, we find that a spin labeled (10% tyrosyls) nucleosome core particle has retained a high degree of the native structure of the nucleosome core particle and we can conclude that our labeled nucleosome core can be used to study the conformational changes of the core structure in different solvent conditions, i.e., urea or NaCl, with the results being applicable to the native core particle itself.

(2) Accessibility and conformational states of the tyrosyl residues in the histone core and nucleosome core particle

N-acetylimidazole reacts with both amino and tyrosyl groups of proteins, but is more selective for tyrosine (120,121,128).

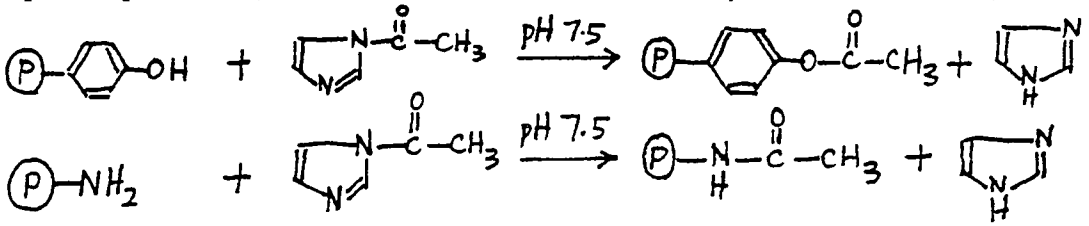

Under appropriate conditions, it has been shown to be specific for the acetylation of "free" tyrosyl residues in protein without affecting amino groups (128,129). Generally, the reaction between N-acetylimidazole with tyrosyl residues is followed by spectral changes at wavelength λ = 278 nm. But such method is not suitable for our system, due to the presence of DNA which has a high absorbance at λ = 278 nm also. A spin labeled imidazole can avoid such problem but maintain the selective reaction with tyrosyl groups. A spin labeled-imidazole can provide

information about the accessibility of the free and buried tyrosyl groups in the nucleosome core particle and also give the information about the conformational environment for the labeled tyrosyls.

An unsaturated N-(2,2,5,5-tetramethyl-1-pyrroline-oxyl)-imidazole has been synthesized and shown to be more specific for poly-L-tyrosine than for poly-L-lysine (130); however, this material was unstable and decomposed rapidly. The preparation and reactivity of a more stable N-(2,2,5,5-tetramethyl-3-carbonyl-pyrrolidine-1-oxyl)-imidazole (IMDSL) has been reported (131), and it is this derivative that has been used in this study. We have shown that this more stable IMDSL is competitive with the non-spin labeled N-acetylimidazole for the tyrosyl residues in the histone core, as shown in Fig. 18. The competitive binding plot shows that the preincubation of the histone core solution with increasing concentration of non-spin labeled acetylimidazole has considerably reduced the amount of tyrosyl groups available for the reaction with imidazole spin label added later. The concentration of the bound spin label (and thus the bound tyrosyls) can be accurately determined by double integration of the ESR spectra with the interfaced computer system. Integration of the conventional first derivative ESR spectrum gives the absorption spectrum and subsequent integration of the absorption spectrum gives a measure of relative concentrations. Figures 19 and 20 show the first derivative, absorption spectrum and its integrals for IMDSL at different immobilized conditions. The double integral values normalized by the spectral gain can be calibrated with respect to relative concentrations of spin labels present by double integrating the ESR spectra of a standard tempol spin label extinction coefficient $E_{242} = 1.44 \times 10^3$ in ethanol) at different concentrations. The standard

Fig. 18 Competitive Binding Plot for N-Acetylimidazole and Imidazole spin label for tyrosines in the histone core

The histone core solution (1 mg/ml) was reacted with varying amounts of N-Acetylimidazole for 2 hours before the addition of 1 mM of IMDSL. After the removal of unreacted imidazole by exhaustive dialysis, the central peak H_o, normalized by the Gain of the ESR spectra, is plotted against the initial N-Acetylimidazole concentration. The concentration of the tyrosine in the histone core was 3×10^{-3} M and the concentration of the IMDSL added was not in molar excess. Therefore, no competition between N-Acetylimidazole and Imidazole spin label was observed when the concentration of the N-Acetylimidazole was less than 2×10^{-3} M.

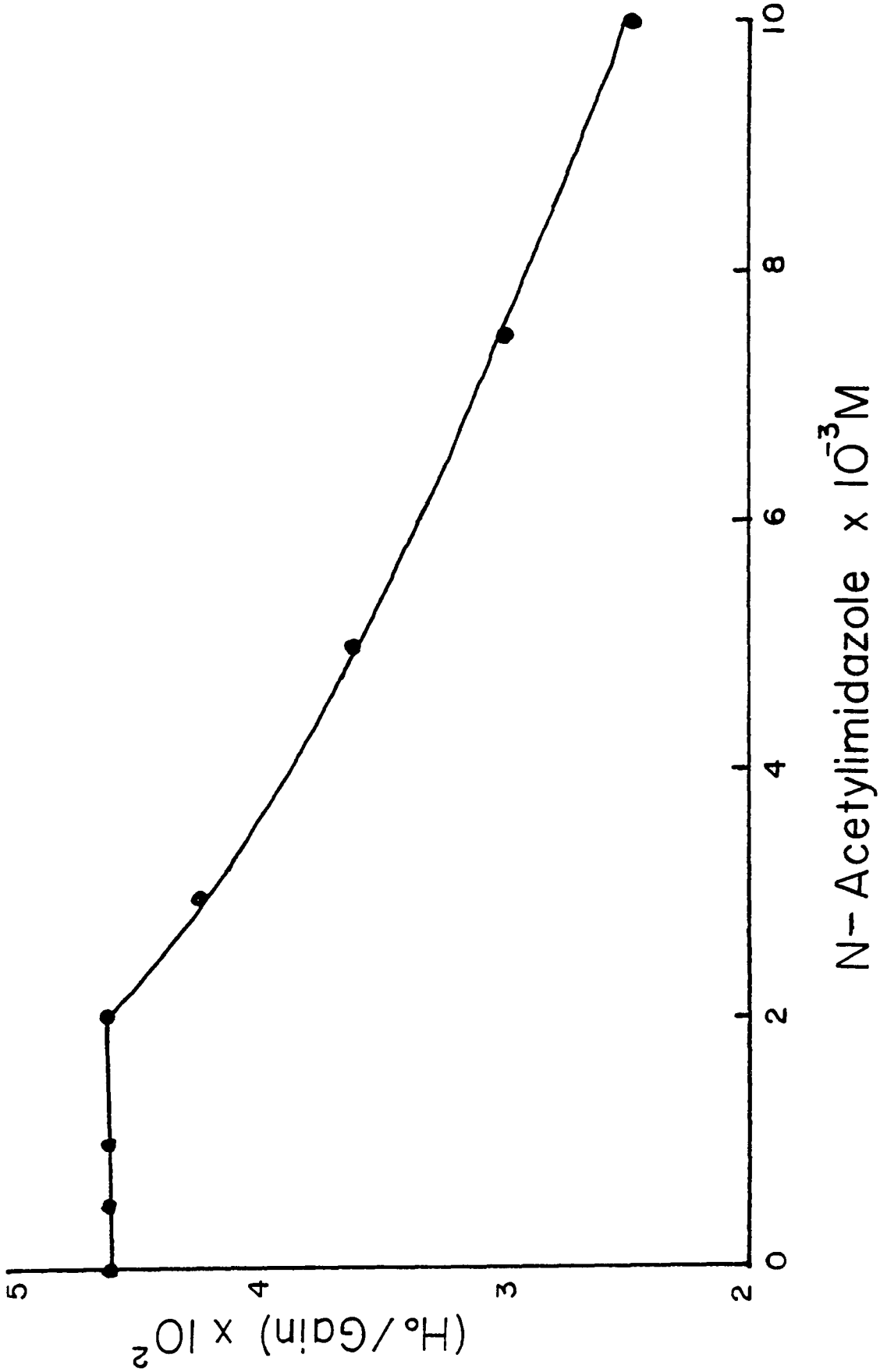
(H₀/Gain) x 10²
5
4
3
2
0
2
4
6
8
10
N-Acetylimidazole x 10⁻³M

Fig. 19 Integration of ESR spectrum of Freely Tumbling IMDSL in Toluene

(a) ESR spectrum

(b) Absorption Spectrum (first Integral)

(c) Second Integral

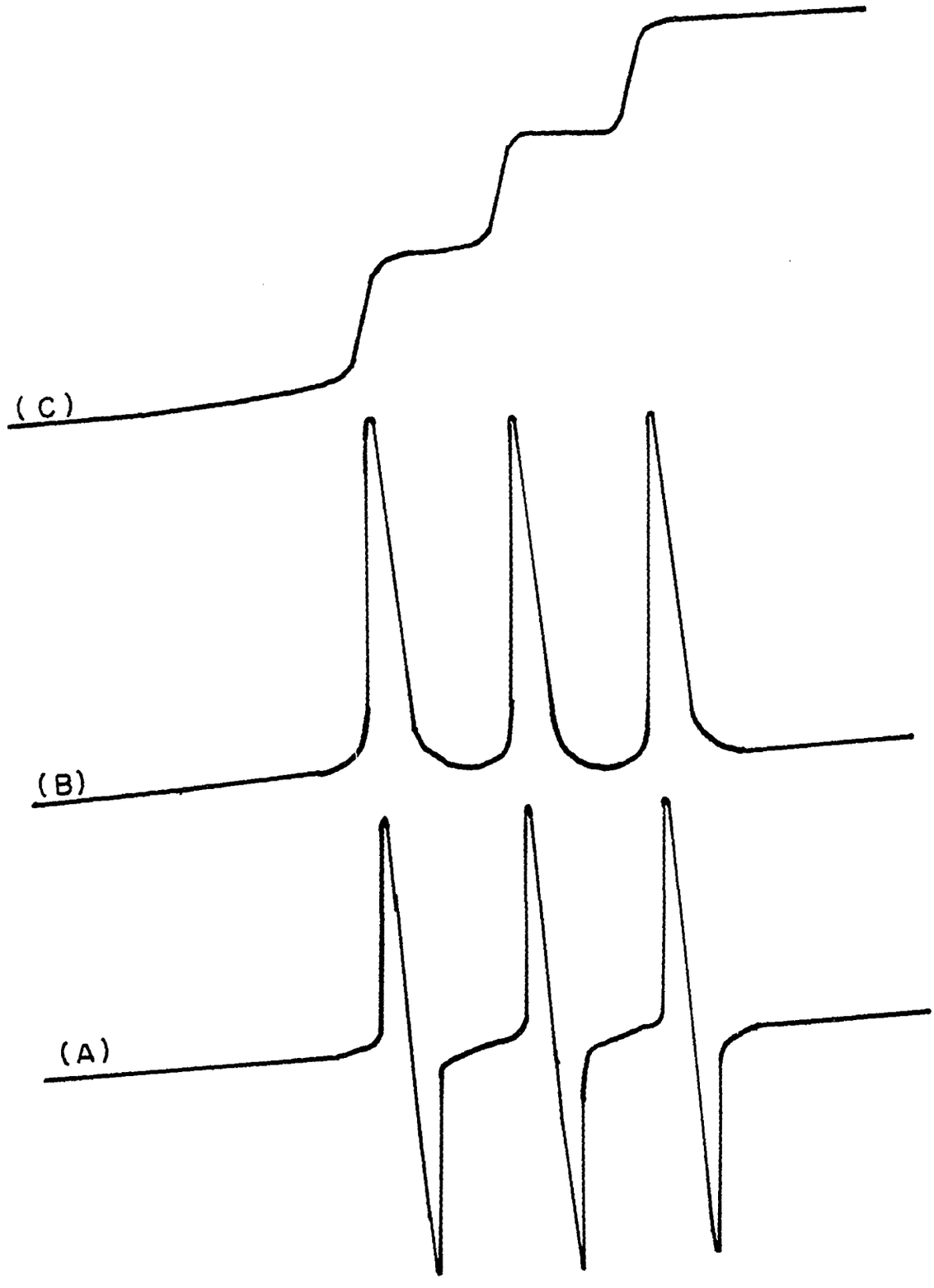
(C)
(B)
(A)

Fig. 20 Integration of the ESR spectrum of the partially immobilized IMDSL in histone core

(a) ESR spectrum

(b) First Integral

(c) Second Integral

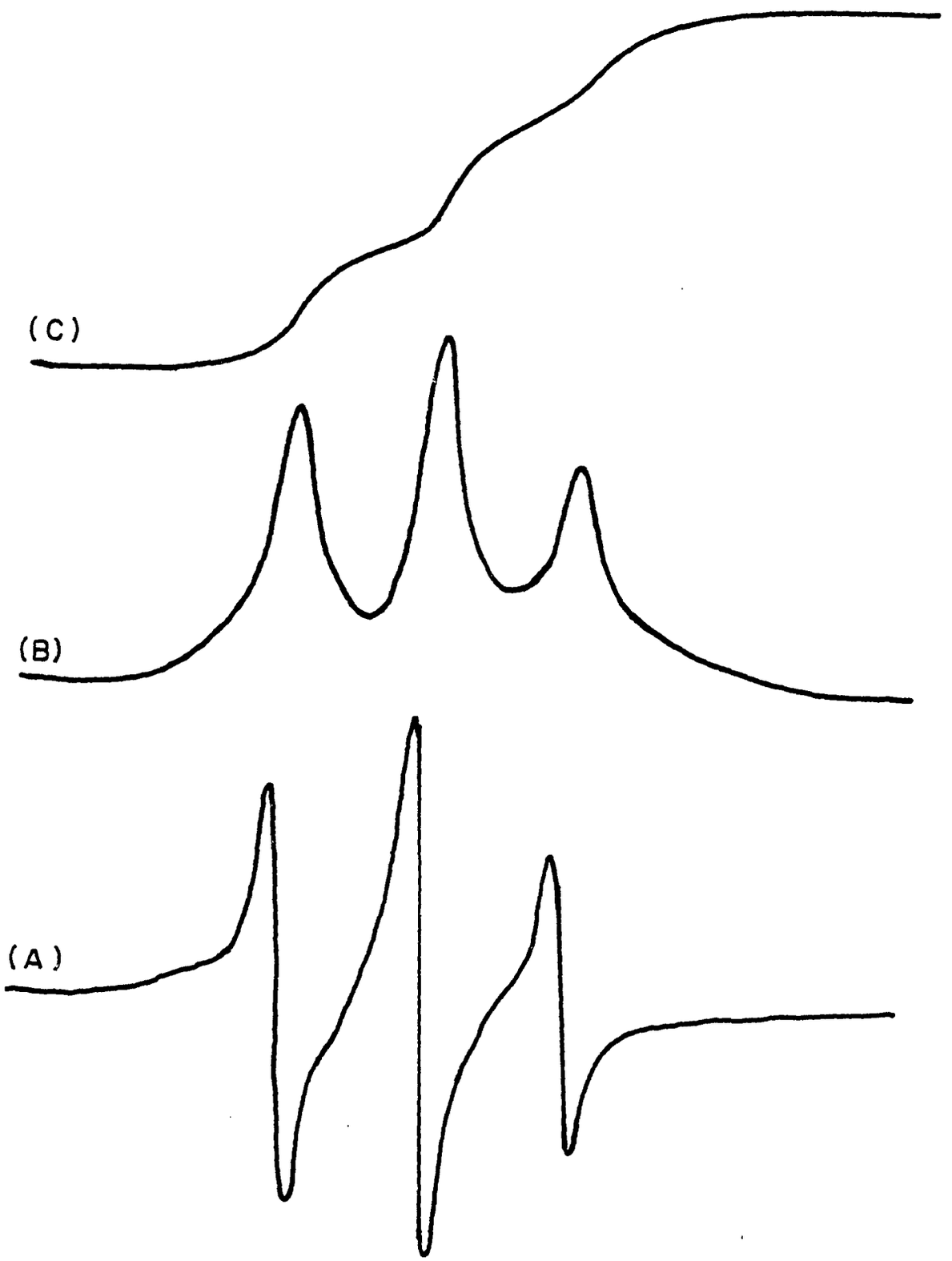
(C)
(B)
(A)

calibration curve obtained by this method is shown in Fig. 21.

When histone cores (without H1 or H5) in 2 M NaCl, 10 mM Tris HCl, 0.2 mM EDTA, pH 7.2, are reacted with various molar excess (1- to 300-fold) of IMDSL, and unbound spin labels removed by exhaustive dialysis, a binding profile is obtained as shown in Fig. 22a. At the highest labeling ratio, a maximum of about 40% of the tyrosyls are being labeled. This suggests that 12 out of the 30 tyrosyls in the histone core are accessible to IMDSL. A higher percentage of tyrosyls (~ 90%) can be labeled when the native histone cores are disrupted by adding urea, by lowering the ionic strength, or by vigorous stirring.

An ESR spectrum, for a histone core in 2 M NaCl, with 20% of the tyrosyls labeled, is shown in Fig. 23a. The histone core-SL shows a weakly immobilized three line spectra. The peak height ratio is $H_+/H_o = 0.67$ and $H_-/H_o = 0.40$ where H_+,H_o, and H_- are the derivative peak heights of the low, central, and high field lines, respectively. The rotational correlation time of 0.60 nsec for these weakly immobilized labels was calculated from the equation given by Likhtenshtein (124),

$$\frac{1}{\tau} = \frac{3.6 \times 10^9}{\left(\sqrt{\frac{H_o}{H_-}} - 1\right) \Delta H_o}$$

where ΔH_o is the width of the central component in Gauss, and H_+, H_o, and H_- are the derivative peak heights of the spectral components.

The spin labels attached at the tyrosyl residues appear to be in a hydrophilic environment and undergo rather free rotational motion. It should be noticed, however, that the environment for the spin-labeled tyrosyls in the histone core is quite complex and inhomogeneous. When the tertiary and secondary structures of the histone core

Fig. 21 Standard Calibration curve of the TEMPOL in ethanol

The relative concentrations of spin label were calculated from the double integral values, normalized by the Gain, of the ESR spectra.

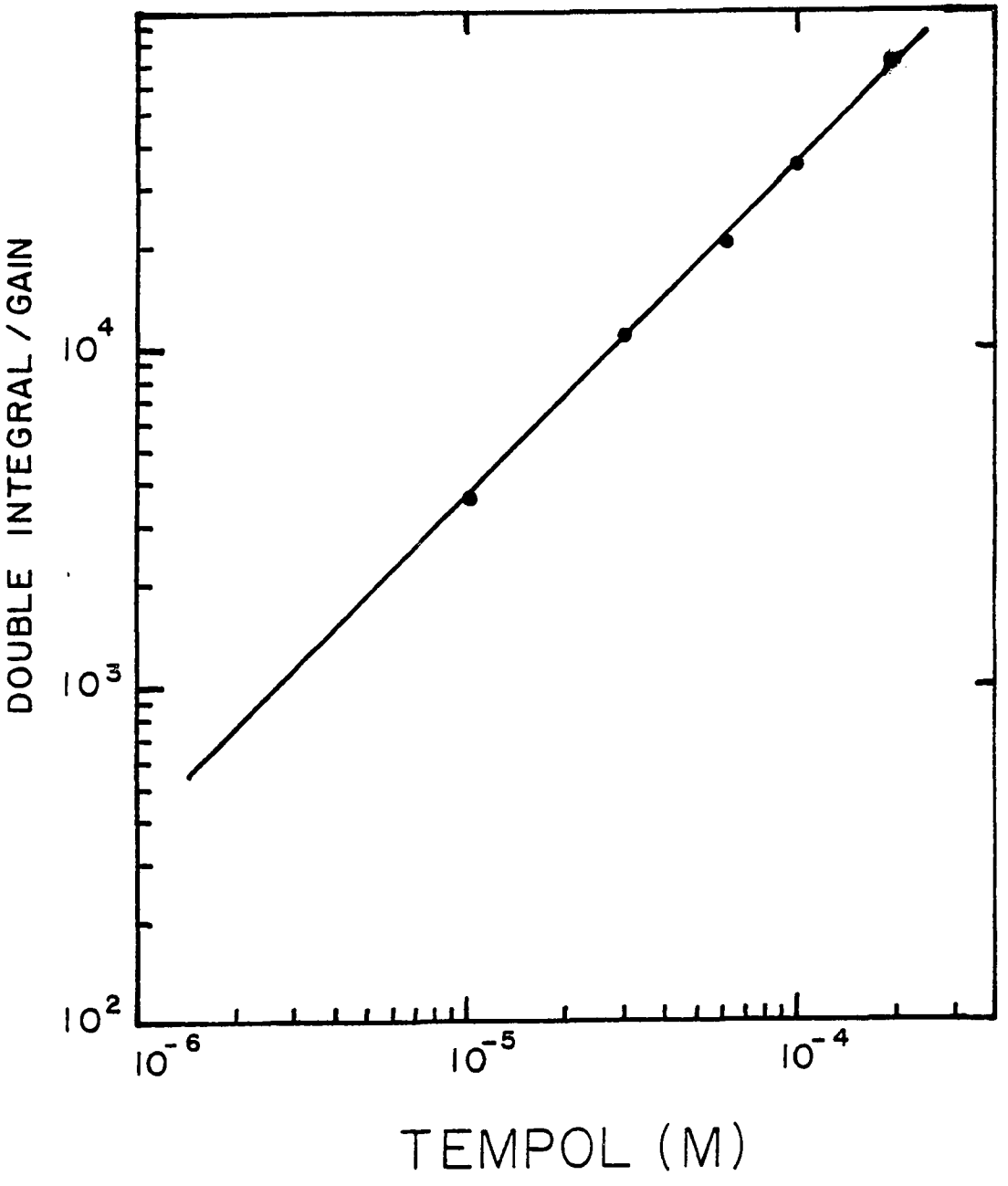
DOUBLE INTEGRAL / GAIN
10^4
10^3
10^2
10^{-6}
10^{-5}
10^{-4}
TEMPOL (M)

Fig. 22 Saturation Binding Plot of histone core and nucleosome core particle

Binding profile for (a) the histone core in 2 M NaCl, 10 mM Tris-HCl, 0.2 mM EDTA, pH 7.2 (_●_●_●_●) and (b) the nucleosome core particle in 10 mM Tris HCl, 0.2 mM EDTA, pH 7.2 (_o_o_o_o) with molar excess of IMDSL respectively.

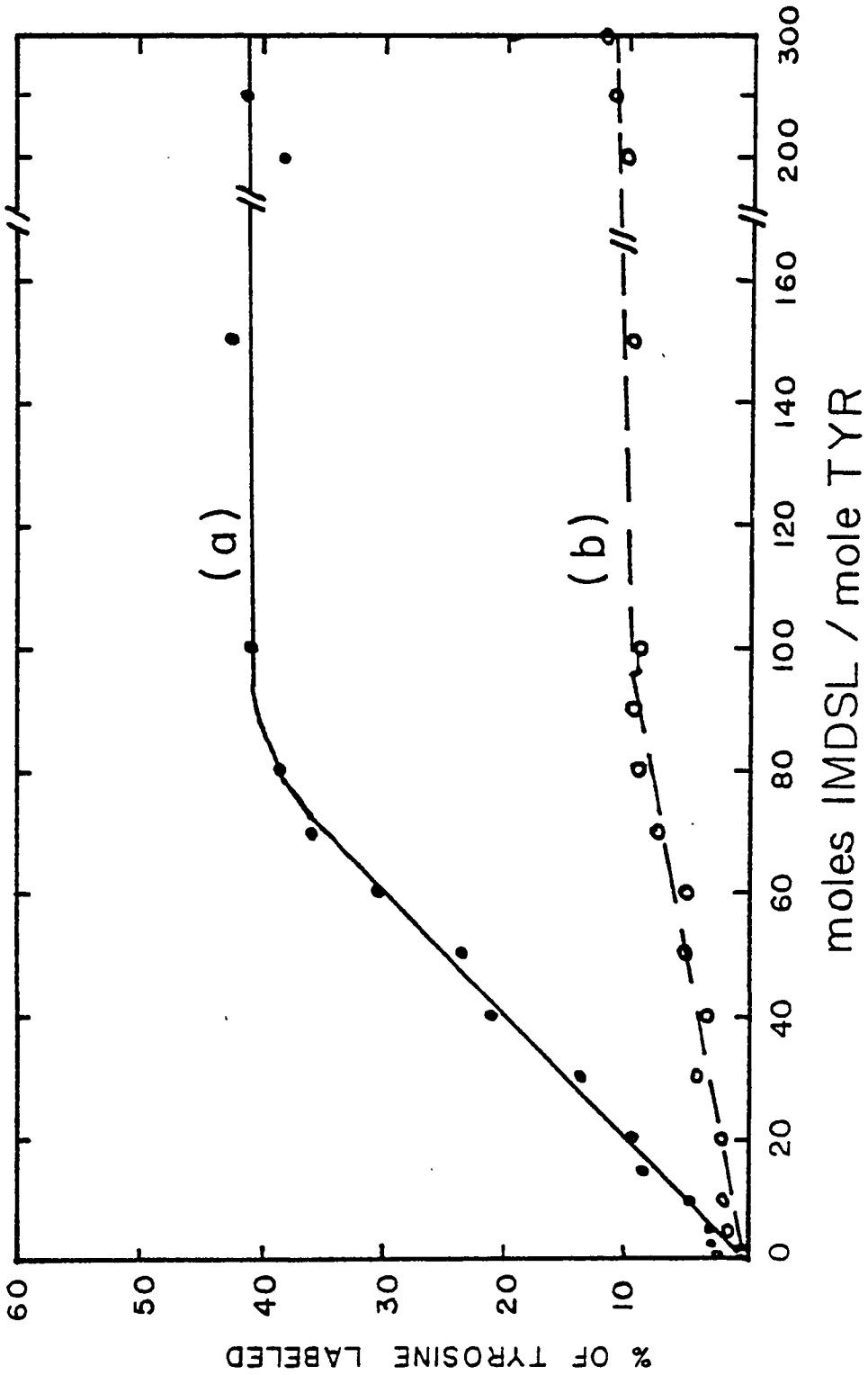
% OF TYROSINE LABELED
60
50
40
30
20
10
0
20
40
60
80
100
120
140
160
200
300
moles IMDSL / mole TYR
(a)
(b)

Fig. 23 ESR spectra for spin labeled histone core

Histone core-SL (20% tyrosyls being labeled) in 10 mM Tris-HCl, 0.2 mM EDTA, pH 7.2, plus (a) 2 M NaCl or (b) 0 M NaCl.

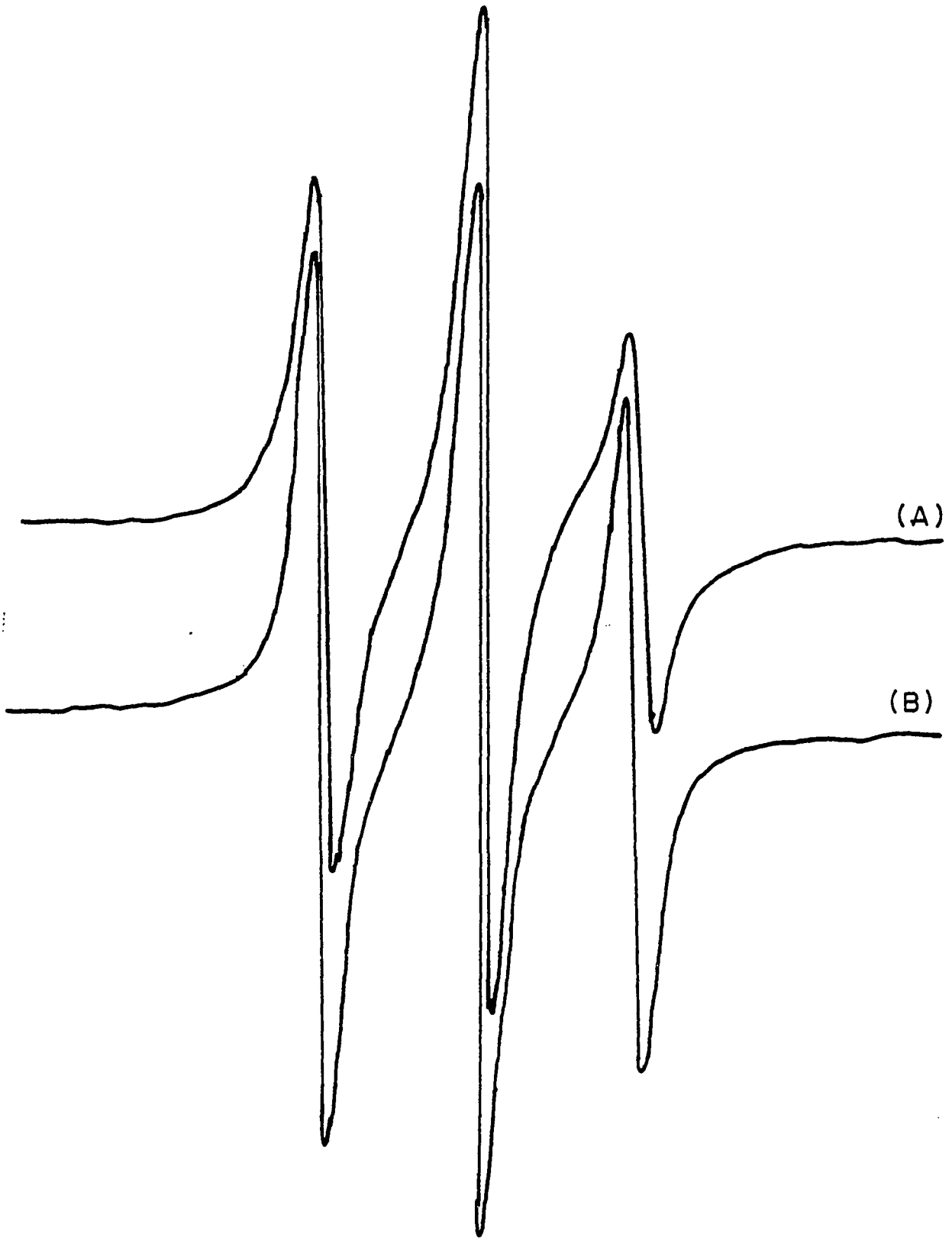
(A)
(B)

are destroyed by lowering the ionic strength of the histone solution, the spin labeled tyrosyls attain their greatest freedom of motion (Fig. 23b), suggesting that the histones are now in an extended, loose form.

When native nucleosome core particles in 10 mM Tris HCl, 0.2 mM EDTA, pH 7.2, are reacted with various molar excesses (5- to 300-fold) of the IMDSL, less than 15% of the tyrosyls are labeled, even at 200- to 300-fold molar excess of IMDSL (Fig. 22b), as compared to 40% labeling for the histone core alone. This suggests that only 4 tyrosyls in the nucleosome core particles are exposed and accessible to IMDSL under these labeling conditions. When the nucleosome cores are partially denatured by high salt or high urea concentrations, more tyrosyls are labeled by IMDSL (data will be shown later).

Fig. 24a shows an ESR weakly immobilized spectrum for the native nucleosome core particle, when 10% of the tyrosyls are labeled. The peak height ratio is $H_+/H_o = 0.57$ and $H_-/H_o = 0.29$, and the rotational correlation time for the label is 0.96 nsec. Again, the spin labeled tyrosyls are in a hydrophilic environment and undergo rather free rotational motion. The environment of the labeled tyrosyls is quite inhomogeneous, and no simple computer ESR spectrum can be simulated. When this labeled nucleosome core is dialyzed against 2 M NaCl, an ESR spectrum (Fig. 24b) is obtained that is similar to the spin labeled histone core in 2 M NaCl (Fig. 23a), suggesting a complete separation of DNA from the inner histone core. Ionic effects on the labeled nucleosome will be discussed in detail later.

(3) Conformational changes of spin labeled histone core and nucleosome core particle due to perturbations

Most proteins, in their native states, are folded into a

Fig. 24 ESR spectra for spin labeled nucleosome core particle

Nucleosome core particle-SL (10% tyrosyls being labeled) in 10 mM Tris-HCl, 0.2 mM EDTA, pH 7.2, plus (a) 0 M NaCl or (b) 2 M NaCl.

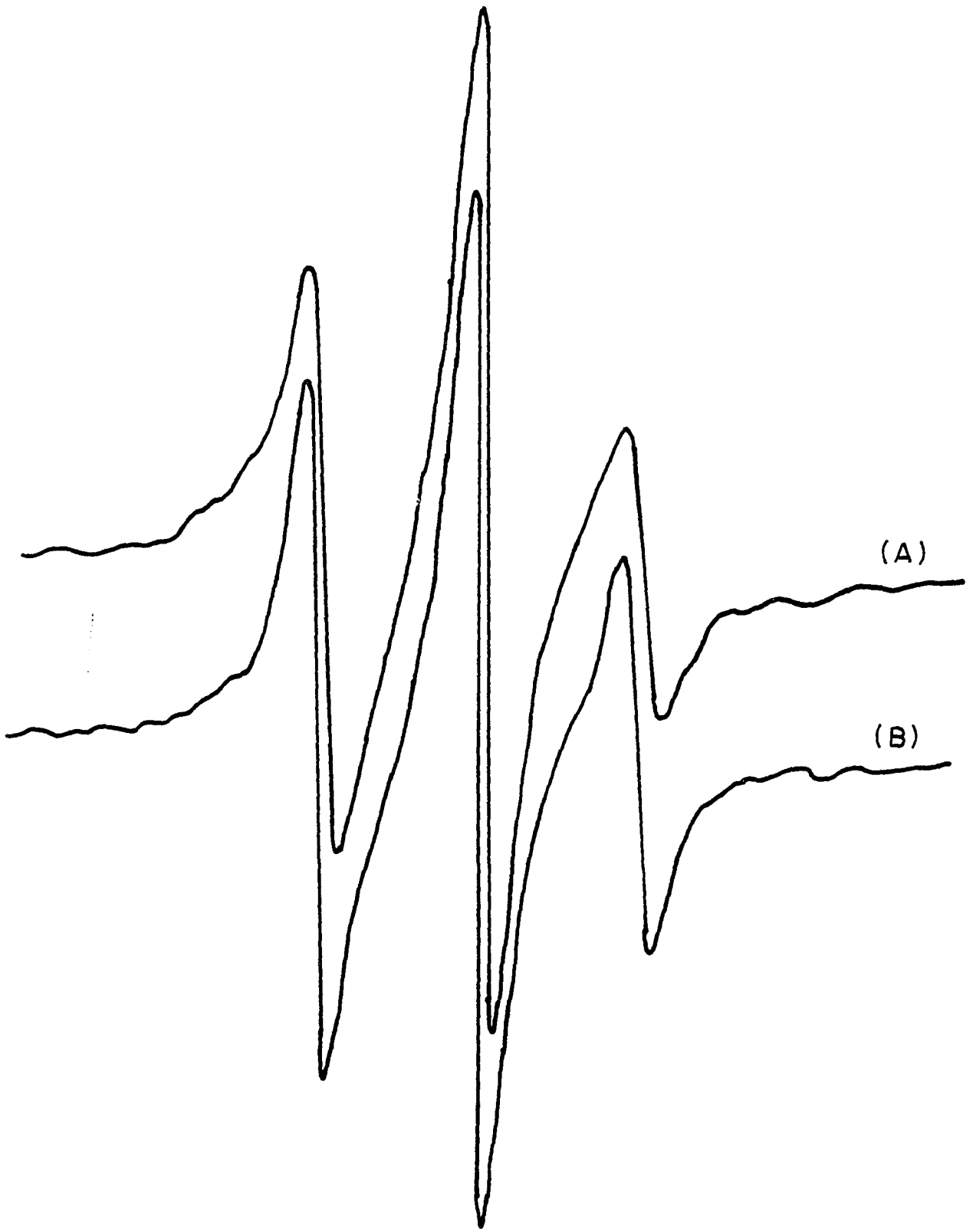
(A)
(B)

large number of well-defined, three-dimensional conformations. The forms that exist in cells are the results of enormous numbers of interactions, primarily noncovalent, that occur between amino acid residues and with components of the cellular environment. The forces that stabilize the proteins are cooperative and exist at various levels of organization: between subunits in multichain structures, and between molecular superstructures. The compact structures of proteins are stable over a range of in vivo and in vitro conditions. However, in regard to biological functions, proteins are capable of undergoing conformational changes by responding in certain ways to the needs of the organisms for expressions of functions by those proteins, for regulations of their activities, or for their destruction, when required (132, 133).

In vitro, proteins can also undergo intramolecular changes in their conformations when their environment is altered. These changes can be brought about by the addition of substances such as urea, or NaCl, or a variation of temperature or pH, or by a number of other means (134,135). Thus, the study of conformational changes in proteins offers means of studying the forces responsible for the secondary, tertiary, or quaternary structures of proteins and the role of different types of interactions in determining active sites (or binding sites) and other properties of the proteins. In this dissertation, we want to report the application of the ESR spin labeling technique on studying the conformational changes in histone core or nucleosome core particle due to external perturbations.

(a) The effect of urea on the spin labeled histone core and nucleosome core particle

After the removal of unreacted spin labels, the labeled histone core was dialyzed overnight against 2 M NaCl, 10 mM Tris HCl, 0.2 mM EDTA, pH 7.2, containing varying amounts of urea (1 M to 10 M). ESR spectra for the samples were recorded, and a plot of the peak height ratio (H_-/H_o) vs. urea concentration is given in Fig. 25a. The peak height ratio (H_-/H_o) is taken as an index of motional freedom of the labeled tyrosyls, the higher the ratio the freer the motion of the labels. Based on the relative sharpness of the ratio, the transition profile for the labeled histone core, due to urea, can be divided into three regions: a gradual change from 0 to 4.5 M, a rather sharp increase from 4.5 M to 7.5 M, and a leveling off from 8 M to 10 M, respectively. The ESR spectrum for the labeled histone core, in 10 M urea (Fig. 26a) clearly indicates that the histone core is completely denatured and that the histones are probably in random coils. The gradual change of the ratio is probably due to a swelling of the overall histone core structure, while the major sharp change is most likely a result of disruption of the secondary structure of the histones, due to the urea.

The effects of urea on the labeled nucleosome core particle are quite different as shown in Fig. 25b. The nucleosome core particle appears to be more sensitive to urea denaturation. This transition profile (a plot of (H_-/H_o) vs. urea concentration) appears to be sigmoidal in shape. The inflection point occurs at around 4 M urea, and the denaturation is complete above 7 M urea. However, although the secondary structure of the inner histone core is destroyed by urea above 7 M, the ESR spectrum (Fig. 26b) for the denatured nucleosome core particle is quite different from that of the denatured histone core (Fig.

Fig. 25 Effects of urea on spin labeled histone core and nucleosome core particle

The effects of urea on (a) the histone core in 2 M NaCl (—●—●—●—) and (b) the nucleosome core particle in 10 mM Tris-HCl, 0.2 mM EDTA, pH 7.2 (—o—o—o—). A plot of the relative peak-height ratio (H_-/H_0) versus urea concentration.

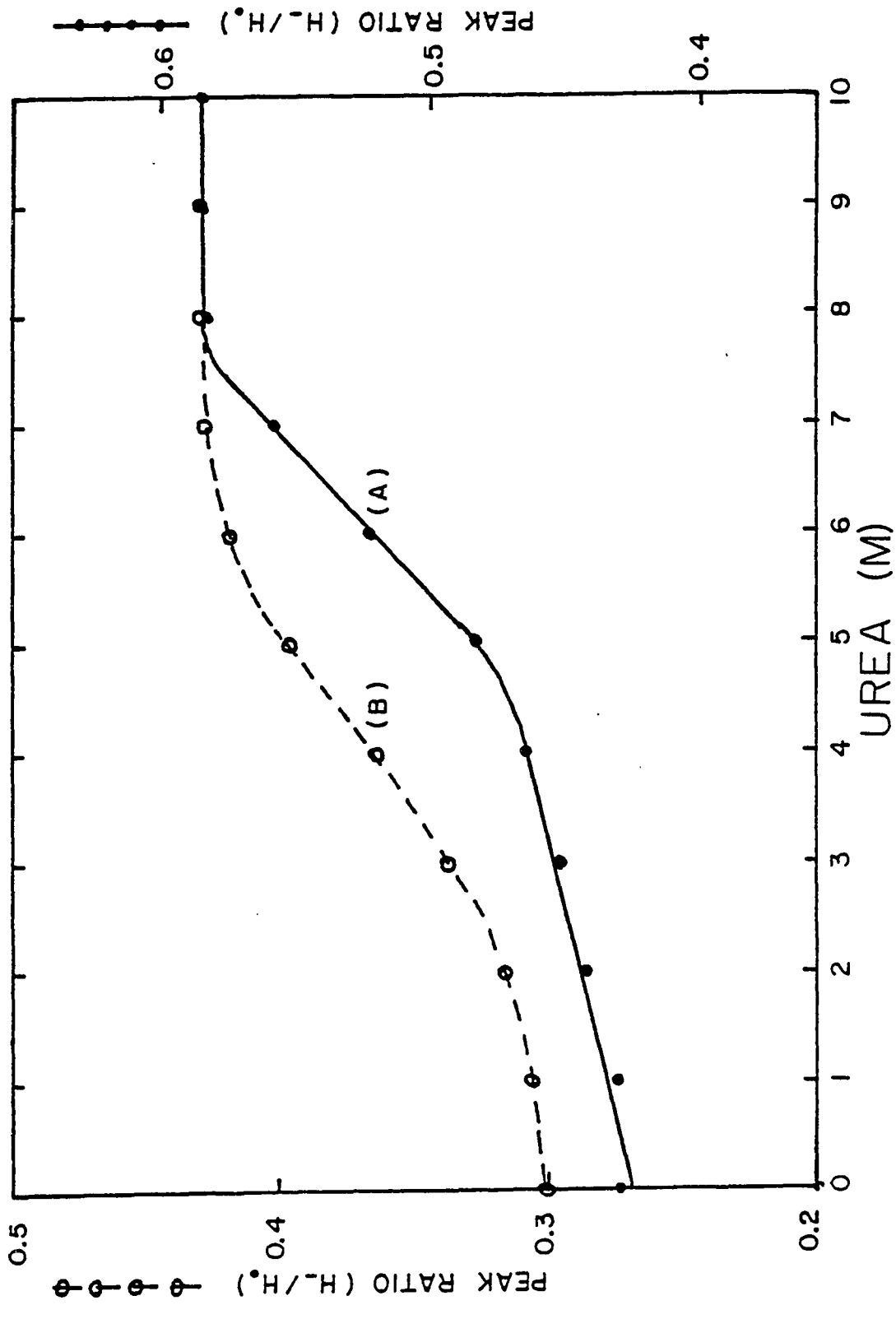
PEAK RATIO (H_/H•)
0.6
0.5
0.4
(A)
(B)
0.5
0.4
0.3
0.2
PEAK RATIO (H_/H•)
0
1
2
3
4
5
6
7
8
9
10
UREA (M)

Fig. 26 ESR spectra of (a) histone core in 10 M urea, 2 M NaCl, 10 mM Tris-HCl, 0.2 mM EDTA, pH 7.2 and (b) nucleosome core particle in 8 M urea, 10 mM Tris-HCl, 0.2 mM EDTA, pH 7.2.

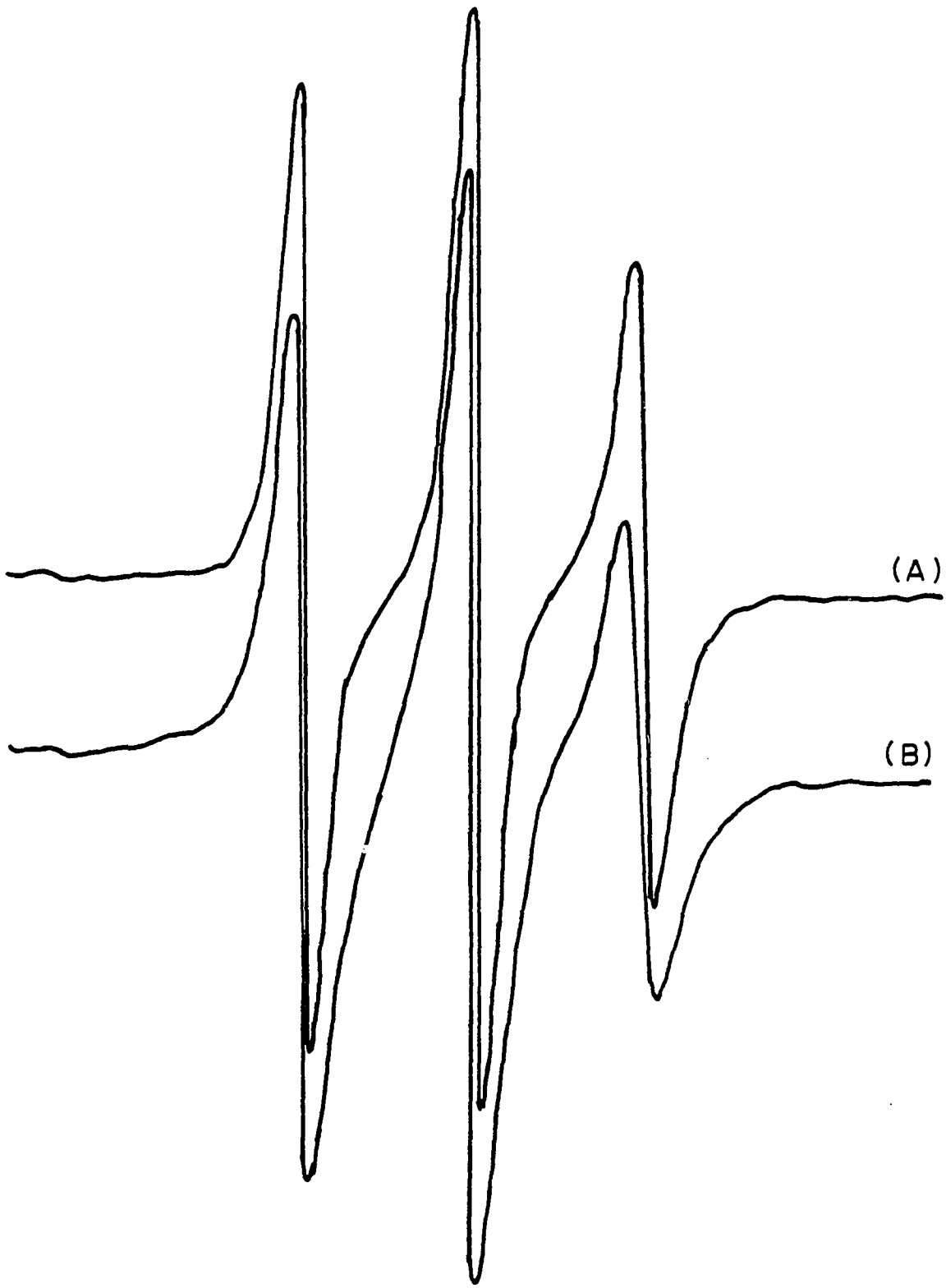
(A)
(B)

26a). The labeled tyrosyls are still in a more constrained environment, in the denatured nucleosome core particle, than in the denatured histone core, as a result of urea treatment. This suggests that the core DNA is still binding to the histones, even though the tertiary and secondary structures of the histones have been destroyed.

(b) Ionic effects on the spin-labeled histone core and nucleosome core particle

When the labeled histone core in 2 M NaCl was dialyzed against either decreasing ionic strength or increasing ionic strength with respect to 2 M NaCl, a plot of the relative peak height ratio (H_-/H_o) vs. ionic strength is shown in Fig. 27. When the ionic strength is less than 1.5 M NaCl, the peak ratio (H_-/H_o) begins to increase, suggesting that the histone core becomes unstable and begins to disintegrate. The labeled tyrosyls achieve their greatest freedom when the histone core is dialyzed into no salt condition, indicating that the histone core has completely dissociated into individual random-coil histones, as shown in Fig. 23b. On the contrary, when the ionic strength is increased to above 2 M, the tumbling environment of the labeled tyrosyls becomes more viscous, suggesting that there is an increased conformational stability. And salting-out of proteins begins to happen when the ionic strength is above 5 M.

The effects of salt concentration on the spin-labeled nucleosome core particle is shown in Fig. 28. Again, the relative peak-height ratio (H_-/H_o) is taken as the index of motional freedom on the labeled tyrosyls. Several structural transitions are observed for the nucleosome core particle in the range of 0.5 mM to 2.5 M NaCl. The peak-height ratio (H_-/H_o) is essentially constant in the range from

Fig. 27 Ionic effects on spin labeled histone core at room temperature

A plot of the relative peak height ratio (H_-/H_o) vs. ionic strength.

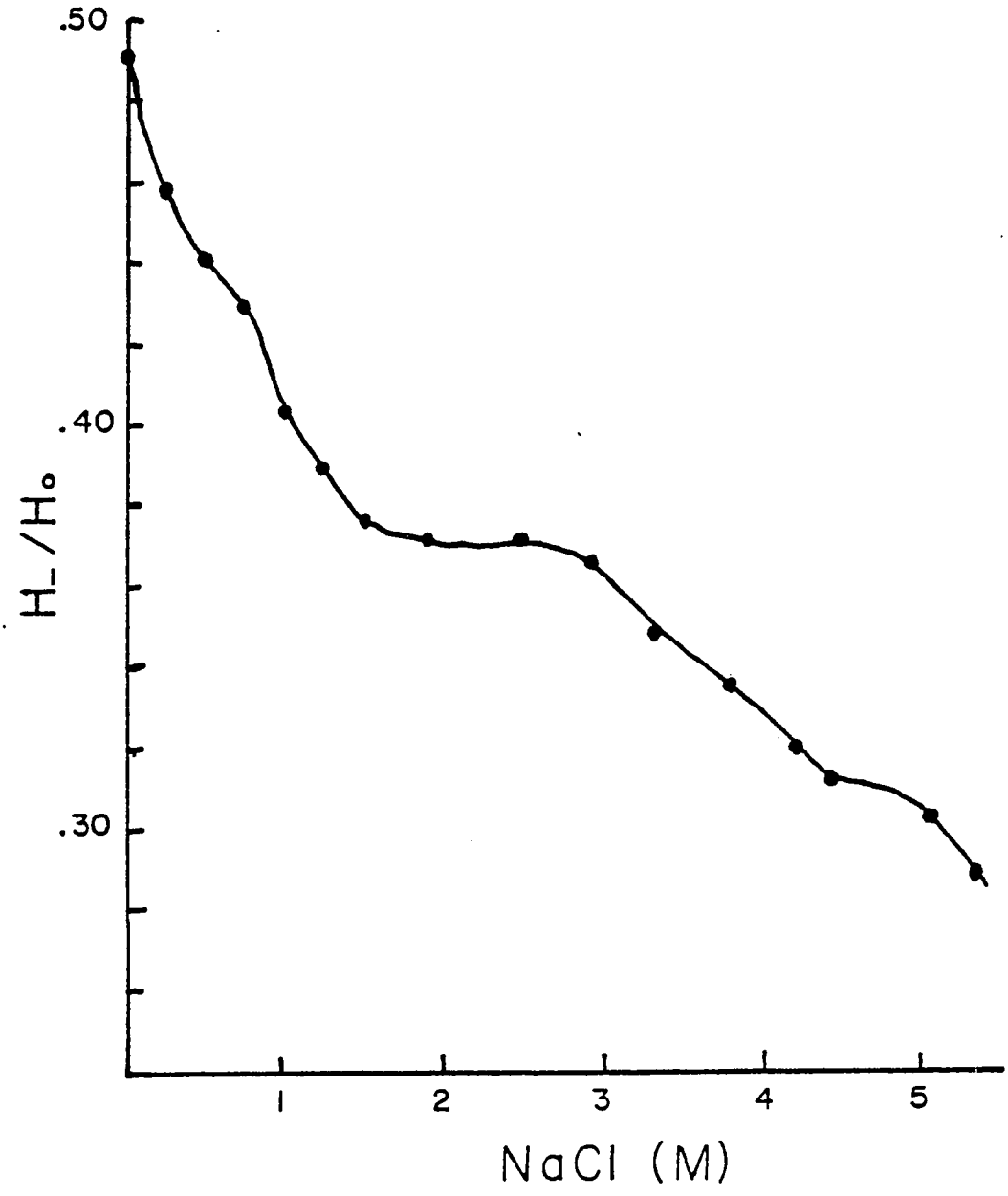
.50
.40
.30
H_/H₀
1
2
3
4
5
NaCl (M)

Fig. 28 Ionic effects on the spin labeled nucleosome core particles at room temperature

A plot of relative peak height ratio (H_-/H_o) vs. ionic strength.

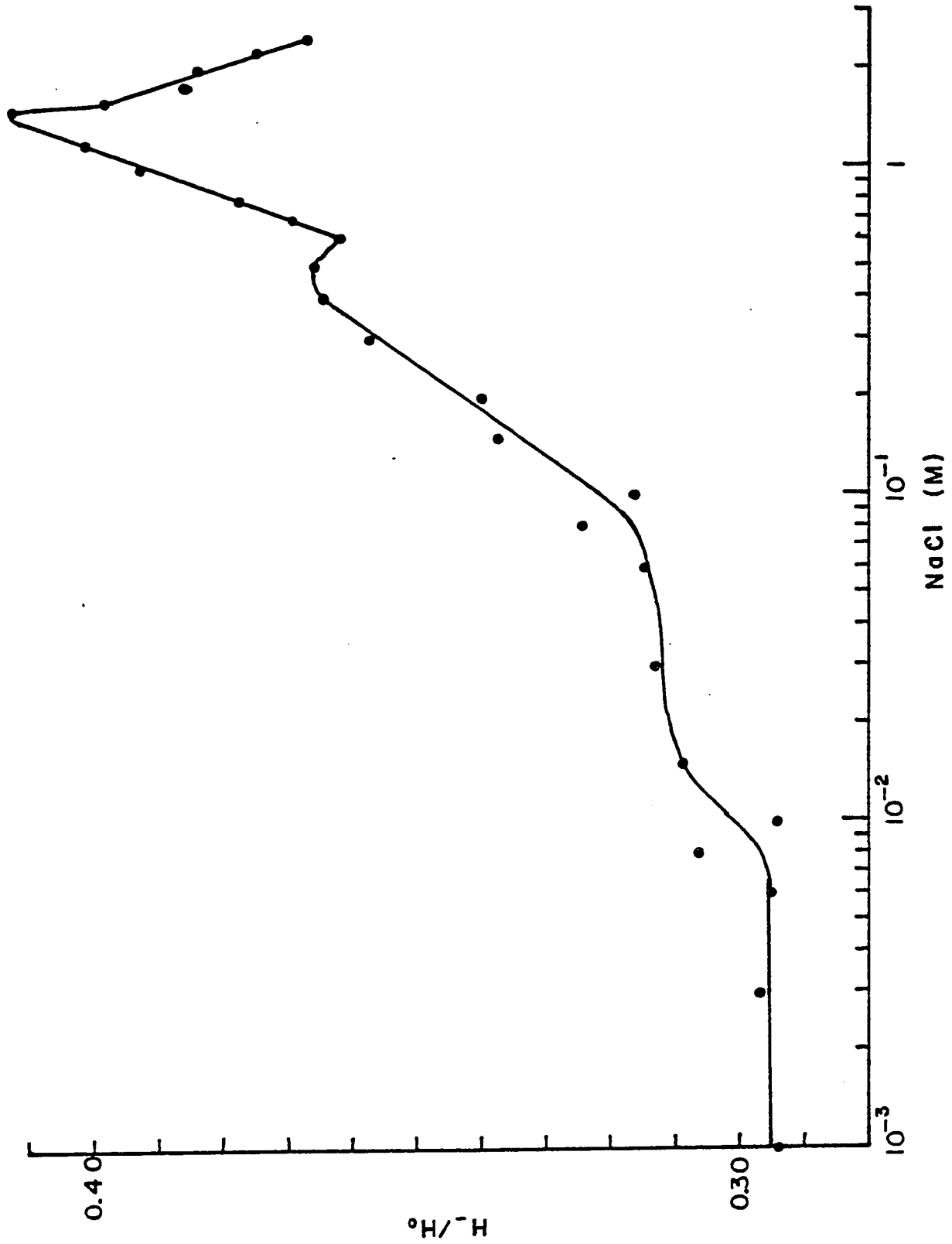
0.40
0.30
H_-/H_0
10^{-3}
10^{-2}
10^{-1}
1
NaCl (M)

0.5 mM to 8 mM NaCl. An abrupt change occurs between 8 mM and 15 mM NaCl. The peak-height ratio remains constant again between 15 mM to 70 mM NaCl. It should be noticed that the actual difference between the peak height ratio in the range from 0.5 mM to 7 mM and 15 mM to 70 mM NaCl is very small.

The peak-height ratio increases linearly as the ionic strength is increased from 0.1 M to 0.5 M. A shoulder occurs at around 0.4 M to 0.6 M. As the ionic strength is further increased from 0.6 M to 1.5 M, the peak-height ratio increases linearly again, but at a different rate from the previous one, and finally, it reaches a maximum value (0.41) at 1.5 M NaCl. Beyond 1.5 M to 2.5 M, the peak-height ratio drops drastically. This experiment has been repeated several times and similar transition profiles have been obtained each time.

To compare these ESR observations, we also measured the CD spectra of the labeled nucleosome core particles at different ionic strengths. The ellipticity $(\theta)_{p,225}$ and $(\theta)_{p,285}$ are plotted as a function of NaCl molarity and are shown in Fig. 29a and Fig. 29b, respectively. The ellipticity $(\theta)_{p,225}$ observed at 225 nm, is due mainly to the conformation of the histone core. It is found that the α-helical content of the histone as measured by a change in $(\theta)_{p,225}$ decreases very slowly as the ionic strength is increased from 0.5 mM to 0.2 M. A sharp decrease in $(\theta)_{p,225}$ occurs between 0.3 M to 0.6 M. However, as the ionic strength is further increased from 0.6 M to 2.5 M, the $(\theta)_{p,225}$, or the α-helical content, returns to the original value observed at the lower ionic strength (Fig. 29a).

The ellipticity of the DNA at 285 nm at the lower ionic strength is found to be 1.4×10^3 deg/cm^2/decimole, identi-

Fig. 29 Ionic effects on nucleosome core particles monitored by circular dichroism

A plot of ellipticity $(\theta)_p$ based on DNA nucleotide concentration at $(a)_\lambda$ = 225 nm (_ ●_ ●_ ●_) or $(b)_\lambda$ = 284 nm (- Δ - Δ -), versus NaCl concentration.

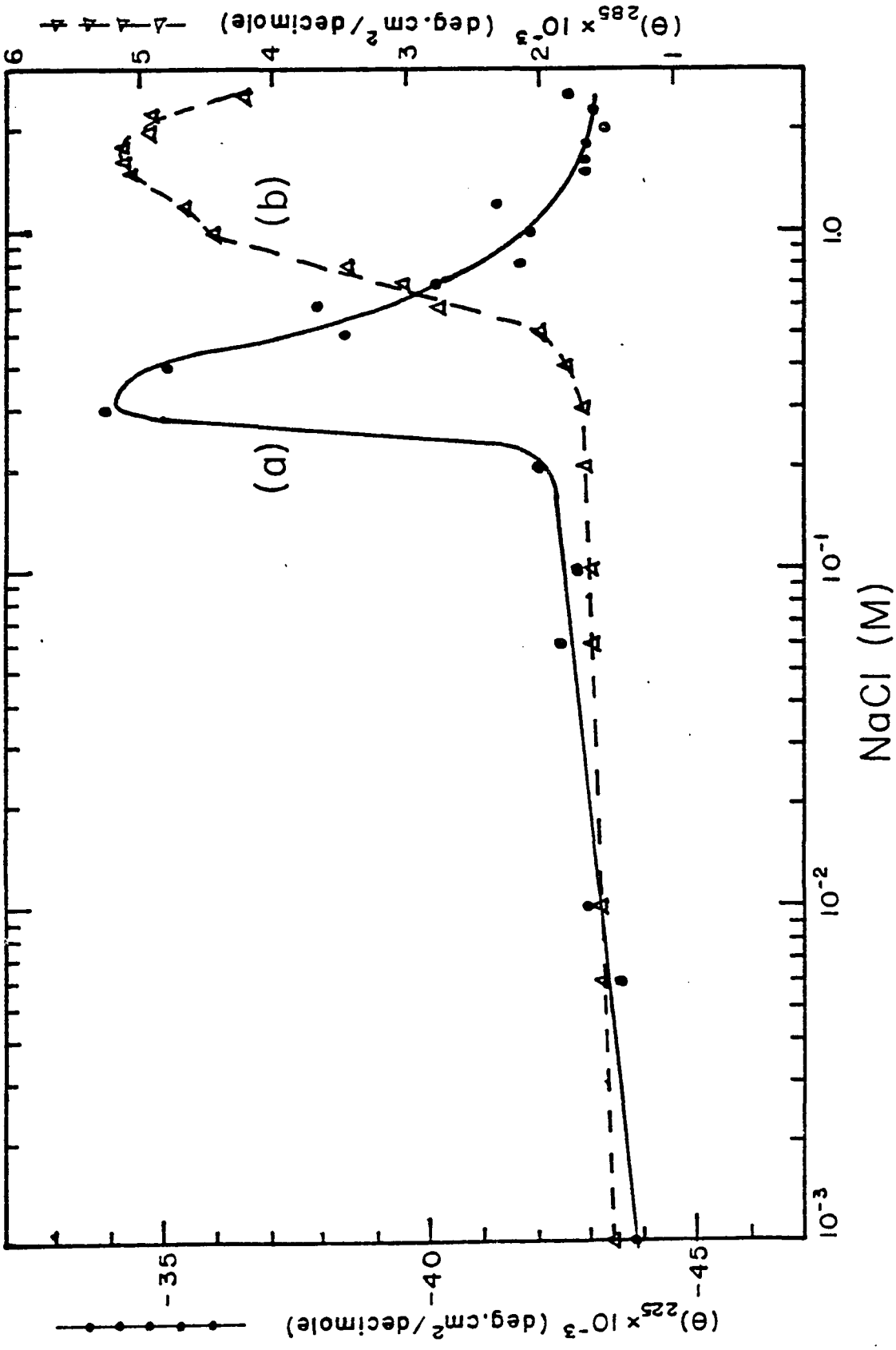
(a)
(b)
NaCl (M)
10^{-3}
10^{-2}
10^{-1}
1.0
$(\theta)_{225} \times 10^{-3}$ (deg.cm^2/decimole)
$(\theta)_{285} \times 10^{-3}$ (deg.cm^2/decimole)
-35
-40
-45
1
2
3
4
5
6

Fig. 30 Ionic effects on spin labeling the nucleosome core particle

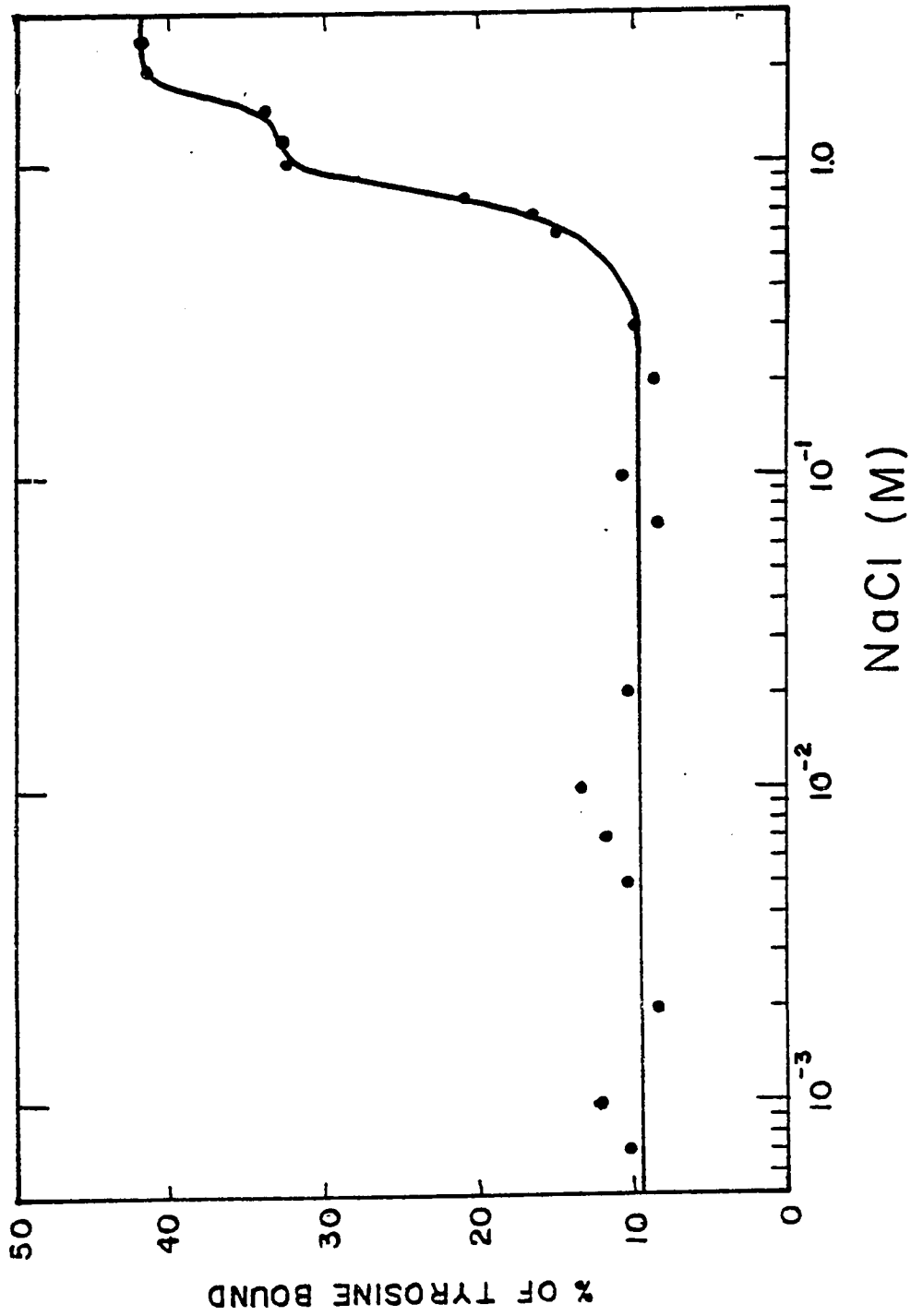
% OF TYROSINE BOUND
50
40
30
20
10
0
1.0
10^{-1}
10^{-2}
10^{-3}
NaCl (M)

cal with what has been reported previously (88). As the ionic strength is increased from 10^{-3} M to 0.3 M, the ellipticity of DNA at 285 nm increases gradually and slowly (from 1.4 x 10^3 to 1.8 x 10^3 deg-cm^2/decimole). The $(\theta)_{p,285}$ increases sharply at 0.5 M NaCl and reaches a maximum (5.2 x 10^3 deg-cm^2/decimole) at about 1.8 M NaCl. A shoulder is found at around 1.0 M to 1.4 M NaCl. The ellipticity then decreases as the ionic strength is further increased from 2 M to 2.5 M.

The accessibility of tyrosyls in the nucleosome core particle in different ionic strengths further confirms our observation on the ionic effect on the nucleosome core particle. Fig. 30 shows a plot of the percentage of the tyrosyls labeled vs. ionic strength of NaCl. When the nucleosome core particle is exposed in the ionic strength of 0.1 mM to 0.5 M, only 8% to 12% of the tyrosyls is available to molar excess of IMDSL. This is consistent with our previous saturation binding of the nucleosome core particle by IMDSL (Fig. 22b), where we have shown that less than 15% of the tyrosyls are labeled even at 200- to 300-fold molar excess of IMDSL. However, when the nucleosome core particle is exposed to a ionic strength higher than 0.4 M, the accessibility of tyrosyls increased considerably from 12% to a 42% maximum at 2 M NaCl. Again, this is consistent with our previous observation that the maximum percentage of tyrosyls available in histone core at 2 M NaCl is 40%.

(c) pH effects on the spin labeled nucleosome core particle

Fig. 31 shows the pH effects on the tumbling environment of the labeled tyrosyls in the nucleosome core particle. It is quite obvious that the conformation of the nucleosome core particle is unaffected by changes of pH in the range of 4 < pH < 9.5. When

Fig. 31 pH effects on the spin labeled nucleosome core particles

A plot of relative peak height ratio (H_-/H_o) vs. pH.

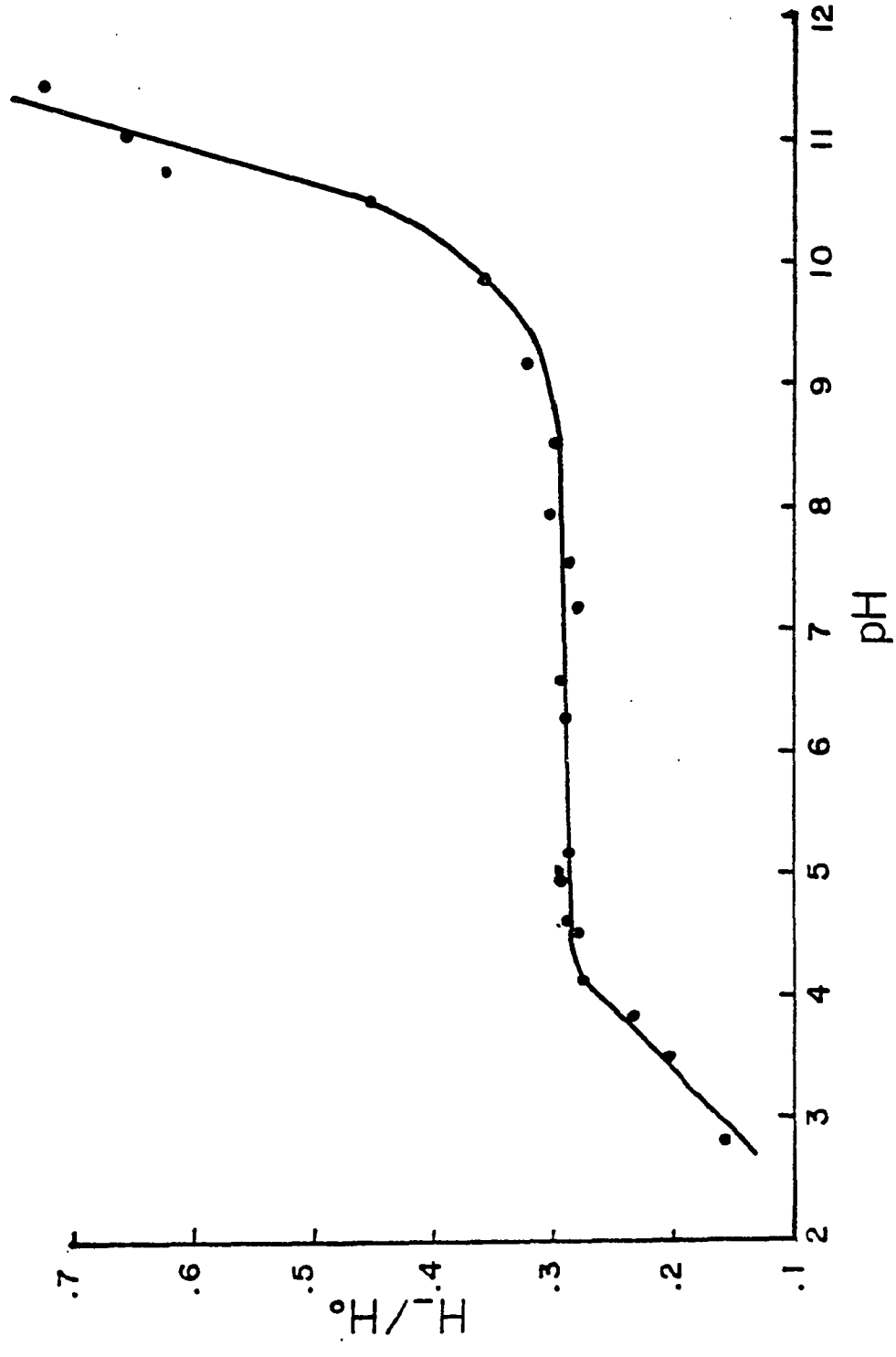
.7
.6
.5
.4
.3
.2
.1
H_{-1}/H_o
2
3
4
5
6
7
8
9
10
11
12
pH

the pH is below 4, the nucleosome core particle begins to aggregate and precipitate. The nitroxide spin label begins to hydrolyze when the pH is raised above 10.5. So, it is kind of difficult to observe any conformational change in the nucleosome when the pH is changed to above 10.5.

(d) Temperature effects on the spin labeled histone core and nucleosome core particle

The peak-height ratio for the labeled tyrosyls in the histone core in 2 M NaCl as a function of temperature is given in Fig. 32. Several fine structural changes are observed for the histone core in responding to a change in temperature over a range of $4^{o}C$ to $50^{o}C$. The histone core appears to be more stabilized at $4^{o}C$ to $18^{o}C$. At room temperature ($22-26^{o}C$), the tumbling environment for the labeled tyrosyls becomes less viscous. The rotational correlation time decreases as the temperature is further increased. And the histone core seems completely dissociated when the temperature is raised above $44^{o}C$.

Temperature effects on the labeled tyrosyls in the nucleosome core particle is shown in Fig. 33. The transition profile obtained for the nucleosome due to the temperature is more complicated when compared with histone core alone. Thermal denaturation profile for the nucleosome core particle monitored by optical method shows a biphasic melting profile ($60^{o}C$ and $75^{o}C$) for the DNA (Fig. 16). However, such optical method does not give any information on the conformational change in the inner histone core due to increasing temperature. A thermal denaturation profile obtained by the ESR method (Fig. 33), on the other hand, shows that gradual conformational changes occur within the inner histone core before the DNA begins to melt. But our data fail to

Fig. 32 Thermal denaturation of the spin labeled histone core

A plot of the relative peak height ratio (H_-/H_o) vs. temperature in ^oC.

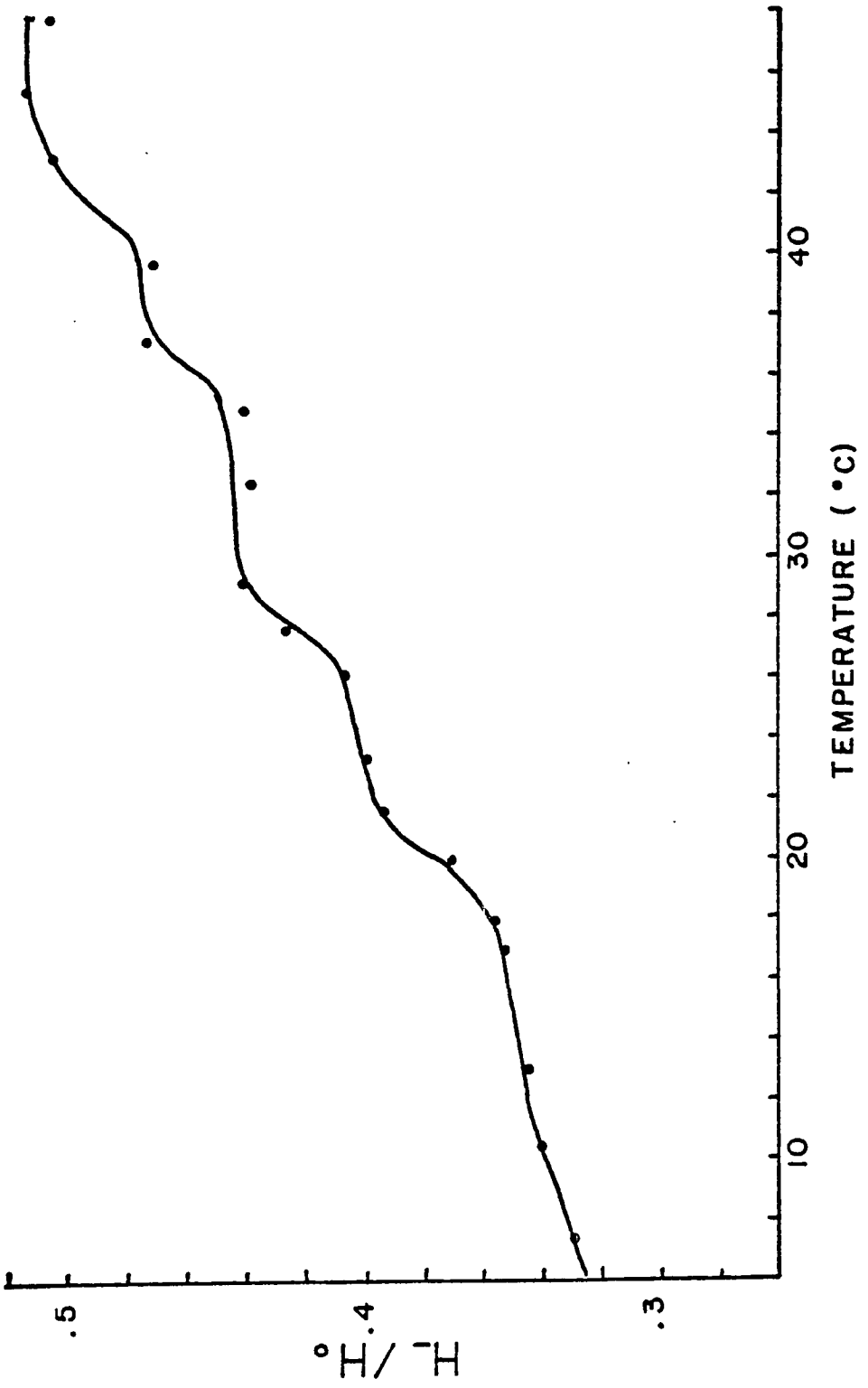
.5
.4
.3
$H_- / H_\circ$
10
20
30
40
TEMPERATURE (°C)

Fig. 33 Thermal denaturation of the spin labeled nucleosome core particles

A plot of the relative peak height ratio (H_-/H_o) vs. Temperature in ^oC.

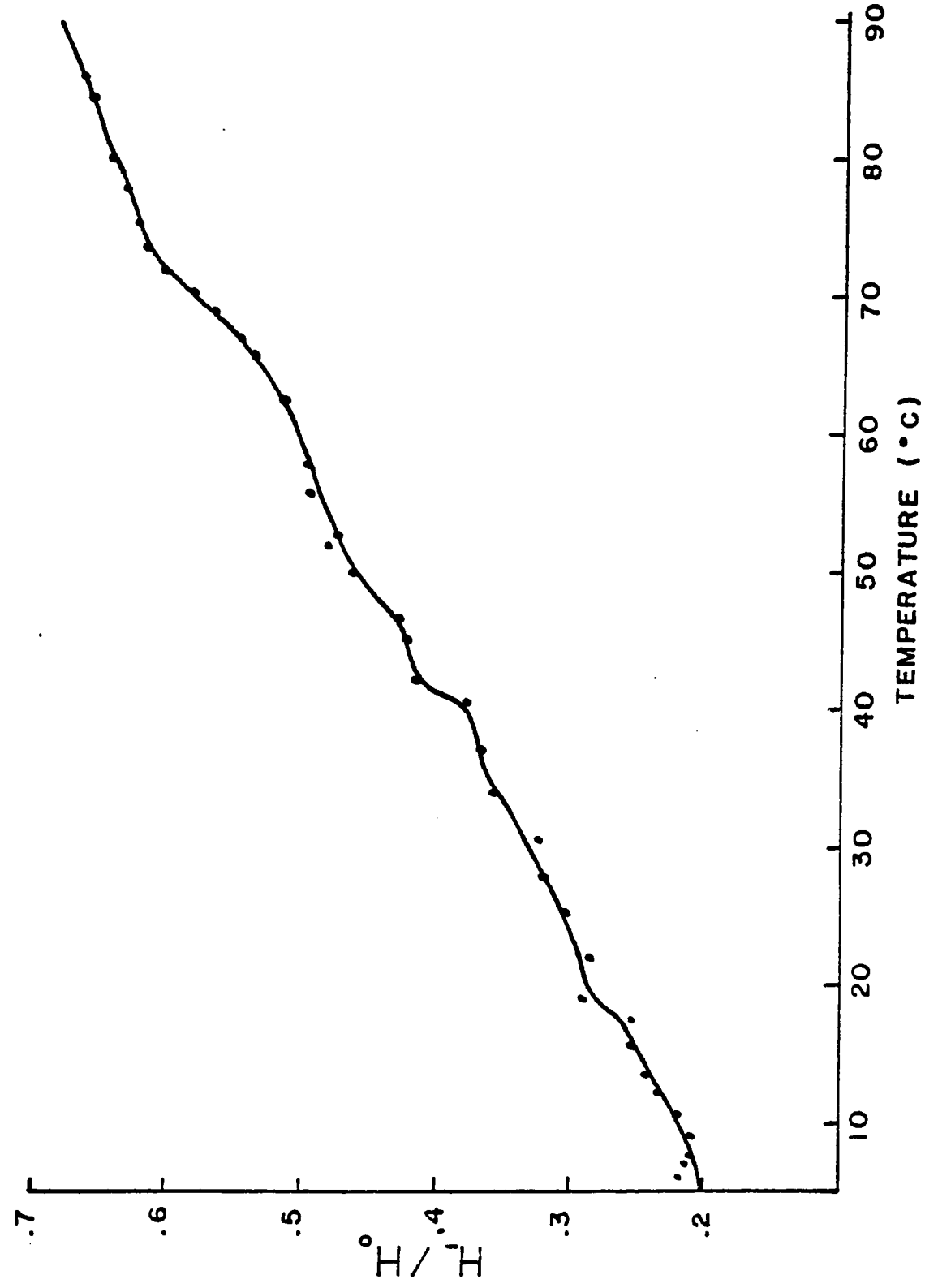
.7
.6
.5
.4
.3
.2
H_- / H_o
10
20
30
40
50
60
70
80
90
TEMPERATURE (°C)

reveal any sharp conformational transitions within the histone core due to changes in temperature.

(E) RECONSTITUTION STUDIES

Reconstitution of chromatin from a mixture of DNA and the four histones H2A, H2B, H3 and H4 has been widely used to investigate chromatin structure (43,73,75,89,136-140). The reconstituted histone-DNA complexes appear to be identical with the native chromatin (or nucleosome) in all physical properties examined (histone content, sedimentation velocity, thermal melting profile and circular dichroism) as well as in their patterns of digestion by DNase I, micrococcal nuclease and proteolytic enzymes (73,75,89,136-140). In this dissertation, we have applied an ESR spin labeling method to determine the mode of reassociation of the spin labeled histone core to the core DNA during the reconstitution and to study the role of tyrosyl groups in the reassociation process.

(1) Mode of reassociation of the spin labeled histone core with DNA during reconstitution

Spin labeled histone cores were mixed with purified core DNA in 2M NaCl. The mixture was reconstituted by the salt step-gradient dialysis as described in the methods. At each step of dialysis, the tumbling condition of the labeled tyrosyls was examined by ESR. Figure 34 shows a plot for the relative peak height ratio vs. the salt concentration during the reconstitution process. In 2M NaCl, the ESR spectrum is identical to Fig. 23a for a spin labeled histone core in the absence of DNA, suggesting that the mixing of DNA at 2M NaCl does not interfere with the labeled tyrosyls. As the ionic strength is gradually decreased, the tumbling freedom of the labeled

Fig. 34 Mode of reconstitution of the nucleosome core particles

A plot of the relative peak height (H_-/H_o) vs. ionic strength at various stages of reconstitution.

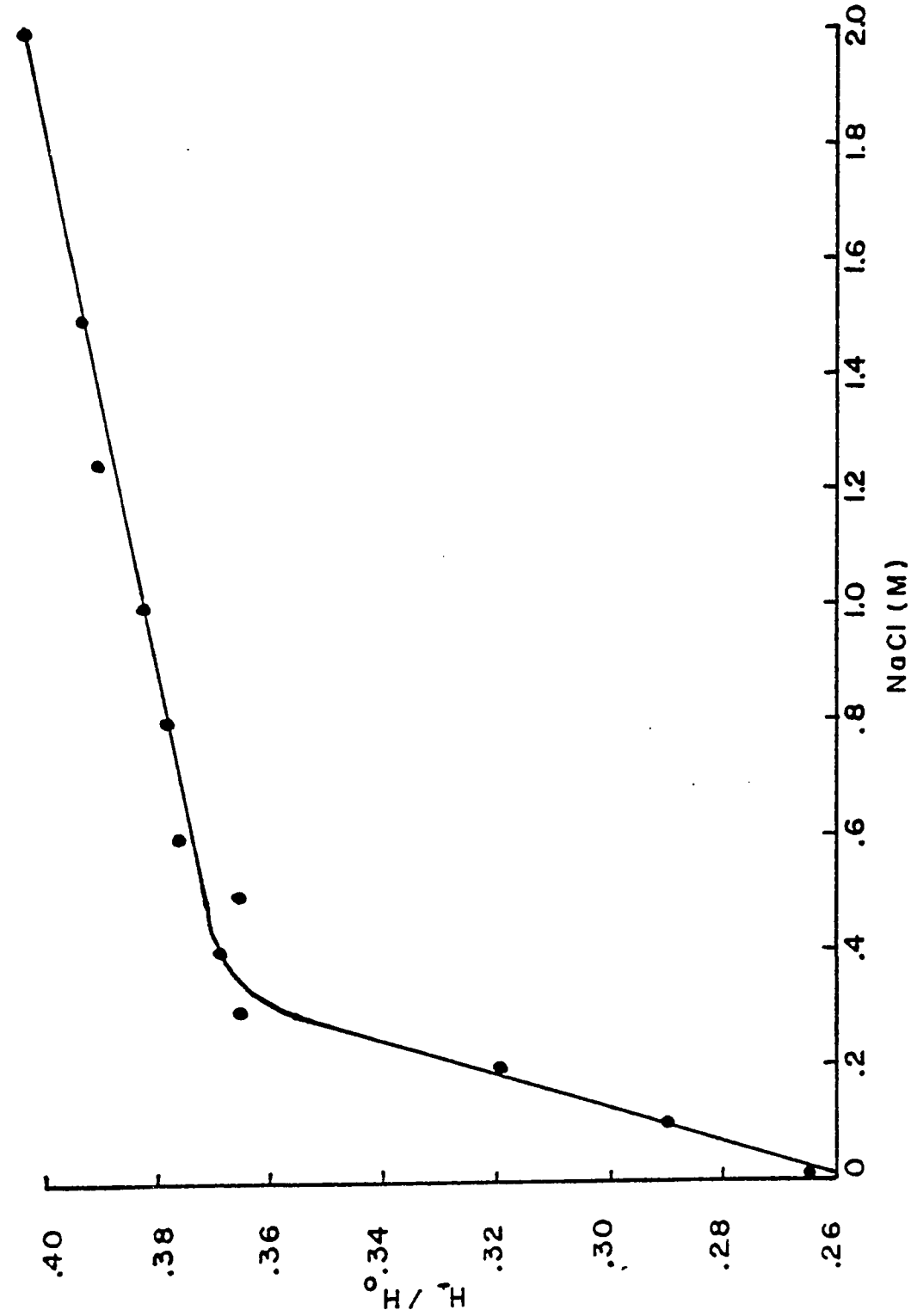
.40
.38
.36
.34
.32
.30
.28
.26
$^{o}H / ^{t}H$
0
.2
.4
.6
.8
1.0
1.2
1.4
1.6
1.8
2.0
NaCl (M)

tyrosines becomes correspondingly hindered. In contrast to what we have observed previously (Fig. 27), that a decrease in the ionic strength has caused the histone core alone to dissociate. The present observation (Fig. 34) strongly indicates that a decrease in the ionic strength has increased the histone-DNA interaction, preventing the histone core from disintegrating. However, no sharp change is found for the labeled tyrosyls in the range of 2M to 0.3M NaCl, suggesting that the histone core binds progressively to the DNA. When the ionic strength is less than 0.3M, the peak height ratio decreases drastically, indicating that full association between histone core and DNA begins to occur and the complex becomes more compact.

The reconstituted complexes were centrifuged through a 5-25% isokinetic sucrose gradient in an SW27 rotor at 27000 rpm for 22 hr., the fractionation pattern is shown in Fig. 35. Two peaks are resolved: one sediments at a position corresponding to the free core DNA ($S_{20,w}$ = 4.5), while the other sediments at the position corresponding to the native nucleosome core particle ($S_{20,w}$ = 10.5). The histone-DNA mixtures were originally reconstituted at a condition in excess of DNA (DNA (w)/Protein (w)=3), giving rise to the unreconstituted free core DNA (as a marker) in the sucrose gradient. The reconstituted nuclesome core-like fractions were pooled and found to have identical physical properties: histone content, sedimentation velocity, biphasic melting profile (Fig. 16) and circular dichroism spectrum (Fig. 17), same as the native nucleosome particle. The ESR spectrum for the reconstituted nucleosome is also found to be quite similar to the labeled native one but with a higher rotational correlation time, τ=1.06 nsec.

Fig. 35 Fractionation of the reconstituted nucleosome core complex

(a) free core DNA, _____

(b) reconstituted nucleosome complex, __ __ __ __ __ __

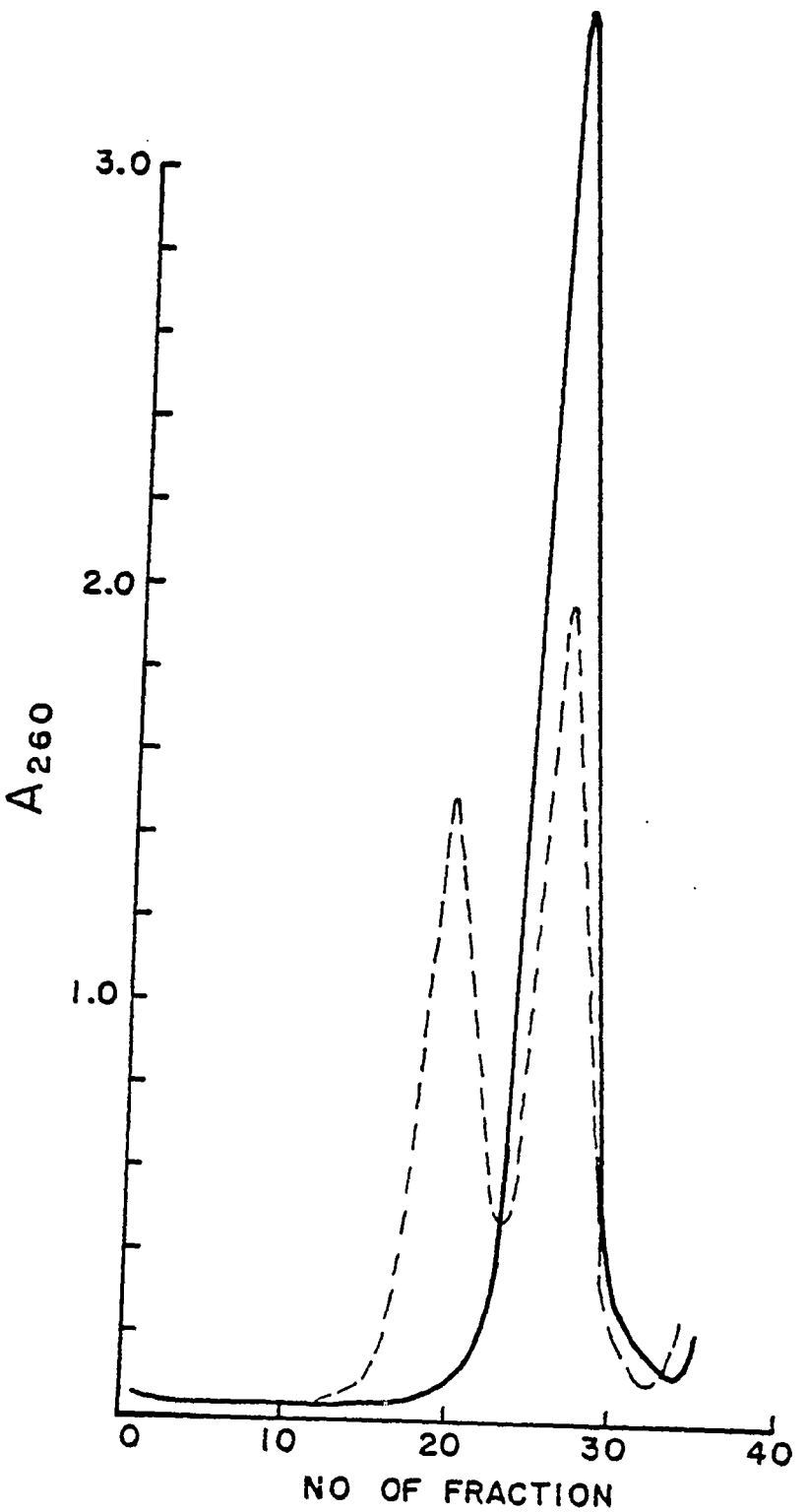
3.0
2.0
1.0
A_{260}
0
10
20
30
40
NO OF FRACTION

(2) Studies of the role of tyrosyl residues in the reassociation process for the nucleosome core complex

In the previous experiments, we have shown that a nucleosome core-like complex can be reconstituted from a mixture of the spin labeled histone core and the core DNA (140 base pairs). The question that is raised, however, is: what degree of modification in labeling the tyrosyls in the histones will prevent the reassociation process for the nucleosome core complex? In other words, is reconstitution of the nucleosome-like complex possible when the "buried" tyrosyls in the histone core become labeled? To answer these questions, we first dissociated the native nucleosome core particles in 10mM TrisHCl, 0.2mM EDTA, pH7.2, containing 2M NaCl, 2M NaCl plus 4M urea, or 2M NaCl plus 6M urea respectively, then, in each case we spin labeled the histone to a different extent. The complexes were reassociated back by salt step-gradient dialysis as described in the methods. The final complexes were concentrated and centrifuged through a 5-20% isokinetic sucrose gradient in an SW27 rotor at 27000 rpm for 26 hours. The fractions were collected and analyzed.

Figure 36 shows the fractionation profiles for the reassociation complexes which have previously been dissociated in 2M NaCl only and labeled by IMDSL to different extents. A major monomer peak, which sediments at a position equivalent to the native nucleosome core particle ($S_{20,w}$ = 10.5S), is found for all the reassociated samples, whether spin labeled or not. This suggests that nearly complete reassociation can be attained even when most of the surface tyrosyls on the histone core have been labeled (4% to 30% tyrosyls). However, when more than 40% of the tyrosyls become labeled, a shoulder

Fig. 36 Fractionation profiles for the Reconstituted nucleosome complexes

The native material was dissociated in 2 M NaCl, plus 10 mM TrisHCl, 0.2 mM EDTA, pH 7.2 and spin labeled with various amount of molar excess IMDSL:

	(SL/tyr)		
(a)	0	:	————————
(b)	20	:	— — — — —
(c)	40	:	.....
(d)	60	:	— . — . — .
(e)	80	:	— — . — — .
(f)	150	:	o o o o o o

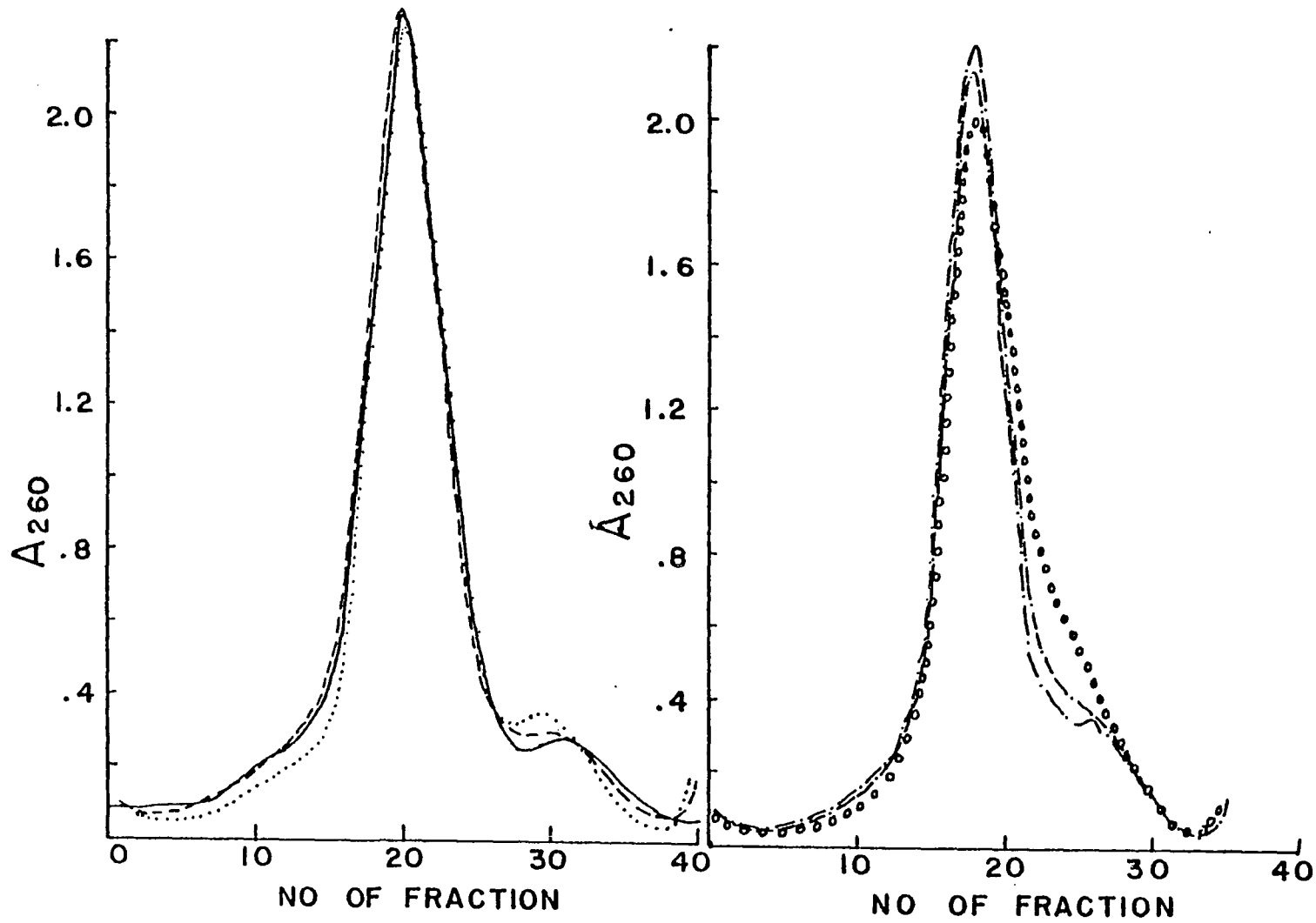
2.0
1.6
1.2
.8
.4
A260
0
10
20
30
40
NO OF FRACTION
2.0
1.6
1.2
.8
.4
A260
10
20
30
40
NO OF FRACTION

Fig. 37 ESR spectra for the reconstituted nucleosome core particles

The percentage of tyrosyls labeled in the reconstituted nucleosome core complexes is

(a) 6.3%

(b) 13.7% and

(c) 27.7%

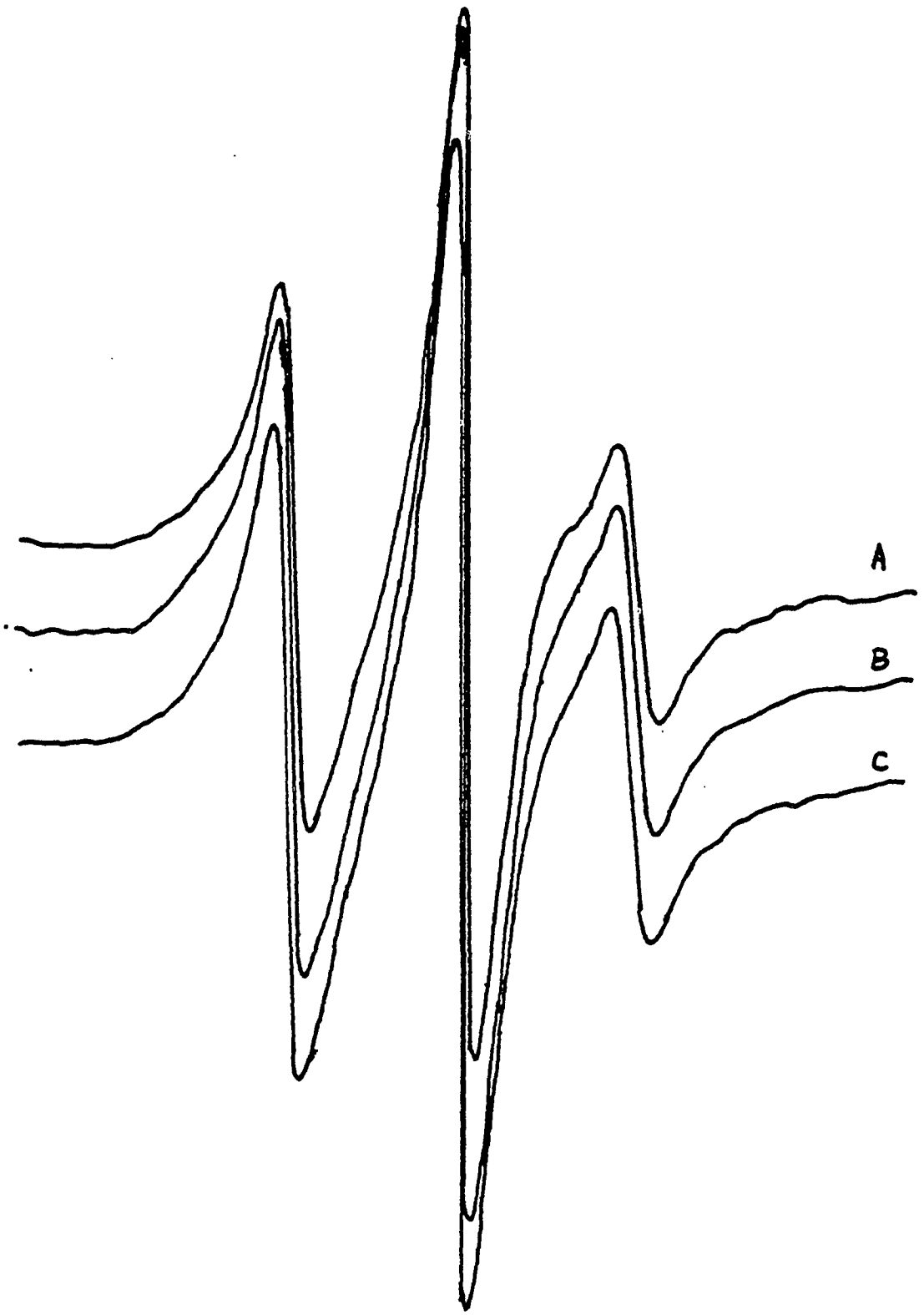
A
B
C

Fig. 38 Fractionation profiles for the reconstituted nucleosome complexes (4 M urea)

The native nucleosome core particles were previously dissociated in 2 M NaCl, 10 mM Tris-HCl, 0.2 mM EDTA, pH 7.2, plus 4 M urea. The partially denatured material was spin labeled with various amounts of molar excess of IMDSL:

	(SL/tyr)		
(a)	0	:	————————
(b)	20	:	— — — — —
(c)	40	:	.....
(d)	60	:	—. —. —.
(e)	80	:	— — . — —., and
(f)	150	:	o o o o o

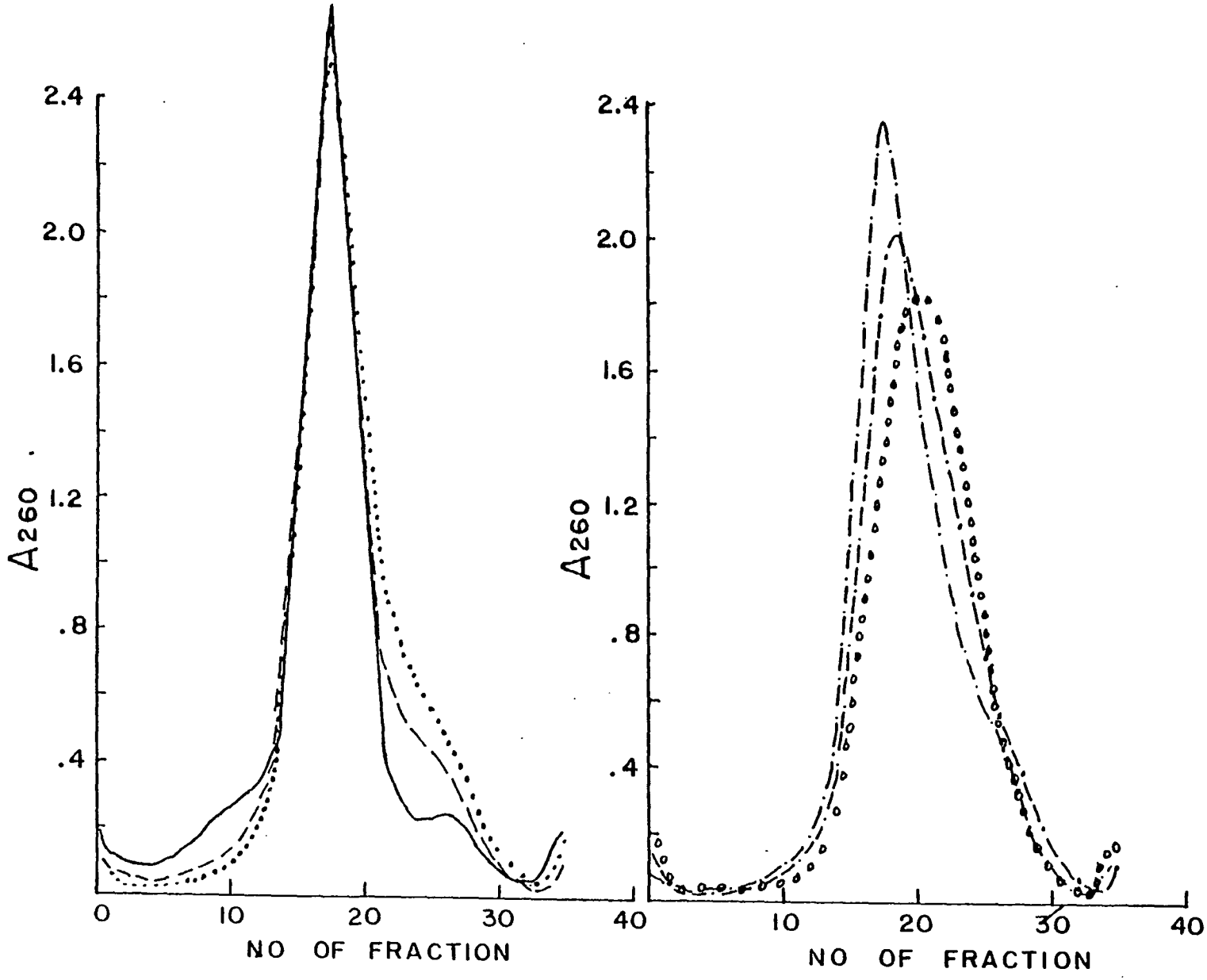
2.4
2.0
1.6
1.2
.8
.4
A260
0
10
20
30
40
NO OF FRACTION
2.4
2.0
1.6
1.2
.8
.4
A260
10
20
30
40
NO OF FRACTION

DNA-histones mixture from reconstituting into a compact nucleosome-like complex.

The physical properties for the reconstituted monomer fractions in Fig. 38a-c are still found to be nearly identical to the native material. However, the other complexes in Fig. 38d, e, f have slightly different physical properties: smaller sedimentation coefficients (10.2 to 8.7S); an increase in DNA ellipticities ($(\theta)_{280}$= 2 to $3x10^3$ deg. cm^2/decimole) and a decrease in α-helical content ($(\theta)_{225}$ = 35 to $30x10^3$ deg. cm^2/decimole); and a decrease in melting temperature, Mp = 72° C. to 70° C.

When the native nucleosome core particles have been denatured in 6M urea plus 2M NaCl and spin labeled to different extents, the fractionation patterns of the reconstituted complexes are shown in Fig. 39 respectively. Again, a major monomer peak has been obtained for the non spin labeled complexes. This further supports that a nucleosome-like complex can be reconstituted from the DNA and the urea-denatured histone cores. When only 4% of the tyrosyls are labeled, a non-nucleosome DNA-histone complexes appears as the "shoulder" in the fractionation profile (Fig. 39a). This shoulder increased as more tyrosyls (8 to 30% tyrosyls) were modified by the IMDSL (Fig. 38c, d and e). At the same time, there was a decrease in the monomer fraction. When 40% of the tyrosyls in the histones were labeled, the resulting complexes sedimented at a position equivalent to 8S (Fig. 39f). These observations further confirm our previous experiments that more of the 'buried' tyrosyls become accessible to the IMDSL when the nucleosome core particles have been treated with higher urea concentration, and the labeling of those'buried' tyrosyls has prevented the proper

Fig. 39 Fractionation prfiles for the reconstituted nucleosome core complexes (6 M urea)

Nucleasome core particles were previously denatured in 2 M NaCl plus 6 M urea and spin labeled with various amounts of molar excess of IMDSL:

	(SL/tyr)		
(a)	0	:	————————
(b)	20	:	- - - - - - - -
(c)	40	:	.....
(d)	60	:	-.-.-.-.-.-.-
(e)	80	:	— — .— —.
(f)	150	:	o o o o o
(g)	$\frac{\text{Acetylimidazole}}{\text{tyr}}$=60	:	X X X X X

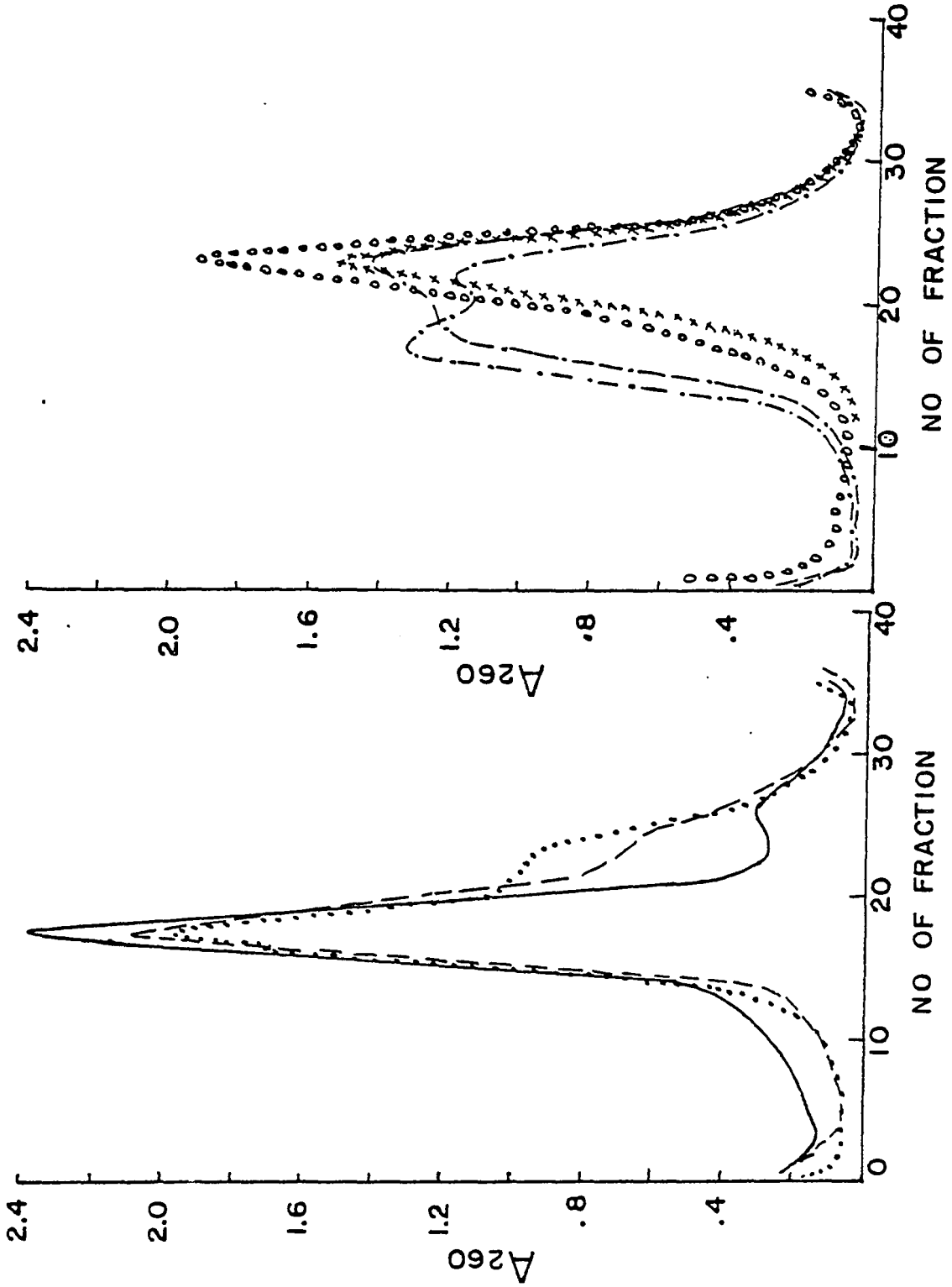
A260
2.4
2.0
1.6
1.2
.8
.4
0
10
20
30
40
NO OF FRACTION
A260
2.4
2.0
1.6
1.2
.8
.4
10
20
30
40
NO OF FRACTION

reassociation process. It is found that the DNA still can bind to the labeled histones, but the modified histones cannot form the proper histone core when some of its "buried" tyrosyls are labeled by the IMDSL.

The effect of the bulky group from the spin label (nitroxide) on preventing the reassociation process has been studied by using the non-spin-labeled N-acetylimidazole. Fig. 39g shows the fractionation profile for the reconstituted complexes when the native material has been previously treated with molar excess of N-acetylimidazole instead of the IMDSL. Again, when the "buried" tyrosyls have been acetylated by the N-acetylimidazole, no nucleosome-like complexes can be reconstituted as shown in Fig. 39f. Thus, all the above experiments clearly demonstrate that the "buried" tyrosyls in the histone core are essential in the proper histone-histone interactions which stabilize the intact inner histone core structure and the size of the reporter nitroxide makes little difference. Modifications on such residues will eventually prevent the compaction of the core DNA into the nucleosome complex.

(3) Distribution of the labeled tyrosyls

In this dissertation, we have found that only 4 tyrosyls in the native nucleosome core particle are accessible to the IMDSL and 12 tyrosyls in the histone core (an octomer with 2 each of the H2A, H2B, H3 and H4) can be modified. This raises the important question: which histone has been labeled? Which tyrosines in that histone have been labeled? At what position? The answers to such questions are not impossible but require tedious and laborious work. We have attempted to answer the question with the following experiments.

Fractionation of the histones into individual fractions by conventional chromatographic methods (see review in 11) requires the treatment of the histone samples with strong acid (below pH2). Such a condition is unfavorable to the labeled tyrosyls because the nitroxide spin label is hydrolyzed at pH below 2. Selective dissociation of the histone pairs from the chromatin by a change of ionic strength has been reported by Ohlenbusch et al. (72). Faulhaber and Bernardi (141) modified such an idea to fractionate histone pairs by using the hydroxyapatite column. Recently, Simon and Felsenfeld (92) have reported a new procedure for purifying histone pairs H2A + H2B and H3 + H4 from the chromatin by using hydroxylapatite. We, with the help of Dr. Tom Grover, have adopted such a procedure to fractionate the histone pairs from the spin labeled nucleosome or the reconstituted and spin labeled nucleosome complex.

Fig. 40 shows the hydroxylapatite column chromatography for the nucleosome. It is found to be quite similar to the one reported by Simon and Felsenfeld (92) although we have used KCl instead of NaCl as suggested by them (note: we have a solubility problem at the high concentration of NaCl in the phosphate buffer). The peak in 0.63M KCl is due to the overloading of the sample and a poorer binding of hydroxylapatite with the core DNA since our samples have been depleted of histone H1 and H5. The peak in 0.93M KCl contains equimolar H2A and H2B while the peak in 2M KCl contains equimolar H3 and H4. The core DNA elutes last in 0.5M potassium phosphate, pH7.6 without KCl.

Fig. 40 Hydroxylapatite column chromatography

Nucleosome core particles containing 5 mg of DNA in 0.63 M KCl, 0.1 M potassium phophate, pH 6.7, was loaded onto a 2x18 cm column, and eluted in 3 ml fractions at 30 ml/hour. The NaCl concentration of the running buffer is indicated by the dashed line. The concentration of potassium phosphate (pH 6.7) was maintained at 0.1 M until tube 120, then stepped to 0.5 M. The optical absorbance of the fractions was monitored at 230 nm (●—●—●) and 260 nm (○—○—○).

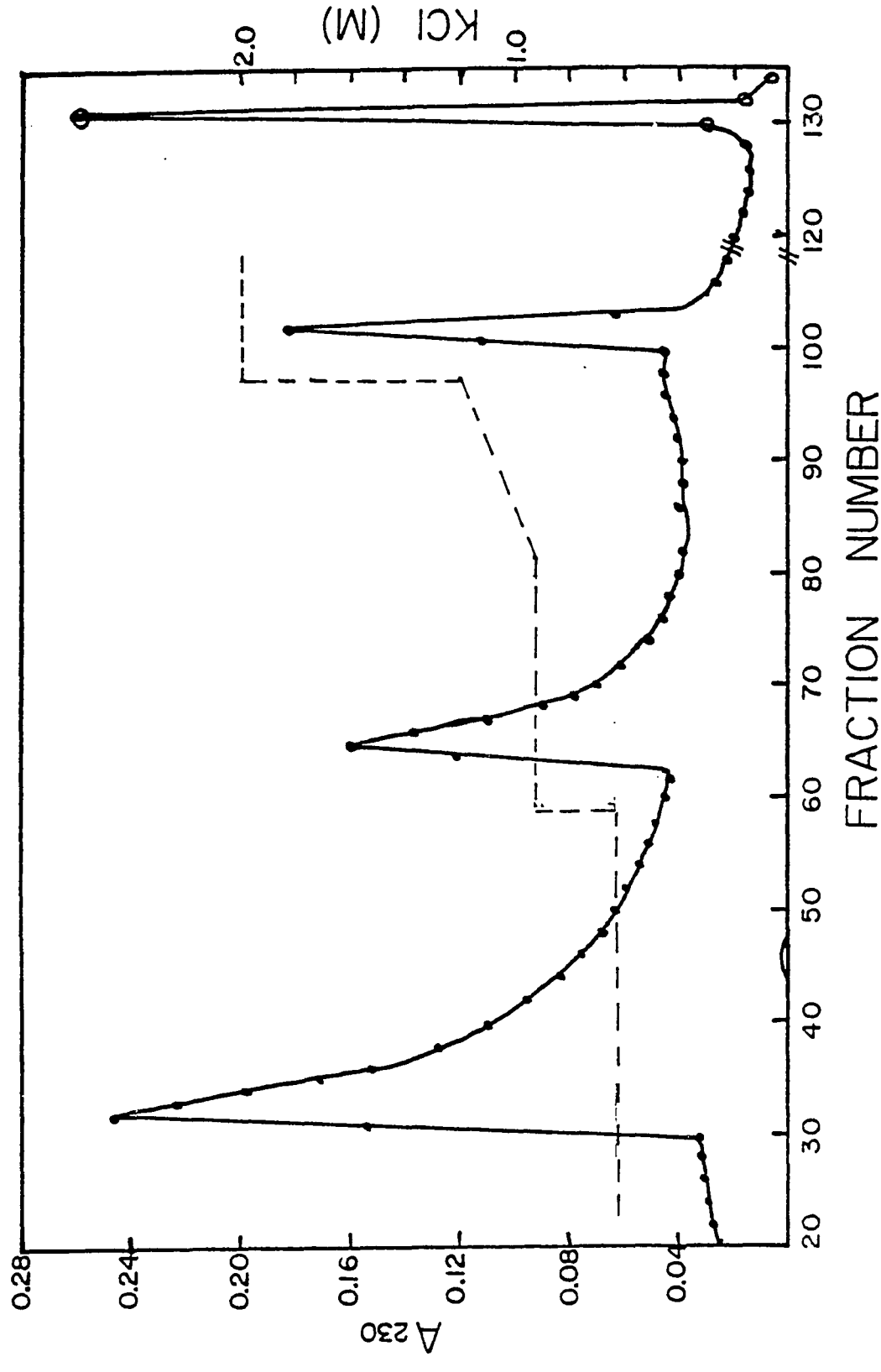
KCl (M)
2.0
1.0
A 230
0.28
0.24
0.20
0.16
0.12
0.08
0.04
20
30
40
50
60
70
80
90
100
120
130
FRACTION NUMBER

Spin labeled histone pairs H2A + H2B and H3 + H4 from the spin labeled uncleosome core particles or from the reconstituted and spin labeled nucleosome complexes were purified by the hydroxyapatite column in the same manner. The histone pairs were pooled, concentrated and analyzed for protein concentrations by the method of Lowry et al(142), using purified calf thymus histone H4 as the standard. The ESR spectra for the fractionated samples were recorded and the concentrations of the bound spin labels were calculated by double integration of the ESR spectra as described previously. The distribution of the labeled tyrosyls among the histone pairs from the nucleosome core particle or the reconstituted nucleosome complex is given in Table 6.

From Table 6, we can see that the four labeled tyrosyls in the nucleosome core particle are distributed in almost equal quantity among the histone pairs H2A + H2B and H3 +H4. For the reconstituted complex, the native sample was dissociated in 2M NaCl and therefore more surface tyrosyls on the histone core were labeled by IMDSL. In this case we find that 2 out of the 8 tyrosyls in the histone pair H2A + H2B have been labeled, while 3 out of 7 tyrosyls in the histone pair H3 + H4 have been modified.

TABLE 6

DISTRIBUTION OF LABELED TYROSYLS IN HISTONE PAIRS

	H2A + H2B FROM NUCLEOSOME	H3 + H4 FROM NUCLEOSOME	H2A + H2B FROM RECONSTITUTED NUCLEOSOME	H3 + H4 FROM RECONSTITUTED NUCLEOSOME
NO OF TYROSYLS LABELED	0.80	1.2	2.1	3.3
TOTAL TYROSYLS	8	7	8	7
% OF TYROSYLS LABELED	10.0%	17%	26%	47%
TOTAL TYROSYLS LABELED IN NUCLEOSOME	4		10.7	

IV. DISCUSSION

(A) Organization of the nucleosomes in the chromatin fiber

There is now good evidence that the organization of DNA into nucleosomes, the repeating subunits of chromatin in the eukaryotic genome, constitutes the first level of packaging of DNA in the interphase nucleus or metaphase chromosome (2,3,23,24). The nucleosomes, generated from brief digestion of chromatin by micrococcal nuclease, contain a histone core (two each of the four histones H2A, H2B, H3 and H4) complexed with a repeat length of about 200 base-pairs of DNA (3,24). However, the contraction in the length of the DNA (about 6.8-fold) achieved in the nucleosome is clearly insufficient to account for the packaging of DNA even in interphase chromatin, and higher levels of folding of the nucleosomes must exist. The two basic levels of folding- the folding of DNA in the nucleosome and the folding of nucleosomes in chromatin fibers - seem to be due solely to the interactions of DNA and histones. In order to better understand the overall structure of the nucleosome and the interactions between the nucleosomes which contribute to the structure and stability of chromatin fiber, chromatin has been briefly digested, and subunits have been isolated and characterized by their circular dichroism spectra as well as their thermal denaturation profiles.

Indeed, the chromatin fiber appears to consist of discrete superbeads, forming from 6 to 8 nucleosomes, along the fiber axis, according to our digestion studies on the rat liver nuclei by the Mg^{+2}, Ca^{+2} dependent endogeneous endonuclease. By plotting the weight average number of subunits against digestion time, as shown in Fig. 9, a slow-down in the rate of change of chromatin fragments is found in the region of around six subunits. This observation may imply that the nucleosomes

are somehow folded into a chain of discrete superstructures, with 6 to 8 subunits per superbead. It is possible, then, that the DNA between such superbeads is more susceptible to the nuclease digestion than the linker DNA between the nucleosomes. Therefore, at the early stage of digestion, there will be an accumulation of the superbeads, or multiples of the superbeads. The mononucleosomes become the dominant species in the fractionation profiles only after longer digestion time (Fig. 8). Our observation here has been confirmed by Hozier et. al. (143) who has found similar results by using micrococcal nuclease instead of the endogeneous endonuclease. Knobby superstructures of 200 Å in diameter along the chromatin fiber have also been reported in the electron microscopy (54,144-147), X-ray diffraction (52,53) and neutron scattering studies (51). A Solenoidal model has been proposed by Finch and Klug (54) to describe the arrangement of the nucleosomes into the superstructure forming the chromatin fiber of 200-300 Å in diameter. Higher-order structure of the mitotic chromosome has also been reported by Bak et. al. (148) to describe the further condensation of the chromatin superstructures in the human mitotic chromatides.

Circular dichroism and thermal denaturation studies on the chromatin and its subunits here, have provided another view on the structure and stability in the chromatin fiber. We have shown that the chromatin and its subunits have suppressed DNA ellipticities in their circular dichroism spectra (Fig. 10). These observations possibly reflect the delicate interactions between DNA and histone core leading to the compact supercoiling of the core DNA on the histone core. Upon assembly of the nucleosomes to form a chromatin fiber, the ellipticity increases until the value of chromatin is achieved and we have found

that at least 8 nucleosomes are required to give the ellipticity of the chromatin (Fig. 12). This suggests that the nucleosomes are possibly assembled in an asymmetric fashion (a superical array) in the chromatin fiber, consistent with the Solenoidal model proposed by Finch and Klug (54).

Perturbation of the DNA helix-coil transition in the chromatin and its subunits by thermal denaturation has reflected the forces which maintain their structures. Monophasic melting profiles have been obtained for the subunits and the chromatin (Fig. 13) which suggest that the electrostatic stabilization of the DNA by the histones is evenly distributed on the chromatin and its subunits. Biphasic melting profiles with a premelt region at 60^{o}C are obtained only for samples with depleted histones H1 and H5 (Fig. 16). The overall thermal denaturation studies on the chromatin and its subunits suggest that the nucleosomes in the native chromatin are closely bound to one another, leading to a rather continuous fiber structure.

(B) Accessibility and conformational state of specific tyrosyl residues in the histone core and in the nucleosome core particle

In this dissertation, we have demonstrated that ESR spin labeling is a powerful technique for probing various structural aspects and conformational changes of the histone core and nucleosome core particle. The spin label, N-(2,2,5,5-tetramethyl-3-carbonyl-pyrrolidine-1-oxyl)-imidazole, is found to be stable and specific for tyrosyls of the histone proteins under appropriate conditions. The specificity of the IMDSL has been shown indirectly through competition studies with N-acetyl imidazole (Fig. 18). Saturation binding studies for IMDSL in both

histone core and nucleosome core particles (Fig. 22) provide further indirect evidence of the specificity of IMDSL towards tyrosyl residues. Since there are about 20% basic residues (His, Lys, and Arg) compared to only 3% of tyrosyls in the histone core, if the IMDSL does bind non-specifically with the free amino groups in the basic residues, a multiplicity of bound spins will result. However, in actual fact, the maximum bound spin concentration is estimated to be only 1.2% of the total 491 x 2 residues in the histone core and less than 0.4% of the amino acids in the nucleosome core particle. Besides, under the labeling conditions used, (pH 7.2), most of the basic residues are protonated, and IMDSL only binds with unprotonated free amino groups besides the free tyrosyls. It has further been demonstrated that labeling of the tyrosyls in the nucleosome core particle is a gentle and specific modification, leading to a high degree of retention of native structure for the particle. Both native and labeled nucleosome core particles have the same sedimentation coefficient ($S_{20,w}$ = 10.5 ± 0.2S); the circular dichroism spectra (Fig. 17) are nearly identical and the thermal denaturation profiles (Fig. 16) are virtually the same, suggesting the integrity of the nucleosome core structure in the labeled particle.

There are 15 tyrosines in the four core histones (H2A, H2B, H3 and H4) and most of these tyrosines are located at the apolar central regions of the histones (2,11). Nuclear magnetic resonance studies by Bradbury and co-workers (149-151) have shown that the histone core is comprised of the histone complexes which are held together by interactions between structured apolar central and carboxyl regions of the proteins. Recently, Whitlock and Stein (152) have demonstrated the importance of these apolar central and carboxyl regions of the four histones in the

formation of the histone core and in the organization and stabilization of the DNA within the nucleosome core complex. Probing the accessibility and conformational state of the tyrosyls then in both native histone core and nucleosome should provide information on the structural aspects of the histone core and nucleosome particles. As we have shown here (Fig. 22), approximately 40% of the tyrosyls in the histone core are accessible to IMDSL under nondenaturing conditions and most of the labeled tyrosyls are located near the surface of the histone core (Fig. 23a). This observation agrees with the Laser-Raman Spectroscopy studies (111,153), which showed that 60% of the tyrosines are hydrogen-bonded within the inner histone core and nucleosome core. Less than 15% of the tyrosyls in the native nucleosome core particle are labeled by the IMDSL (Fig. 22), and most of these labeled tyrosyls are located in a rather hydrophilic but quite viscous environment (Fig. 24a). The 3- to 4-fold difference in reactivity between histone core and nucleosome core towards IMDSL supports the notion that DNA is indeed wrapped around the histone core, thus decreasing the accessibility of the tyrosyls. Saturation binding studies, on both histone core and nucleosome core, suggest that the labeled tyrosyls are distributed on well defined and stable three dimensional structures of both samples. It is found that the labeled tyrosyls are in a more viscous and more constrained environment in the nucleosome core particle than in the histone core, indicating a certain amount of histone-DNA interaction near the labeled tyrosyls in the nucleosome complex.

When the histone pairs H2A + H2B and H3 + H4 have been purified from the spin labeled nucleosome core particle by the hydroxylapatite column, we have found that 10% of the 8 tyrosyls residues in

histone pair H2A + H2B have been labeled by the IMDSL, while 17% of the 7 tyrosyls in the histone pair H3 + H4 have been modified. We have also found that, when the nucleosome core particle has been spin labeled in 2 M NaCl, 26% of the tyrosyl residues in the histone pair H2A + H2B have been modified and 47% of the tyrosyls in the H3 + H4 have been spin labeled. At present, unfortunately, we do not have any further information to locate the exact position of the labeled tyrosyls among the individual histones.

(C) Conformational changes in the spin labeled histone core and nucleosome core particle

Conformational perturbation of native chromatin by urea is a useful method for studying chromatin structure. In fact, an abundance of data about disruptive effects of urea on chromatin have been reported using circular dichroism, electron microscopy, hydrodynamics, low-angle X-ray scattering, nuclease digestion, sedimentation and thermal denaturation methods (see ref. in 154 and 155). In this dissertation, the ESR spin labeling technique has also been shown to be a very powerful method for detecting conformational changes in the histone core due to urea treatment. The effect of urea on the conformational state of labeled tyrosyls in both the nucleosome core and histone core suggest that the microenvironment of the labeled tyrosyls is very sensitive to conformational pertubation by this denaturant. The transition profile for the labeled histone core shown here (Fig. 25a) is very similar to that obtained from CD studies reported by Olins et. al. (Fig. 5D in 154), even though ESR and CD techniques are measuring two different properties of the histone core. ESR spin labeling measures the rigidity of the labeled tyrosyls, while CD measures the orientation of the peptide planes

relative to one another in the histones. Olins et. al. (154) have demonstrated by CD studies that 50% denaturation of $(\theta)_{223}$ occurs at approximately 6 M urea and the disruption of the α-helix in the histone core by urea is highly cooperative. Since we have observed a parallel sharp change in the labeled tyrosyls at 6 M urea, this may imply that the spin labels are located at or near the α-helical regions of the histone core. Olins et. al. (154) have also demonstrated the disruptive effects of urea on the nucleosome core particle by CD studies. They have shown that the denaturation of the α-helix in the inner histone core is highly cooperative, 50% denaturation (of the ellipticity at λ = 223 nm) occurs at approximately 5 M urea, with no significant effect up to 3 M urea; denaturation is complete at 7 M urea. They have also shown a linear release of the suppressed spectrum for the core DNA with increased urea concentration (0 to 7 M). Thus, we see that the sigmoidal transition profile for the nucleosome core particle (Fig. 25b) obtained by the ESR spin labeling method has revealed the composite disruptive effects of urea on both DNA and the inner histone core. A conformational change of the superhelical core DNA as detected by CD is also reflected in the ESR spectra as a change in the mobility of the labeled tyrosyls. This may imply that the labeled tyrosyls are located close to some of the DNA-histone binding sites.

The effect of ionic strength on chromatin structure is an interesting phenomenon and has yielded a good deal of information about DNA-histone and histone-histone interactions (2,3,13,23). Earlier work by Ohlenbusch et. al. (72) showed that histones (H1, H2A, H2B, H3 and H4) could be selectively dissociated from the calf thymus nucleoprotein by varying the ionic strength. Complex formation studies on

histones by Isenberg et. al. (see ref. in 57-59) suggest that the histones are able to form both dimeric or tetrameric complexes under appropriate ionic conditions. Weintraub et. al. (60) have presented evidence for a stable heterotypic tetramer (H2A, H2B, H3 and H4) in 2 M NaCl solution. Olins and co-workers supported Weintraub's finding and further suggested that an octamer could be formed from a pair of the heterotypic tetramers when the ionic strength was further increased from 2 M NaCl to 4 M NaCl. Electron microscopic and nuclease digestion studies by Oudet et. al. (158) suggested that, at very low ionic strength and low temperature, the compact nucleosomal structure could be converted to half-nucleosomes and to extended structures. Recently, hydrodynamic studies by Gordon et. al. (159) showed that two salt-dependent conformational transitions occurred in the nucleosome. Structural transitions of the nucleosome due to ionic effects as detected with fluorescent probes have also been reported (160-162). More recently, cross-linking agents, such as tetranitromethane and UV irradiation, have also been applied to study the mechanism of nucleosome unfolding by ionic effect (163).

The ESR spin-labeling results presented here provide additional insight as to the effect of ionic strength on the nucleosome core particle. From the above ESR spin labeling and CD data, we see that the overall conformation of the nucleosome core particle is not greatly affected by NaCl in the range of 1 mM to 80 mM. The tumbling environment for the labeled tyrosines (Fig. 28) is only slightly less viscous in the range of 15 mM to 80 mM than in the range of 1 mM to 8 mM. The DNA ellipticity and α-helical content of the histone core changes only slightly in this range of NaCl. These observations suggest that there is only a minor change in the quarternary or tertiary structure of the

nucleosome core, as the ionic strength is increased from 1 mM to 80 mM. The linear increase in the tumbling motion for the labeled tyrosyls in the range of 0.1 M to 0.5 M (Fig. 28), however, correlates very well with changes in some of the tertiary and secondary structures within the inner histone core, as evidenced from the CD data (Fig. 29a). Another linear increase in tumbling motion of the labeled tyrosyls occurs between 0.7 M and 1.8 M NaCl (Fig. 28), and this can be correlated with the gradual release of DNA from the histone core, as shown in the CD data (Fig. 29b). It is obvious that the DNA is completely released from the histone core at 1.8 M NaCl. The shoulder, observed between 0.4 M and 0.7 M NaCl for the labeled tyrosyls, is due possibly to the overlapping effect of the conformational changes in the histone core and the gradual release of the DNA from the histones. Above 2 M NaCl, the DNA is completely released from the histone core; this is followed by a decrease in tumbling motion for the labled tyrosyls, suggesting that there is a tightening in the overall structure of the histone core as the ionic strength is further increased. However, the α-helical content of the histone core remains constant, and is the same as its original value at lower ionic strength, as shown by the CD data (Fig. 29a). It is known that the ellipticity at 285 nm for free DNA at lower ionic strengths is around 8×10^3 deg-cm^2/decimole. The suppression in ellipticity for the core DNA at 2 M NaCl and above is possibly due to the dehydration-induced shift in the tilt of the DNA bases as suggested by Li et. al. (164). We see that both ESR and CD methods provide complementary information on the conformational changes due to the ionic effect. It is suggested that the three major transitions observed here between 0.1 M to 2.5 M can be interpreted as: swelling and conformational changes in the inner

histone core; gradual separation of DNA from the histone core; and tightening of the histone core.

Based on the identical α-helical contents, it has been generally assumed that the conformation of the histone core in 2 M NaCl is the same (or close) as it is in the native nucleosome under lower ionic strength. However, we have noticed that before the separation of the DNA from the inner histone core, there is a conformational change within the inner histone core. Unless such a conformational change is reversible, the integrity of the histone core in 2 M NaCl being the same as it is in the native state is questionable. Indeed, our spin labeling and CD data confirmed that the conformational change of the inner histone core in 0.1 M to 0.7 M NaCl is reversible. Our CD data clearly has shown that the α-helical content of the histone core returns close to its original value as the ionic strength is increased to above 1.5 M NaCl. And our spin labeling data has demonstrated that the ESR spectrum (Fig. 24b) for the labeled nucleosome core particle in 2 M NaCl is almost the same as the labeled histone core (Fig. 23a) in 2 M NaCl. However, we do not have evidence to show that the labeled histone core in 2 M NaCl is an octamer or a heterotypic tetramer.

The minor changes observed in the lower ionic strength range for the labeled tyrosyls are difficult to interpret since circular dichroism data in the same ionic strength range do not show any drastic change in ellipticity for either DNA or the histone core. Changes in peak-height ratio for the labeled tyrosyls, from 15 mM to 70 mM NaCl may suggest that there is a small swelling of the nucleosome core particle. We do not have enough evidence, however, to suggest that swelling of the labeled nucleosome core at room temperature at this low ionic strength

has caused a splitting of the particle into two half-nucleosomes. The study of the accessibility of tyrosyl residues in the nucleosome core particle in different ionic strengths has further supported the above observation. An increase of labeling will be expected if the nucleosome core particle indeed splits into two half-nucleosomes at very low ionic strength. Contrarily, only 10% of the tyrosyl residues are accessible to the IMDSL in the range of 0.1 mM to 0.3 M NaCl as shown in Fig. 30. A maximum of 40% of the tyrosyl residues can be labeled only when the nucleosome core particle has been treated with 2 M NaCl. Oudet et. al. (158), however, have observed the formation of two half-nucleosomes at very low ionic strengths and at low temperatures ($0^{o}C$). Gordon et. al. (159) have also reported the observation of conformational changes for the nucleosome core at a low ionic strength by hydrodynamic studies. We suspect that in vitro, additional factors such as low temperature or high centrifugal forces are needed, besides the lower ionic strength condition in order for the whole nucleosome to split into two half-nucleosomes.

According to the spin labeling studies present here, spin labeled nucleosome core particle is found to be stable over a pH range of 9.5 > pH > 4.5. Beyond this pH range, the nucleosome either aggregates or the nitroxide becomes hydrolyzed. However, a conformational change in the nucleosome at pH below 4.5 has been reported by Zama et. al. (165), using circular dichroism, fluorescent probe and laser Raman speatroscopy. At 4.6 > pH > 4.2, they find a large change in DNA conformation, with a slight loss of histone α-helix content.

(D). Reconstitution of nucleosome core particles

An important aspect of the chromatin research comes from the study of reconstitution. Reconstitution is one of the most useful biochemical methods for examining the role of individual components in a macromolecular assembly such as the chromatin complex. Full potential of this approach is achieved only when individual histones and DNA can be purified and reintegrated into the complex in a native state. The reconstituted product is valid only when it is shown to be functionally and (or) structurally identical with the native material. In the absence of a suitable biologically functional assay for the fidelity in the reconstituted product, several biophysical and biochemical methods are always employed (43, 73-75, 89, 136-140). For example, both individually purified histones and histone complexes, used in the reconstitution of chromatin, have resulted in the ultrastructure of nucleosome in electron micrographs (43), characteristic X-ray diffraction maxima (74), and limited nuclease digestion products (73). Tatchell and Van Holde (89) have demonstrated that nucleosome core particles can be reconstituted from salt-extracted histone cores and core DNA. The purified reconstituted particles appear to be identical with native core particle by a variety of criteria (sedimentation, velocity, histone content, circular dichroism, DNA melting profile, and patterns of digestion by micrococcal nuclease, DNase I, and tyrpsin).

In this report, we have demonstrated that ESR spin labeling is also a very powerful technique for studying the mode of nucleosome reconstitution and identifying the role of tyrosyl residues in the reassociation process. Judging from the tumbling

constraint on the labeled tyrosyls in the histone core, we find that DNA binds to histone core progressively in the range of 2M to 0.3M NaCl. Full association between DNA and histone core occurs when the ionic strength is below 0.25M. However, our experiments cannot distinguish any preferential binding between DNA and individual histones at various stages of reconstitution. Using SDS gel electrophoresis, Wilhelm, et al (138) have found that H3 + H4 bind first to the DNA and H2A + H2B bind to the DNA only after H3 + H4 are completely bound. Their data seems to suggest that histones H3 + H4 appear as a tetramer and H2A + H2B as a dimer in 2M NaCl before reconstitution begins. We have started our reconstitution with native histone core and core DNA. Our data suggests that binding of DNA to the histone core has prevented the histone core from dissociating into (H3)2 (H4)2 tetramer and (H2A + H2B) dimer during various stages of reassociation.

The role of tyrosines in the association of proteins and nucleic acids has been recently reported by Mayer et al (166). They have shown that tyrosyl side chains from the oligopeptides can give rise to both stacking and hydrogen-bonding interactions in the complex formation with nucleic acids. They have also suggested that tyrosine may be involved through the stacking interactions in the selective recognition of single stranded nucleic acids by proteins (166). The contact site cross-linkers tetranitromethane and UV irradiation have been used to generate H2A-H2B dimers and H2A-H2B-H4 trimers from nuclei and chromatin by Martinson et al (167). They have demonstrated that some of the tyrosyl residues in H2B are involved in the H2A-H2B and H4-H2B interactions (163, 167). In this dissertation, we have

shown that spin labeled histone core can be reconstituted or re-associated back into nucleosome core-like complex, provided that the 'buried' tyrosyls in the histone core have not been modified. The ESR spectra for the purified, reconstituted nucleosome complex do not show any strong immobilization of the labeled tyrosyl residues. These experiments suggest that the 'surface' tyrosyls are possibly not involved in the histone-DNA interactions.

On the contrary, when the 'buried' tyrosyl residues have been labeled, even in small quantity, we find that the results of the reconstituted nucleosome complexes are affected as shown in Fig. 38 and Fig. 39. Some other histone-DNA complexes are formed instead of nucleosome particles, when more 'buried' tyrosyls have been modified. Our results clearly demonstrate that urea has disrupted the tertiary and secondary structures of the histones, exposing those 'buried' tyrosyl residues to the IMDSL. If those tyrosyl residues remain unmodified by the IMDSL, the dissociated complex can still reassociate back into native structure (Fig. 38a, Fig. 39a), showing that urea denaturation of histones is reversible. However, if those 'buried' tyrosyl residues have been modified, then proper histone-histone interactions leading to the histone core structure will be interupted. Eventually, these modifications will prevent the compact supercoiling of DNA into the nucleosome core particle.

In conclusion, ESR spin labeling technique has been applied to study various structural aspects and conformational changes of the hsitone core and nucleosome core particle. It is concluded that the labeling of the tyrosyl residues in the nucleosome core particle is a gentle and specific modification, leading to a high degree of retention of native structure for the particle. Saturation binding studies, on both histone core and nucleosome core particle, suggest that the labeled tyrosyls are distributed on well defined and stable three dimensional structures of both samples. Reconstitution of nucleosome studies as presented here, has illustrated that the compaction of core DNA in the nucleosome depends heavily on a well defined histone core structure. We have shown that some of those 'buried' tyrosyls are involved closely in the specific histone-histone interactions which are the vital forces for stabilizing the histone core structure. On the other hand, we have also demonstrated that the nucleosome core particle is a dynamic structure capable of undergoing reversible conformational transitions under appropriate conditions. Such conformational flexibility, therefore, could be an important factor in chromatin transcription and replication.

H1

```
                                                  10                                                  20
RTL-3  Ac -Ser-Glu-Ala-Pro-Ala-Glu-Thr-Ala-Ala-Pro-Ala-Pro-Ala-Glu-Lys-Ser-Pro-Ala-Lys- — - — -Lys-
Trout  Ac -Ala-Glu-Ala-Pro-Ala-Glu-Val-Ala- — -Pro-Ala-Pro-Ala-Ala-Ala-Pro-Ala-Ala-Lys-Ala-Pro-Lys-

                                        30                                                  40
RTL-3      Lys-Lys-Ala-Ala-Lys-Lys-Pro-Gly- — -Ala-Gly-Ala-Ala-Lys-Arg-Lys-Ala-Ala-Gly-Pro-Pro-Val-
Trout      Lys-Lys-Ala-Ala-Ala-Lys-Pro-Lys-Lys-Ala-Gly- — - — - — - — - — - — - — -Gly-Pro-Ala-Val-

                                  50                                                  60
RTL-3      Ser-Glu-Leu-Ile-Thr-Lys-Ala-Val-Ala-Ala-Ser-Lys-Glu-Arg-Asn-Gly-Leu-Ser-Leu-Ala-Ala-Leu-
Trout      Gly-Glu-Leu-Ile-Gly-Lys-Ala-Val-Ala-Ala-Ser-Lys-Glu-Arg-Ser-Gly-Val-Ser-Leu-Ala-Ala-Leu-

                            70                                                  80
RTL-3      Lys-Lys-Ala-Leu-Ala-Ala-Gly-Gly-Tyr-Asp-Val-Glu-Lys-Asn-Asn-Ser-Arg-Ile-Lys-Leu-Gly-Leu-
Trout      Lys-Lys-Ser-Leu-Ala-Ala-Gly-Gly-Tyr-Asp-Val-Glu-Lys-Asn-Asn-Ser-Arg-Val-Lys-Ile-Ala-Val-

                 90                                                 100                                                 110
RTL-3      Lys-Ser-Leu-Val-Ser-Lys-Gly-Thr-Leu-Val-Glu-Thr-Lys-Gly-Thr-Gly-Ala-Ser-Gly-Ser-Phe-Lys-
Trout      Lys-Ser-Leu-Val-Thr-Lys-Gly-Thr-Leu-Val-Glu-Thr-Lys-Gly-Thr-Gly-Ala-Ser-Gly-Ser-Phe-Lys-

                                             120                                                 130
RTL-3      Leu-Asn-Lys-Lys-Ala-Ala-Ser-Gly-Glu-Ala-Lys-Pro-Lys-Pro- — -Lys-Lys-Ala-Gly-Ala-Ala-Lys-
Trout      Leu-Asn-Lys-Lys-Ala- — - — -Val-Glu-Ala-Lys- — -Lys-Pro-Ala-Lys-Lys-Ala-Ala-Ala-Pro-Lys-

                                       140                                                 150
RTL-3      Pro-Lys-Lys-Pro-Ala-Gly- — - — - — -Ala-Thr-Pro-Lys-Lys-Pro-Lys-Lys-Ala-Ala-Gly-Ala-Lys-
Trout      Ala-Lys-Lys-Val-Ala-Ala-Lys-Lys-Pro-Ala-Ala-Ala-Lys-Lys-Pro-Lys-Lys-Val-Ala- — -Ala-Lys.

                                  160                                                 170
RTL-3      Lys-Ala-Val- — - — -Lys-Lys-Thr-Pro-Lys-Lys-Ala-Pro-Lys-Pro-Lys-Ala-Ala-Ala-Lys-Pro-Lys-
Trout      Lys-Ala-Val-Ala-Ala-Lys-Lys-Ser-Pro-Lys-Lys-Ala- — -Lys- — - — - — - — - — - — -Lys-Pro- — -

                            180                                                 190
RTL-3      Val-Ala-Lys-Pro-Lys-Ser-Pro-Ala-Lys-Val-Ala-Lys-Ser-Pro-Lys-Lys-Ala- — -Lys-Ala-Val-Lys-
Trout      — -Ala- — - — - — - — -Thr-Pro-Lys-Lys-Ala-Ala-Lys-Ser-Pro-Lys-Lys-Ala-Thr-Lys-Ala-Ala-Lys-

                       200                                                 210
RTL-3      Pro-Lys-Ala-Ala-Lys-Pro-Lys- — -Ala-Pro-Lys- — -Pro-Lys-Ala-Ala-Lys-Ala-Lys-Lys-Thr-Ala-
Trout      Pro-Lys-Ala-Ala-Lys-Pro-Lys-Lys-Ala-Ala-Lys-Ser-Pro-Lys-Lys-Val-Lys- — -Lys-Pro-Ala-Ala-

                                  225
RTL-3      Ala-Lys-Lys-Lys-Lys
Trout      Ala-Lys-Lys
```

H_{2A}

```
                                                                  10                                                  20
          Calf  Ac- Ser-Gly-Arg-Gly-Lys-Gln-Gly-Gly-Lys-Ala-Arg-Ala-Lys-Ala-Lys-Thr-Arg-Ser-Ser-Arg-
         Trout  Ac- Ser-Gly-Arg-Gly-Lys-Thr-Gly-Gly-Lys-Ala-Arg-Ala-Lys-Ala-Lys-Thr-Arg-Ser-Ser-Arg-
P. Miliaris  Ac- Ser-Gly-Arg-Gly-Lys-——-Gly-Ala-Lys-Gly-Lys-Ala-Lys-Ala-Lys-Ser-Arg-Ser-Ser-Arg-

                                                                  30                                                  40
          Ala-Gly-Leu-Gln-Phe-Pro-Val-Gly-Arg-Val-His-Arg-Leu-Leu-Arg-Lys-Gly-Asn-Tyr-Ala-
          Ala-Gly-Leu-Gln-Phe-Pro-Val-Gly-Arg-Val-His-Arg-Leu-Leu-Arg-Lys-Gly-Asn-Tyr-Ala-
          Ala-Gly-Leu-Gln-Phe-Pro-Val-Gly-Arg-Val-His-Arg-Phe-Leu-Arg-Lys-Gly-Asn-Tyr-Ala-

                                                                  50                                                  60
          Glu-Arg-Val-Gly-Ala-Gly-Ala-Pro-Val-Tyr-Leu-Ala-Ala-Val-Leu-Glu-Tyr-Leu-Thr-Ala-
          Glu-Arg-Val-Gly-Ala-Gly-Ala-Pro-Val-Tyr-Leu-Ala-Ala-Val-Leu-Glu-——-Leu-Thr-Ala-
          Asn-Arg-Val-Gly-Ala-Gly-Ala-Pro-Val-Tyr-Leu-Ala-Ala-Val-Leu-Glu-Tyr-Leu-Ala-Ala-
```

H_{2A}

```
                                                  70                                                  80
Glu-Ile-Leu-Glu-Leu-Ala-Gly-Asn-Ala-Ala- - - - - - - - -Arg-Asp-Asn-Lys-Lys-Thr-Arg-

Glu-Ile-Leu-Glu-Leu-Ala-Gly-Asx-Ala-Ala-Arg-Ile-Pro-Arg-Asx-Asx-Lys-Lys-Thr-Arg-

Glu-Ile-Leu-Glu-Leu-Ala-Gly-Asn-Ala-Ala- - - - - - - - -Arg-Asp-Asn-Lys-Lys-Thr-Arg-


                                                  90                                                  100
Ile-Ile-Pro-Arg-His-Leu-Gln-Leu-Ala-Ile-Arg-Asn-Asp-Glu-Glu-Leu-Asn-Lys-Leu-Leu-

- - -Ile-Pro-Arg-His-Leu-Gln-Leu-Ala-Val-Arg-Asn-Asp-Glu-Glu-Leu-Asx-Lys-Leu-Leu-

Ile-Ile-Pro-Arg-His-Leu-Gln-Leu-Ala-Ile-Arg-Asn-Asp-Glu-Glu-Leu-Asn-Lys-Leu-Leu-


                                                  110                                                 120
Gly-Lys-Val-Thr-Ile-Ala-Gln-Gly-Gly-Val-Leu-Pro-Asn-Ile-Gln-Ala-Val-Leu-Leu-Pro-

Gly-Gly-Val-Thr-Ile-Ala-Glx-Gly-Gly-Val-Leu-Pro-Asx-Ile-Glx-Ala-Val-Leu-Leu-Pro-

Gly-Gly-Val-Thr-Ile-Ala-Gln-Gly-Gly-Val-Leu-Pro-Asn-Ile-Gln-Ala-Val-Leu-Leu-Pro-


                                                  130
Lys-Lys-Thr-Glu-Ser-His-His-Lys-Ala-Lys-Gly-Lys

Lys-Lys-Thr-Glu- - - - - - - - -Lys-Ala-Lys-Val-Ala-Lys

Lys-Lys-Thr-Gly-Ser- - - - - - -Lys-Ser-Ser- - - - - - -Lys
```

H_{2B}

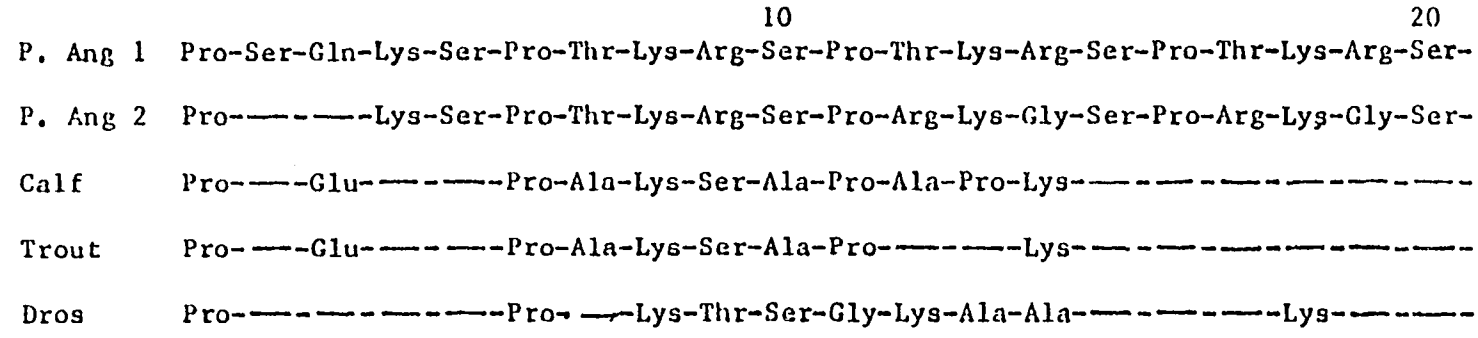
10
20
P. Ang 1 Pro-Ser-Gln-Lys-Ser-Pro-Thr-Lys-Arg-Ser-Pro-Thr-Lys-Arg-Ser-Pro-Thr-Lys-Arg-Ser-
P. Ang 2 Pro-------Lys-Ser-Pro-Thr-Lys-Arg-Ser-Pro-Arg-Lys-Gly-Ser-Pro-Arg-Lys-Gly-Ser-
Calf Pro---Glu-------Pro-Ala-Lys-Ser-Ala-Pro-Ala-Pro-Lys----------
Trout Pro---Glu-------Pro-Ala-Lys-Ser-Ala-Pro-------Lys----------
Dros Pro----------Pro---Lys-Thr-Ser-Gly-Lys-Ala-Ala-------Lys-------

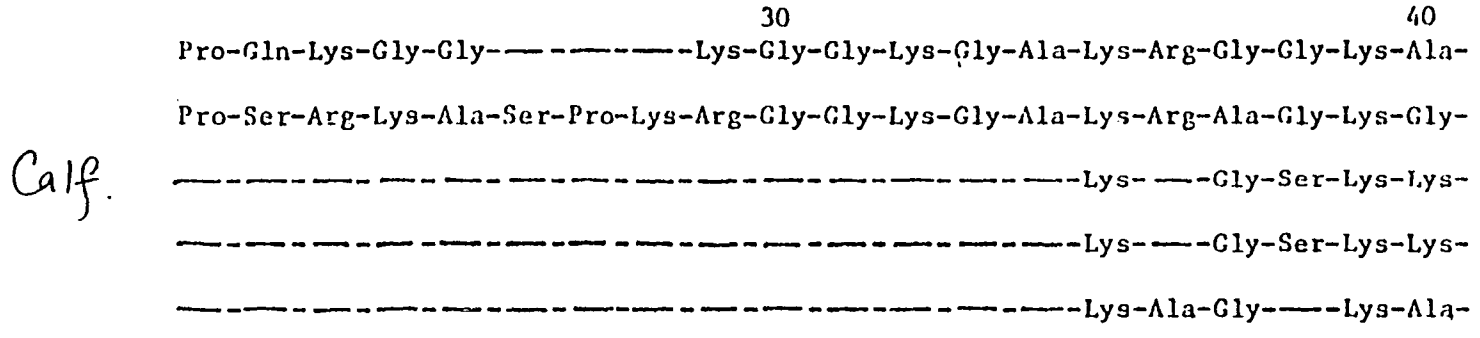
30
40
Pro-Gln-Lys-Gly-Gly---------Lys-Gly-Gly-Lys-Gly-Ala-Lys-Arg-Gly-Gly-Lys-Ala-
Pro-Ser-Arg-Lys-Ala-Ser-Pro-Lys-Arg-Gly-Gly-Lys-Gly-Ala-Lys-Arg-Ala-Gly-Lys-Gly-
Calf.
----------Lys---Gly-Ser-Lys-Lys-
----------Lys---Gly-Ser-Lys-Lys-
----------Lys-Ala-Gly---Lys-Ala-

H_{2B}

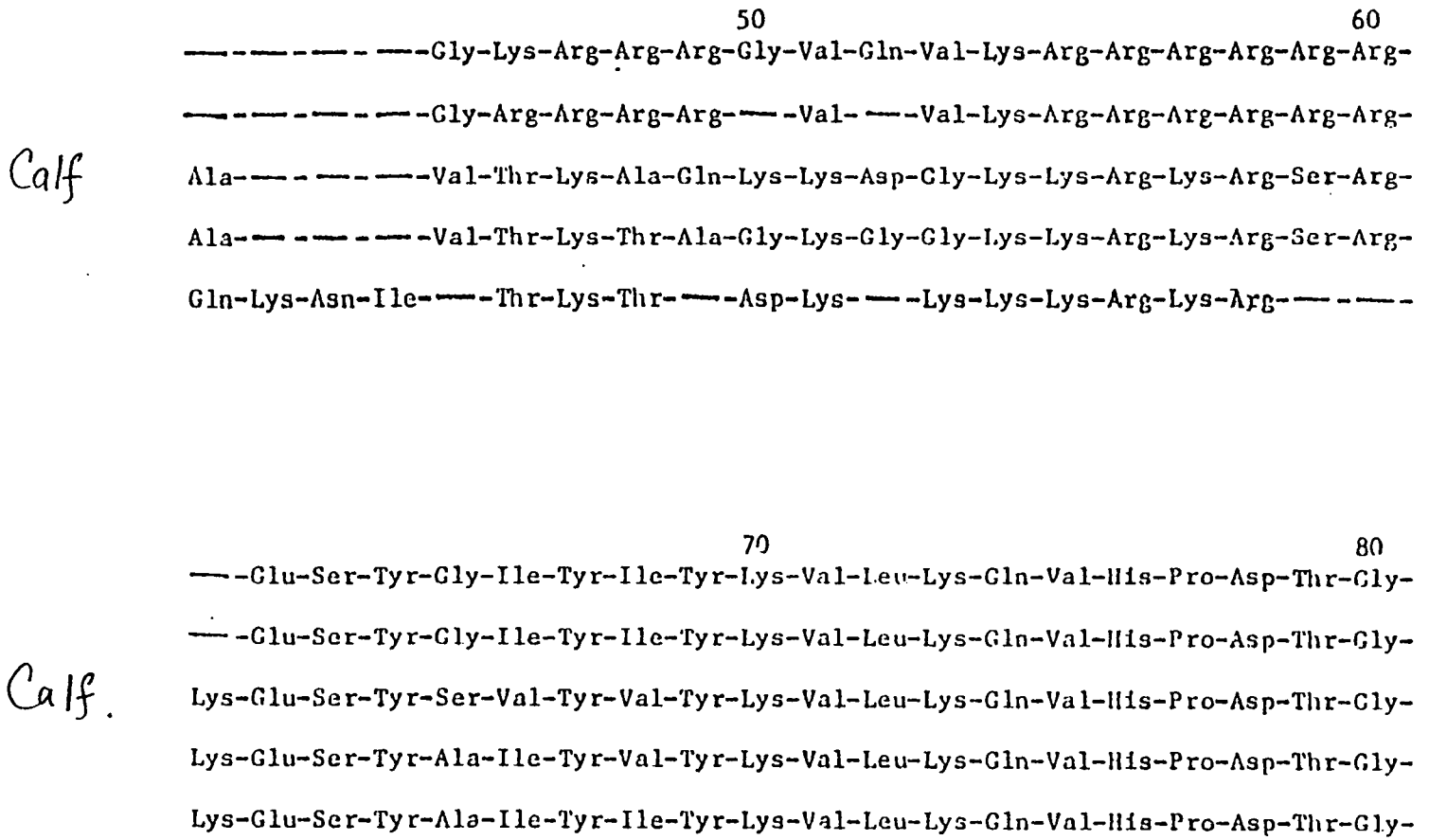
50
60
Gly-Lys-Arg-Arg-Arg-Gly-Val-Gln-Val-Lys-Arg-Arg-Arg-Arg-Arg-Arg-
Gly-Arg-Arg-Arg-Arg-Val-Val-Lys-Arg-Arg-Arg-Arg-Arg-Arg-
Calf
Ala-Val-Thr-Lys-Ala-Gln-Lys-Lys-Asp-Gly-Lys-Lys-Arg-Lys-Arg-Ser-Arg-
Ala-Val-Thr-Lys-Thr-Ala-Gly-Lys-Gly-Gly-Lys-Lys-Arg-Lys-Arg-Ser-Arg-
Gln-Lys-Asn-Ile-Thr-Lys-Thr-Asp-Lys-Lys-Lys-Lys-Arg-Lys-Arg-
70
80
Glu-Ser-Tyr-Gly-Ile-Tyr-Ile-Tyr-Lys-Val-Leu-Lys-Gln-Val-His-Pro-Asp-Thr-Gly-
Glu-Ser-Tyr-Gly-Ile-Tyr-Ile-Tyr-Lys-Val-Leu-Lys-Gln-Val-His-Pro-Asp-Thr-Gly-
Calf.
Lys-Glu-Ser-Tyr-Ser-Val-Tyr-Val-Tyr-Lys-Val-Leu-Lys-Gln-Val-His-Pro-Asp-Thr-Gly-
Lys-Glu-Ser-Tyr-Ala-Ile-Tyr-Val-Tyr-Lys-Val-Leu-Lys-Gln-Val-His-Pro-Asp-Thr-Gly-
Lys-Glu-Ser-Tyr-Ala-Ile-Tyr-Ile-Tyr-Lys-Val-Leu-Lys-Gln-Val-His-Pro-Asp-Thr-Gly-

H_{2B}

90 100

Ile-Ser-Ser-Arg-Ala-Met-Ser-Val-Met-Asn-Ser-Phe-Val-Asn-Asp-Val-Phe-Glu-Arg-Ile-

Ile-Ser-Ser-Arg-Ala-Met-Ser-Val-Met-Asn-Ser-Phe-Val-Asn-Asp-Val-Phe-Glu-Arg-Ile-

Calf Ile-Ser-Ser-Lys-Ala-Met-Gly-Ile-Met-Asn-Ser-Phe-Val-Asn-Asp-Ile-Phe-Glu-Arg-Ile-

Ile-Ser-Ser-Lys-Ala-Met-Gly-Ile-Met-Asn-Ser-Phe-Val-Asn-Asp-Ile-Phe-Glu-Arg-Ile-

Ile-Ser-Ser-Lys-Ala-Met-Ser-Ile-Met-Asn-Ser-Phe-Val-Asn-Asp-Ile-Phe-Glu-Arg-Ile-

110 120

Ala-Ala-Glu-Ala-Gly-Arg-Leu-Thr-Thr-Tyr-Asn-Arg-Arg-Ser-Thr-Val-Ser-Ser-Arg-Glu-

Ala-Gly-Glu-Ala-Ser-Arg-Leu-Thr-Ser-Ala-Asn-Arg-Arg-Ser-Thr-Val-Ser-Ser-Arg-Glu-

Calf Ala-Gly-Glu-Ala-Ser-Arg-Leu-Ala-His-Tyr-Asn-Lys-Arg-Ser-Thr-Ile-Thr-Ser-Arg-Glu-

Ala-Gly-Glu-Ser-Ser-Arg-Leu-Ala-His-Tyr-Asn-Lys-Arg-Ser-Thr-Ile-Thr-Ser-Arg-Glu-

Ala-Ala-Glu-Ala-Ser-Arg-Leu-Ala-His-Tyr-Asn-Lys-Arg-Ser-Thr-Ile-Thr-Ser-Arg-Glu-

H_{2B}

130 140

Val-Gln-Thr-Ala-Val-Arg-Leu-Leu-Leu-Pro-Gly-Glu-Leu-Ala-Lys-His-Ala-Val-Ser-Glu-

Ile-Gln-Thr-Ala-Val-Arg-Leu-Leu-Leu-Pro-Gly-Glu-Leu-Ala-Lys-His-Ala-Val-Ser-Glu-

Calf Ile-Gln-Thr-Ala-Val-Arg-Leu-Leu-Leu-Pro-Gly-Glu-Leu-Ala-Lys-His-Ala-Val-Ser-Glu-

Ile-Gln-Thr-Ala-Val-Arg-Leu-Leu-Leu-Pro-Gly-Glu-Leu-Ala-Lys-His-Ala-Val-Ser-Glu-

Ile-Gln-Thr-Ala-Val-Arg-Leu-Leu-Leu-Pro-Gly-Glu-Leu-Ala-Lys-His-Ala-Val-Ser-Glu-

150

Gly-Thr-Lys-Ala-Val-Thr-Lys-Tyr-Thr-Thr-Ser-Arg

Gly-Thr-Lys-Ala-Val-Thr-Lys-Tyr-Thr-Thr-Ser-Arg

Calf Gly-Thr-Lys-Ala-Val-Thr-Lys-Tyr-Thr-Ser-Ser-Lys

Gly-Thr-Lys-Ala-Val-Thr-Lys-Tyr-Thr-Ser-Ser-Lys

Gly-Thr-Lys-Ala-Val-Thr-Lys-Tyr-Thr-Ser-Ser-X

H_3

Calf

```
                                                  10                                                  20
Ala-Arg-Thr-Lys-Gln-Thr-Ala-Arg-Lys-Ser-Thr-Gly-Gly-Lys-Ala-Pro-Arg-Lys-Gln-Leu-

                                                  30                                                  40
Ala-Thr-Lys-Ala-Ala-Arg-Lys-Ser-Ala-Pro-Ala-Thr-Gly-Gly-Val-Lys-Lys-Pro-His-Arg-

                                                  50                                                  60
Tyr-Arg-Pro-Gly-Thr-Val-Ala-Leu-Arg-Glu-Ile-Arg-Arg-Tyr-Gln-Lys-Ser-Thr-Glu-Leu-

                                                  70                                                  80
Leu-Ile-Arg-Lys-Leu-Pro-Phe-Gln-Arg-Leu-Val-Arg-Glu-Ile-Ala-Gln-Asp-Phe-Lys-Thr-

                                                  90                                                  100
Asp-Leu-Arg-Phe-Gln-Ser-Ser-Ala-Val-Met-Ala-Leu-Gln-Glu-Ala-Cys-Glu-Ala-Tyr-Leu-

                                                  110                                                 120
Val-Gly-Leu-Phe-Glu-Asp-Thr-Asn-Leu-Cys-Ala-Ile-His-Ala-Lys-Arg-Val-Thr-Ile-Met-

                                                  130
Pro-Lys-Asp-Ile-Glu-Leu-Ala-Arg-Arg-Ile-Arg-Gly-Glu-Arg-Ala
```

H_4 Calf

```
                                                  10                                                  20
Ser-Gly-Arg-Gly-Lys-Gly-Gly-Lys-Gly-Leu-Gly-Lys-Gly-Gly-Ala-Lys-Arg-His-Arg-Lys-

                                                  30                                                  40
Val-Leu-Arg-Asp-Asn-Ile-Gln-Gly-Ile-Thr-Lys-Pro-Ala-Ile-Arg-Arg-Leu-Ala-Arg-Arg-

                                                  50                                                  60
Gly-Gly-Val-Lys-Arg-Ile-Ser-Gly-Leu-Ile-Tyr-Glu-Glu-Thr-Arg-Gly-Val-Leu-Lys-Val-

                                                  70                                                  80
Phe-Leu-Glu-Asn-Val-Ile-Arg-Asp-Ala-Val-Thr-Tyr-Thr-Glu-His-Ala-Lys-Arg-Lys-Thr-

                                                  90                                                 100
Val-Thr-Ala-Met-Asp-Val-Val-Tyr-Ala-Leu-Lys-Arg-Gln-Gly-Arg-Thr-Leu-Tyr-Gly-Phe-Gly-Gly
```

APPENDIX-II

CHARGES DISTRIBUTION OF THE HISTONES

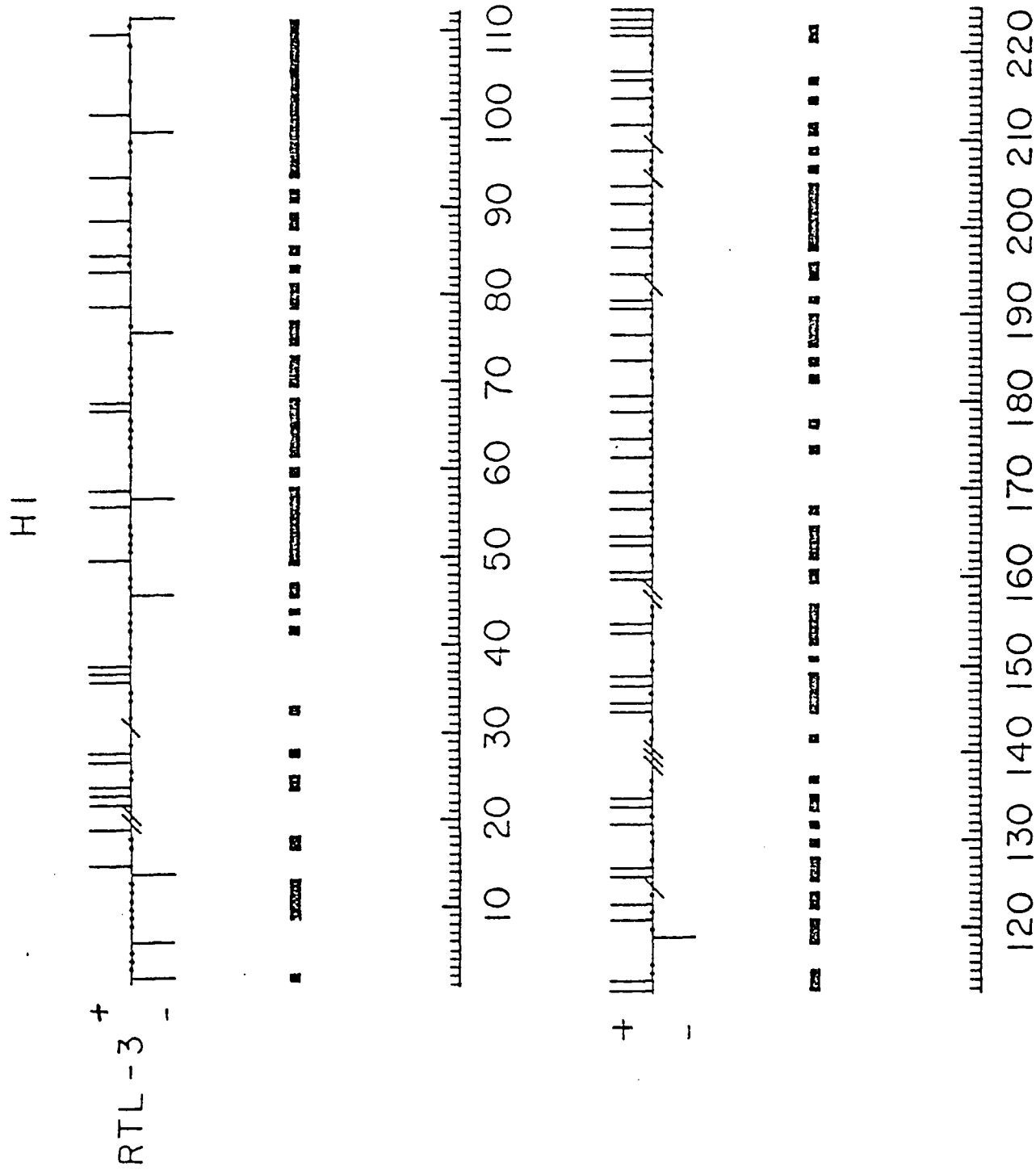

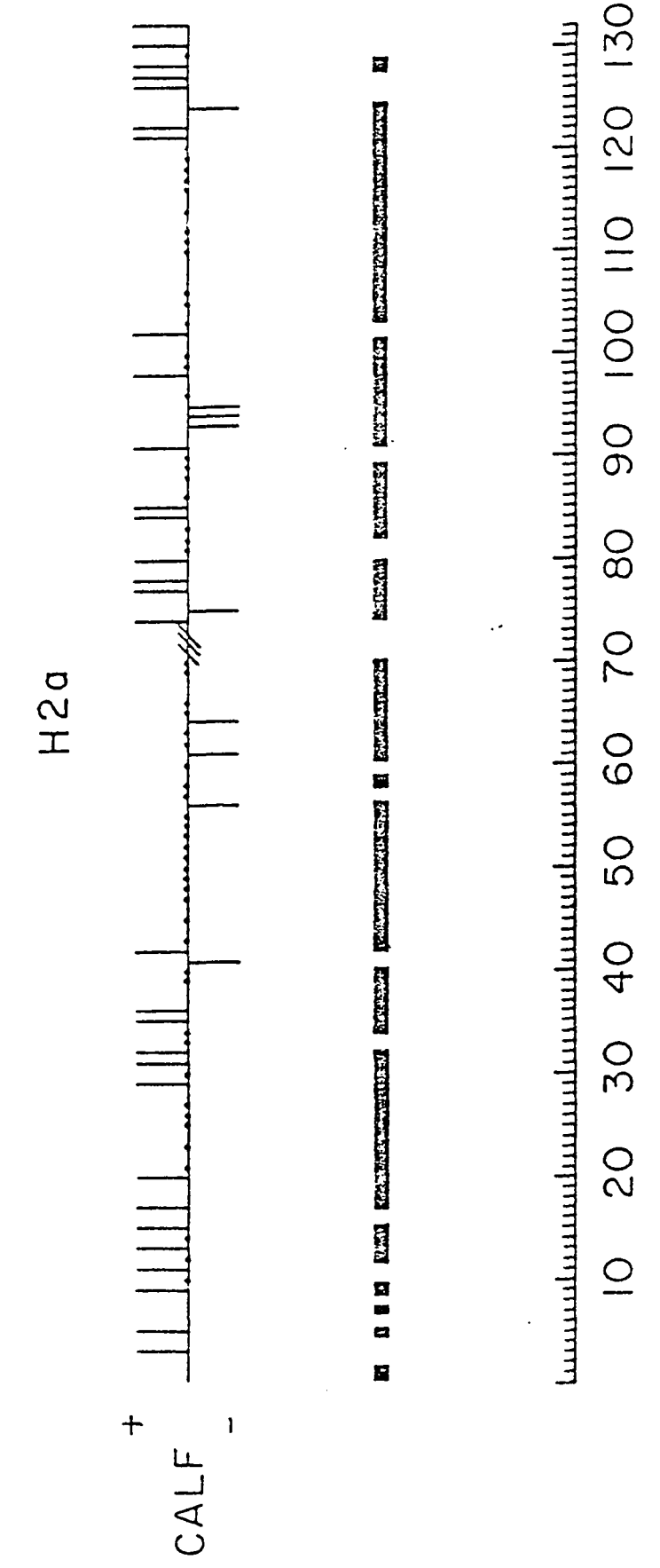
H2a
+
CALF
-
10 20 30 40 50 60 70 80 90 100 110 120 130

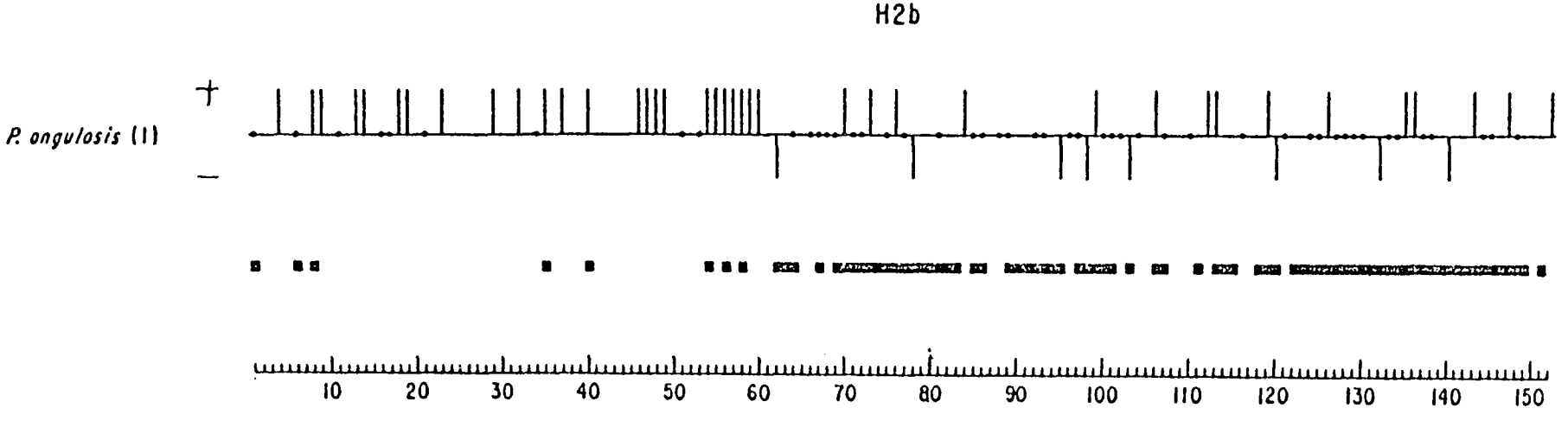
H2b
P. angulosis (1)
+
—
10
20
30
40
50
60
70
80
90
100
110
120
130
140
150

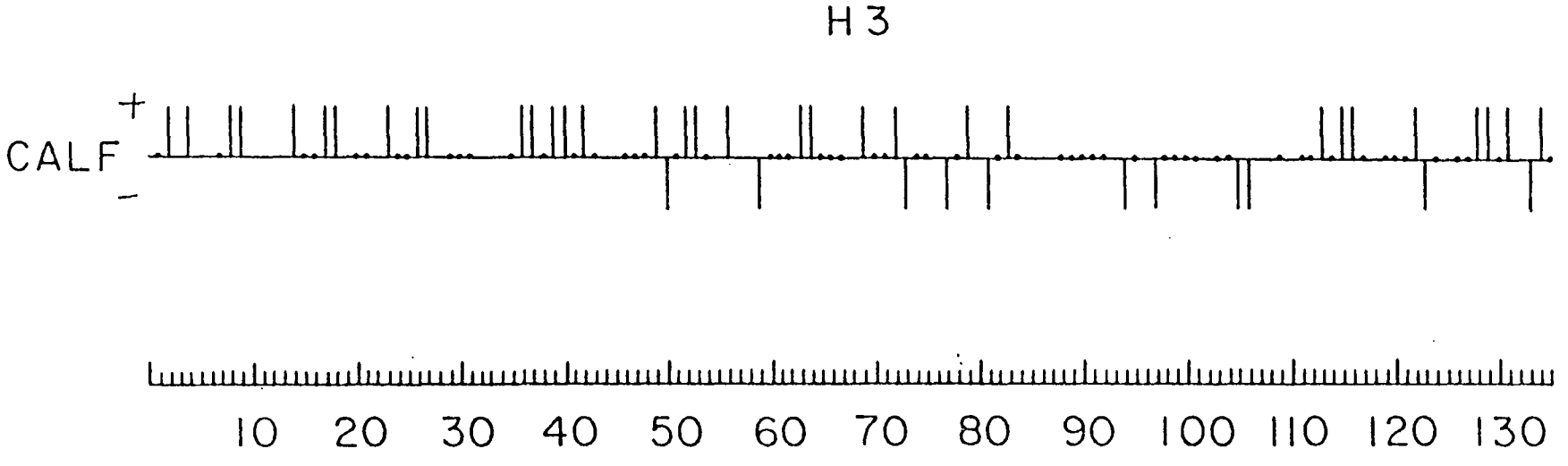
H 3
CALF
+
−
10 20 30 40 50 60 70 80 90 100 110 120 130

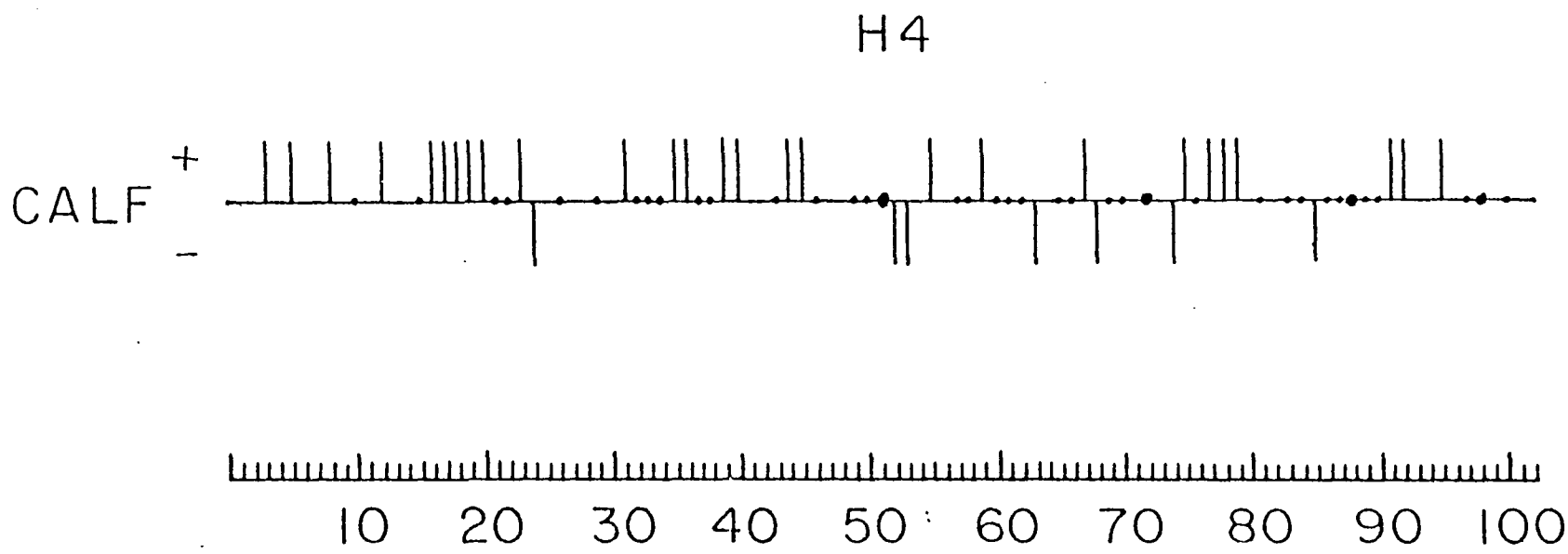
H4
CALF
+
−
10
20
30
40
50
60
70
80
90
100

REFERENCES

1. Huberman, J. A. (1973) Ann. Rev. Biochem. 42, 355.
2. Elgin, S. C. and Weintraub, H. (1975) Ann. Rev. Biochem. 44, 725.
3. Kornberg, R. (1977) Ann. Rev. Biochem. 46, 931.
4. Grouse, L., Chilton, M. D. and McCarthy, B. J. (1972) Biochem. 11, 798.
5. Davis, D. R. (1967) Ann. Rev. Biochem. 36, 321.
6. Bonner, J., Dahmus, M., Fambrough, D., Huang, R. C., Marushige, K., and Tuan, D. (1968) Science 159, 47.
7. Holmes, D. and Bonner, J. (1973) Biochem. 12, 2330.
8. Jacobson, R. A. and Bonner, J. (1968) Bioch. Biophys. Res. Comm. 33, 716.
9. Dahmus, M. and McConnell, D. (1969) Biochem. 8, 1534.
10. Mayfield, J. E. and Bonner, J. (1971) Proc. Natl. Acad. Sci. U.S.A. 68, 2652.
11. Von Holt, C., Strickland, W. N., Brandt, W. F., and Strickland, M. S. (1979) FEBS Letters 100 (2), 201.
12. DeLange, R. J. and Smith, E. L. (1973) Accounts of Chem. Res. 5, 368.
13. Van Holde, K. E. and Isenberg, I. (1975) Accounts of Chemical Research 8, 327.
14. Bradbury, E. M. (1975) Ciba Symposium 28, 1.
15. Stedman, E. and Stedman, E. (1950) Nature 166, 780.
16. Elgin, S. C. and Bonner, J. (1970) Biochem. 9, 4440.
17. Elgin, S. C. and Bonner, J. (1972) Biochem. 11, 772.
18. MacGillivray, A. J., Cameron, A., Krauze, R. J., Rickwood, D., and Paul, J. (1972) Bioch. Biophys. Acta 277, 384.
19. Wu, F. C., Elgin, S. C. and Hood, L. E. (1973) Biochem. 12, 2792.
20. Gilmour, R. S. and Paul. J. (1973) Proc. Natl. Acad. Sci. U.S.A. 70, 3440.
21. Pardon, J. F. and Wilkins, M. H. (1972) J. Mol. Biol. 68, 115.

REFERENCES

22. Brams, S. and Ris, H. (1971) J. Mol. Biol. 55, 325.

23. Chambon, P. (1977) Cold Spring Harbor Symposia 42 (II), 1209.

24. Felsenfeld, G. (1978) Nature (London) 271, 115.

25. Williamson, Robert (1970) J. Mol. Biol. 51, 157.

26. Clark and Felsenfeld (1971) Nature New Biol. 229, 101.

27. Hewish, D. R. and Burgoyne, L. A. (1973) Bioch. Biophys. Res. Comm. 52 (2), 504.

28. Noll, M. (1974) Nature 251, 249.

29. Shaw, B., Corden, J., Sahasrahuddhe, C. and Van Holde, K. (1974) Bioch. Biophys. Res. Comm. 61, 1193.

30. Honda, B. M., Baillie, D. L. and Candido, E. P. (1974) FFBS Letters 84, 156.

31. Sollner-Webb, B. and Felsenfeld, G. (1975) Biochem. 14, 2915.

32. McGhee, J. and Engel, J. (1975) Nature 254, 449.

33. Lohr, D. and Van Holde, K. (1975) Science 188, 165.

34. Spadafora, C. and Graci, G. (1975) FEBS Letters 57, 79.

35. Compton, J. L., Bellard, M. and Chambon, P. (1976) Proc. Natl. Acad. Sci., U.S.A. 73, 4382.

36. Morris, N. R. (1976) Cell 8, 357.

37. Rill, R. and Van Holde, K. (1973) J. Biol. Chem. 248, 1080.

38. Sahasrabuddhe, O. C. G. and Van Holde, K. E. (1974) J. Biol. Chem. 249, 152.

39. Woodcock, C. L. (1973) J. Cell Biol. 59, 368a.

40. Olins, A. L. and Olins, D. E. (1973) J. Cell Biol. 59, 2529.

41. Olins, D. E. and Olins, A. L. (1974) Science 183, 330.

42. Senior, M. B., Olins, A. L. and Olins, D. E. (1975) Science 187, 173.

43. Oudet, P., Groso-Bellard, M. and Chambon, P. (1975) Cell 4, 281.

REFERENCES

44. Finch, J., Noll, M. and Kornberg, R. (1975) Proc. Nat. Acad. Sci. U.S.A. 72, 3320.

45. Bakayev, V., Melnickor, A., Osicka, V. and Varshavsky, A. (1975) Nucleic Acids Res. 2, 1401.

46. Van Holde, K. E., Sahasrabuddhe, C. G., Shaw, B. R. (1974) Nucleic Acids Res. 1 (11), 1579.

47. Simpson, R. T. and Whitlock, J. P., Jr. (1976) Nuclei Acids Res. 3 (1), 117.

48. Weintraub, H., Worcel, A., and Alberts, B. (1976) Cell 9, 409.

49. Kornberg, R. and Thomas, J. O. (1974) Science 184, 865.

50. Baldwin, J. P., Boseley, P. G. and Bradbury, E. M. (1975) Nature 253, 245.

51. Carpenter, B. G., Baldwin, J. P., Bradbury, E. M. and Ibel, Konrad (1976) Nucleic Acids Res. 3 (7), 1739.

52. Subirana, J. A. and Martinez, A. B. (1976) Nucleic Acids Res. 3(11), 3025.

53. Sperling, L. and Klug, A. (1977) J. Mol. Biol. 112, 253.

54. Finch, J. T. and Klug, A. (1976) Proc. Natl. Acad. Sci. U.S.A. 73, 1897.

55. Hzelm, R. P., Kreale, G. G., Suan, P., Baldwin, J. P. and Bradbury, E. M. (1977) Cell 10, 139.

56. Pardon, J. F., Worcester, D. L., Wooley, J. C. , Tatchell, K., Van Holde, K. E. and Richards, B. M. (1975) Nucleic Acids Research 2 (11), 2163.

57. Spiker, S. and Isenberg, I. (1977) Cold Spring Harbor Symposia, 42, (1), 157.

58. Isenberg, I. (1977) In "Search and Discovery" (ed. by B. Kaminer), 195, Acad. Press, N. Y.

59. D'Anna, J. A., Jr. and Isenberg, I. (1977) Biochem. 16, 1819.

60. Weintraub, H., Patter, K., and Van Lente, F. (1975) Cell 6, 85.

61. Lewis, P. N. (1976) Bioch. Biophys. Res. Comm. 68, 2.

REFERENCES

62. Skandrani, E., Mizon, J., Santiere, P., and Biserte, G. (1972) Biochemie 54, 1267.

63. Kelley, R. (1973) Bioch. Biophys. Res. Comm. 54, 1588.

64. Roark, D. E., Geoghegan, T. E. and Kellen, G. H. (1974) Bioch. Biophys. Res. Comm. 59, 542.

65. Van Lente, F., Jackson, J. F., and Weintraub, H. (1975) Cell 5, 45.

66. Chalkley, R. (1975) Bioch. Biophys. Res. Comm. 64, 587.

67. Thomas, J. O., and Kornberg, R. (1975) Proc. Natl. Acad. Sci. U.S.A. 72, 2626.

68. Martinson, H. G., and McCarthy, B. J. (1975) Biochem. 14, 1073.

69. Martinson, H. G., Shetlar, M. D. and McCarthy, B. J. (1976) Biochem. 15, 2002.

70. Bonner, W. M., and Pollard, H. B. (1975) Bioch. Biophys. Res. Comm. 64, 782.

71. Isenberg, I. (1979) in "The Cell Nucleus", Vol. 4, ed. by Stein, G., Acad. Press, N. Y.

72. Ohlenbusch, H., Olivera, B., Tuan, D. and Davidson, N. (1967) J. Mol. Biol. 25, 299.

73. Camerini-Otero, R. D., Sollner-Webb, B. and Felsenfeld, G. (1976) Cell 8, 333-347.

74. Boseley, P. G., Bradbury, E. M., Butler-Browne, G. S., Carpenter, B. G., and Stephen, R. M. (1976) Eur. J. Bioch. 62, 21.

75. Oudet, P., Germond, J. E., Bellard, M., Spadafora, C. and Chambon, P. (1978) Phil. Trans. R. Soc. Lond. B. 283, 241-258.

76. Mirzabekov, A. D., Schick, V. V., Belyavsky, A. V., Karpov, V. L., and Bavykin, S. G. (1978) Cold Spring Harbor Symposia 42 (I), 149.

77. Simpson, R. T. (1976) Proc. Natl. Acad. Sci. U.S.A. 73, 4400.

78. Finch, J. T., Lutter, L. C., Rhodes, D., Brown, R. S., Rushton, B., Lewitt, M. and Klug, A. (1977) Nature 269, 29.

79. Langmore, J. P. and Wooley, J. C. (1975) Proc. Natl. Acad. Sci. U.S.A. 72, 2691.

REFERENCES

80. Richards, B., Pardon, J., Lilley, D., Cotter, R., and Wooley, J. (1977) Cell Biol. Intern. Rept. 1, 107.

81. Suau, P., Kneale, G. G., Braddock, G. W., Baldwin, J. P. and Bradbury, E. M. (1977) Nucleic Acids Res. 4, 3759.

82. Noll, M. (1977) J. Mol. Biol. 116, 49.

83. Lutter, L. C. (1977) J. Mol. Biol. 117, 53.

84. Sollner-Webb, B. and Felsenfeld, G. (1977) Cell 10, 537.

85. Sussman, J. L. and Trifonov, E. N. (1978) Proc. Natl. Acad. Sci. U.S.A. 75, 103.

86. Crick, F. H. C. and Klug, A. (1975) Nature 255, 530.

87. Sobell, H. M., Tsai, C., Gilbert, S. G., Jain, S. C. and Sakore, T. D. (1976) Proc. Natl. Acad. Sci. U.S.A. 73, 3068.

88. Lawrence, J. J., Chan, D. C. F., and Piette, L. H. (1976) Nucleic Acids Res. 3, 2879.

89. Tatchell, K. and Van Holde, K. E. (1977) Biochem. 16, 5295.

90. Noll, M., Thomas, J. O. and Kornberg, R. D. (1975) Science 187, 1203.

91. Johns, E. W. (1971) in "Histones and Nucleohistones," pp. 1-45, ed. by Phillips, D. M. P., Plenum Press.

92. Simon, R. H. and Felsenfeld, G. (1979) Nucleic Acids Res. 6 (2), 689.

93. Bohm, E. L., Strickland, W. N., Strickland, M., Thwaits, B. H., Van Der Westhuizen, D. R. and Von Holt, C. (1973) FEBS Letters 34 (2), 217.

94. Olins, A. L., Carlson, R. D., Wright, E. B. and Olins, D. E. (1976) Nucleic Acids Res. 3 (12), 3271.

95. Noll, M. and Kornberg, R. D. (1977) J. Mol. Biol. 109, 393.

96. Loening, U. E. (1967) Biochem. J. 102, 251.

97. Laemmli, V. K. (1970) Nature (London), 227, 680.

98. Cotter, R. I. and Lilley, D. M. (1977) FEBS Letters 82, 63.

99. Adackaparayil, M. and Smith, J. H. (1977) J. Organic Chem. 42, 1655.

REFERENCES

100. Noll, H. (1969) in "Techniques in Protein Biosynthesis," Vol. 2, pp. 101-179, ed. by Campell, Acad. Press.

101. Johnson, W. C., Jr., and Tinoco, I., Jr. (1969) Biochem. 8, 4108.

102. Greenfield, N. and Fasman, G. D. (1969) Biochem. 8, 4108.

103. Tunis-Schneider, M. J. and Maestre, M. F. (1970) J. Bol. Biol. 52, 521.

104. Jirgenson, B. (1973) in "Optical Rotatory Dispersion of Proteins and Other Macromolecules" Springer-Verlag, Berlin and N. Y.

105. Wagner, T. E., Vandegrift, V. and Moore, D. S. (1975) "Meth. of Enzymology", 40, 209.

106. Mandel, R. and Fasman, G. (1974) Biochem. Biophys. Res. Comm. 59, 672.

107. Fasman, G. (1978) Methods in Cell Biology 18, 327.

108. Fuller, W., Wilkins, M. H. F., Wilson, H. R. and Hamilton, L. D. (1965) J. Mol. Biol. 12, 60.

109. Li, H. J. (1975) Nucleic Acids Res. 2, 1275.

110. Mandel, R. and Fasman, G. D. (1976) Nucleic Acids Res. 3 (8), 1839.

111. Thomas, G. J., Jr., Prescott, B. and Olins, D. E. (1977) Science 197, 385.

112. Li, H. J. (1973) Biopolymers 12, 287.

113. Subirana, J. A. (1973) J. Mol. Biol. 74, 363.

114. Angenlicht, L., Nicolini, C. and Baserga, R. (1974) Bioch. Biophys. Res. Comm. 59, 920.

115. Worcel, A. and Benyajati, C. (1977) Cell 12, 83.

116. Li, H. J. (1976) in "Chromatin and Chromosome Structure," ed. by Li, H. J. and Eckhardt, R. A., pp. 37, Acad. Press, N. Y.

117. Schildkraut, C. and Lifson, S. (1965) Biopolymers 3, 195.

118. Wittig, B. and Wittig, S. (1977) Nucleic Acids Res. 4 (11), 3901.

119. Witlock, J. P., Jr. and Simpson, R. T. (1976) Nucleic Acids Res. 3, 2255.

REFERENCES

120. Means, G. E. and Feeney, R. E. (1971) in "Chemical Modification of Proteins," Holden-Day, Inc.

121. Kronman, M. J. and Robbins, F. M. (1970) in "Fine Structure of Proteins and Nucleic Acids," ed. by Fasman, G. D. and Timasheff, S. N., Chapter 4, 'Buried and Exposed Groups in Proteins,' M. Dekker, Inc., N. Y.

122. Berliner, L. (1976) in "Spin Labeling, Theory and Applications," Academic Press, N. Y.

123. Berliner, L. (1978) in "Spin Labeling II, Theory and Applications," Academic Press, N. Y.

124. Likhtenshtein, G. I. (1976) in "Spin Labeling Methods in Molecular Biology," J. Wiley and Sons, N. Y.

125. Berliner, L. (1974) in "Progress in Bioorganic Chemistry," ed. by Kaiser, E. T. and Kezdy, Vol. 3, 1.

126. Berliner, L. (1978) in "Methods of Enzymology," Vol. 49, part G, 418.

127. Smith, I. C. P., Schreier-Muccillo, S. and Marsh, D. (1976) in "Free Radicals in Biology," ed. by Pryor, W., Chapter 4, 149, Acad. Press, N. Y.

128. Riordan, J. F., Wacker, W. E. C. and Vallee, B. L. (1965) Biochem. 4, 1758.

129. Simpson, R. T., Riordan, J. F. and Vallee, B. L. (1963) Biochem. 2, 616.

130. Barratt, M. D., Dodd, G. H. and Chapman, D. (1969) Biochim. Biophys. Acta 194, 600.

131. Adackaparayil, M. and Smith, J. H. (1977) J. Organic Chem. 42, 1655.

132. Haschemeyer, R. H. and Haschemeyer, A. E. V. (1973) in "Proteins: A Guide to Study by Physical and Chemical Methods," Chapter 15, J. Wiley and Sons, N. Y.

133. Timasheff, S. N. and Fasman, G. D., eds. (1969) in "Structure and Stability of Biological Macromolecules," Marcel Dekker, Inc., N. Y.

134. Tanford, C. (1968) in "Adv. Protein Chem.," 23, 121.

135. Tanford, C. (1970) in "Adv. Protein Chem.," 24, 1.

136. Gadski, R. A. and Chi-Bom Chae (1976) Biochem. 15, 3812.

REFERENCES

137. Stein, A., Bina-Stein, M. and Simpson, R. T. (1977) Proc. Natl. Acad. Sci. U.S.A. 74, 2780.

138. Wilhelm, F. X., Wilhelm, M. L., Erard, M. and Daune, M. P. (1978) Nucleic Acids Res. 5 (2), 505.

139. Steinmetz, M., Streeck, R. E., and Zachau, H. G. (1978) Phil. Trans. R. Soc. Lond. Series B, 283, 259.

140. Fulmer, A. W. and Fasman, G. D. (1979) Biochem. 18 (4), 659.

141. Faulhaber, I. and Bernardi, G. (1967) Biochim. Biophys. Acta 140, 561.

142. Lowry, O. H., Rosenbrough, N. J., Farr, A. L. and Randall, R. J. (1951) J. Biol. Chem. 193, 265.

143. Hozier, J., Nehls, P., and Renz, M. (1977) Chromosoma 62, 301.

144. DuPraw, E. J. (1970) in "DNA and chromosomes," pp. 132, 172, Holt, Rinehart and Winston, N. Y.

145. Davies, H. G. and Haynes, M. E. (1976) J. Cell. Sci. 21, 315.

146. Olins, A. L. (1977) Cold Spring Harbor Symposia 42 (I), 325.

147. Renz, M., Nehls, P. and Hozier, J. (1977) Proc. Natl. Acad. Sci. 74, 1879.

148. Bak, A. L., Zeuthen, J. and Crick, F. H. C. (1977) Proc. Natl. Acad. Sci. U.S.A. 74 (4), 1595.

149. Moss, T., Cary, P. D., Abercrombie, B. A., Crane-Robinson, C. and Bradbury, E. M. (1976) Eur. J. Biochem. 71, 337.

150. Moss, T., Crane-Robinson, C. and Bradbury, E. M. (1976) Biochem. 15, 2261.

151. Bohm, L., Hayashi, H., Crane-Robinson, C., Cary, P.D. and Bradbury, E. M. (1977) Eur. J. Biochem. 77, 487.

152. Whitlock, J. P., Jr., and Stein, A. (1978) J. Biol. Chem. 253, 3857.

153. Olins, D. E. (1977) in "Molecular Human Cytogenetics," ed. by Sparkes, R. S., Comings, D. E. and Fox, C. F. pp. 1-16, Academic Press, N. Y.

154. Olins, D. E., Bryan, P. N., Harrington, R. E., Hill, W. E. and Olins, A. L. (1977) Nucleic Acids Res. 4, 1911.

REFERENCES

155. Harrington, R. E. (1977) Nucleic Acids Res. 4, 3821.

156. Olins, D. E. (1978) Federation Proceedings, Abstract 37 (6), 1065.

157. Butler, A., Harrington, R. E. and Olins, D. E. (1979) Nucleic Acids Res. 6 (4), 1509.

158. Oudet, P., Spadafora, C. and Chambon, P. (1977) Cold Spring Harbor Symposia 42, 301.

159. Gordon, V. C., Knobler, C. M., Olins, D. E., and Schumaker, V. N. (1978) Proc. Nat. Acad. Sci. U.S.A. 75, 660.

160. Zama, M., Bryan, P. N., Harrington, R. E., Olins, A. L. and Olins, D. E. (1977) Cold Spring Harbor Symposia 42, 31.

161. Dieterich, A. E., Axel, A. and Cantor, C. R. (1977) Cold Spring Harbor Symposia 42, 199.

162. Shiffman, M. L., Maciewicz, R. A., Hu, A. W., Howard, J. C. and Li, H. J. (1978) Nucleic Acids Res. 5, 3409.

163. Martinson, H. G. and True, R. J. (1979) Biochem. 18 (6), 1089.

164. Li, H. J., Isenberg, I. and Johnson, W. C., Jr. (1971) Biochem. 10, 2587.

165. Zama, M., Olins, D. E., Presscott, B. and Thomas, G. J., Jr. (1978) Nucleic Acids Res. 5 (10), 3881.

166. Mayer, R., Toulme, F., Montenay-Garestier, T. and Helene, C. (1979) J. Biol. Chem. 254 (1), 75.

167 Martinson, H.G., True, R., Lau, C.K. and Mehrabian, M. (1979) Biochem. 18 (6), 1075.

168. Urry, D.W. (1969) in "Spectroscopic Approaches to Biomolecular Conformation," edited by Urry, D.W., Chapter 3, pp. 34, American Medical Association, Illinois.